

NORTHWESTERN UNIVERSITY

Wireless Sensor Networks for Monitoring Cracks in Structures

A THESIS

SUBMITTED TO THE GRADUATE SCHOOL  
IN PARTIAL FULFILLMENT OF THE REQUIREMENTS

for the degree

Master of Science

Field of Civil Engineering

By

Mathew P. Kotowsky

EVANSTON, ILLINOIS

June 2010



## **ABSTRACT**

Autonomous Crack Monitoring (ACM) and Autonomous Crack Propagation Sensing (ACPS) are two types of structural health monitoring in which characteristics of cracks are recorded over long periods of time. ACM seeks to correlate changes in widths of cosmetic cracks in structures to nearby blasting or construction vibration activity for the purposes of litigation or regulation. ACPS seeks to track growth of cracks in steel bridges, supplementing regular inspections and alerting stakeholders if a crack has grown.

Both ACM and ACPS may be implemented using wired data loggers and sensors, however, the cost of installation and intrusion upon the use of a structure makes the use of these systems impractical if not completely impossible. This thesis presents the implementation of these systems using wireless sensor networks (WSNs) and evaluates the effectiveness of each.

Three wireless ACM test deployments are presented: the first a proof of concept, the second to show long-term functionality, and the third to show the effectiveness of a newly invented device for low-power event detection. Each of these case studies was performed in a residential structure.

Four laboratory experiments of ACPS systems and sensors are presented: the first three show the functionality of commercially available crack propagation sensors and a WSN system adapted from the agricultural industry. The final experiment shows the functionality of a newly invented form of crack propagation gage that allows for a more flexible installation of the sensor.



## Acknowledgements

This thesis represents the climax of a serendipitous chapter in my career in which I found an unexpected outlet in civil engineering for my interest and skills in computers and electronics. Many teachers, co-workers, family and friends have been a part of this process, and to them I give my most sincere thanks.

First, I would like to thank my M.S. thesis committee, Professor Charles H. Dowding and Professor David J. Corr for their guidance and direction during my entire graduate school experience. Entering the field of civil engineering with an undergraduate background in computer engineering was a challenge through which these two gentlemen saw me with advice on everything from course selection to conference attendance and everything in between.

While I was a sophomore in computer engineering at the University of Illinois at Urbana-Champaign, Professor Dowding hired me as an undergraduate programmer to assist over the Internet and on school breaks in his Autonomous Crack Monitoring project sponsored by Northwestern University's Infrastructure Technology Institute (ITI). This unusual employment arrangement blossomed into a summer internship at ITI, employment after graduation, and eventually entrance into graduate school. Instead of moving to California to write software for a large company in Silicon Valley, I have spent the last several years of my life travelling the country and applying my computer and civil engineering education to exciting instrumentation projects.

Professor Corr only recently joined the ITI team, but his industry experience and expertise in structural engineering immediately strengthened my work at ITI and gave me a fresh perspective on all of my efforts. Both in the classroom and in the field, Professor Corr reinforced my understanding of structural engineering concepts that were newer to me than to my classmates and gave me the confidence to go forward with my experiments in custom-designed crack propagation sensors.

The late Professor David F. Schulz, founding director of ITI, brought together a team of engineers that have turned my college job into a viable career path. Professor Schulz, and current ITI Director Joseph L. Schofer, have made available to me a world of engineering experiences that I could not have imagined as an undergraduate. To these gentlemen I am deeply

indebted. Nearly all of the research described in this thesis was funded by ITI via its grant from the Research and Innovative Technology Administration of the United States Department of Transportation.

The ITI Research Engineering Group, Daniel R. Marron, David E. Kosnik, and the late Daniel J. Hogan, have been my closest partners during my time at Northwestern. From these three gentlemen I have learned more than from any classroom teacher. We have travelled the country together from the Everglades to the Pacific Northwest, at every destination encountering unique challenges and meeting them as a team. From Mr. Hogan, I learned that befriending a man with a welder can solve more problems than you might think, especially when you need to drop the anchor. From Mr. Marron I learned that any engineering task is possible if you're near enough to a hardware store. From Mr. Kosnik I learned that I can be as fascinated by a coincidental juxtaposition of municipal and private water towers as by staring upward from inside the construction site at the World Trade Center. These and other life lessons learned while part of the Research Engineering Group will stay with me for the rest of my engineering career.

Without the contributions of undergraduate research assistant Ken Fuller, the experiments in Chapter 4 would have been impossible. Mr. Fuller assisted me by completing almost all of the preparation of the test coupons, accompanying me to the industrial paint warehouse, and making himself available for long hours in the mechanical testing lab. His reliability, work ethic, attention to detail, and camaraderie were invaluable to me.

Melissa Mattenson, an old friend and more recently my next-door neighbor at the office, contributed vastly to my graduate work with a steady stream of gummy stars, needless (or were they?) lunch trips to the best Evanston eateries, and moral support mere steps from my desk.

For longer than near-decade I have been associated with ITI, Autonomous Crack Monitoring (ACM) has been a research focus of the Institute. The published work of several students, some of whom I have never met, has been essential to the research presented in this thesis. I would especially like to thank three of these former students for their individual roles in ACM project:

Damien R. Siebert received his M.S. in 2000 after publishing his thesis, *Autonomous Crack Comparometer*, five months before I first began work at ITI. His work, heavily referenced in this document, provided the basic principles on which I based my research.

Hasan Ozer, who received his M.S. in 2005, was my partner in ITI's first exploration of wireless sensor networks. Mr. Ozer and I, with our respective undergraduate backgrounds in civil and computer engineering, found ourselves learning together and teaching each other how to make wireless sensor networks work for us. He was my partner in the project that

received third place honors at the Second Annual TinyOS Technology Exchange in 2005, and his contributions to wireless ACM have been invaluable.

Jeffrey E. Meissner, research assistant to Professor Dowding, took on the arduous task of analyzing data collected by one of the systems in Chapter 3 several years after it was archived. Mr. Meissner worked diligently with this unfamiliar data and, in extremely short order, produced information that I used to further my analysis.

Martin Turon, Director of Software Engineering at Crossbow Technology, was not only responsible for the development of all of the software which I later modified to implement the systems described in Chapter 3, but he made himself available to me for personal consultation after I met him at Crossbow's headquarters in 2005. Mr. Turon's patience and helpful insights as I struggled to understand the vastness of the Crossbow code library were invaluable.

Mohammad Rahimi of the Center for Embedded Networked Sensing at the University of California, Los Angeles, designed and developed the MDA300CA sensor board which was integral to all of the work described in Chapter 3. Dr. Rahimi provided me with technical support and guidance in my efforts to adapt the MDA300CA to wireless ACM.

The experiments in Chapter 3 would not have been possible without the University Lutheran Church at Northwestern. Reverend Lloyd R. Kittlaus provided me with virtually unlimited access to the property to deploy and test the wireless sensor hardware in a real occupied environment to which I could walk from my office in no more than five minutes. I would also like to thank Aaron Miller and Amanda Hakemian, the tenants of the third floor apartment, for allowing me to place a wireless sensor node in their home for several months.

Professors Peter Dinda and Robert Dick of Northwestern University's Department Electrical Engineering and Computer Science led a team of engineering undergraduates and graduate students, faculty, and staff in a collective research group funded by the National Science Foundation under award CNS-0721978. They acted in an advisory role to Sasha Jevtic in the *Shake 'n Wake* project described in Chapter 3, and provided the funds to purchase the eKo Pro Series WSN described in Chapter 4. Their insightful commentary and advice aided greatly in my software work.

Sasha Jevtic, a graduate student then graduate of Northwestern University's Electrical and Computer Engineering Department, was the chief developer of the Shake 'n Wake board described in Chapter 3. Mr. Jevtic brought to the project not only his considerable electronics and engineering expertise but the willingness to spend late nights in the lab with me debugging hardware and software after we had both finished working full days.

Mark Seniw of Northwestern University's Department of Materials Science and Engineering was crucial in performing the experiments described in Chapter 4. With his extensive experience in mechanical testing, Mr. Seniw guided me through every step of the process of creating then destroying compact test specimens and dedicated a great deal of his time to the often slow and laborious process of test setup.

Steve Albertson of Northwestern University's Department of Civil and Environmental Engineering made himself and his lab available to me to do last-minute mechanical testing when my intended machine suddenly broke down. Without Mr. Albertson's assistance, the custom crack propagation gages described in Chapter 4 would not have been tested in time for the publication of this thesis.

This thesis was typeset using the `nuthesis` class for L<sup>A</sup>T<sub>E</sub>X2<sub>ε</sub>, developed by Miguel A. Lerma of Northwestern's Department of Mathematics and amended by David E. Kosnik of Northwestern University's Infrastructure Technology Institute.

To my parents, Janet and Arnold Kotowsky, and to my grandmother Anne Horwitz and my late grandfather Lawrence Horwitz, I give thanks for their constant support through the times that I have struggled and instilling in me the work ethic and stubborn insistence on perfection that have come to define my attitude toward all my endeavors.

Finally, to Kristen Pappacena, who came into my life only a few short years ago, I must give thanks for her inspirational example as she completed her Ph.D. in front of my eyes. Her attitude and accomplishments served as an example for me as I worked toward my degree, and her kind and caring ways have, time and again, seen me through the difficult times.

## Table of Contents

ABSTRACT	i
Acknowledgements	iii
List of Tables	xiii
List of Figures	xv
Chapter 1. Introduction	1
Chapter 2. Fundamentals of the Monitoring of Cracks	5
2.1. Overview of Autonomous Crack Monitoring	5
2.2. Crack Width	6
2.3. A Wired ACM System	7
2.3.1. Crack Width Sensors	10
2.3.2. Velocity Transducers	13
2.3.2.1. Traditional Buried Geophones	13
2.3.2.2. Miniature Geophones	14
2.3.3. Temperature and Humidity Sensors	15
2.4. Types of Crack Monitoring	15
2.4.1. Width Change Monitoring	16
2.4.1.1. ACM Mode 1: Long-term	17

2.4.1.2. ACM Mode 2: Dynamic	17
2.4.2. Crack Extension Monitoring	20
2.4.2.1. Traditional Crack Propagation Patterns	21
2.4.2.2. Custom Crack Propagation Patterns	21
2.5. Examples of the output of an ACM system	22
2.6. Chapter Conclusion	24
Chapter 3. Techniques for Wireless Autonomous Crack Monitoring	25
3.1. Chapter Introduction	25
3.1.1. Wireless Sensor Networks	25
3.1.1.1. Motes	26
3.1.1.2. Base Station	26
3.1.1.3. Wireless Communication	27
3.1.2. Challenges of Removing the Wires from ACM	27
3.2. Crack Displacement Sensor of Choice	30
3.3. WSN Selection	33
3.3.1. The Mote	34
3.3.2. Sensor Board Selection	35
3.3.2.1. Precision Sensor Excitation	37
3.3.2.2. Precision Differential Channels with 12-bit ADC	37
3.3.3. Software and Power Management	38
3.3.4. MICA2-Based Wireless ACM Version 1	38
3.3.4.1. Hardware	38
3.3.4.2. Software	41

3.3.4.3.	Operation	41
3.3.4.4.	Deployment in Test Structure	42
3.3.4.5.	Results	44
3.3.5.	MICA2-Based Wireless ACM Version 2 – <i>XMesh</i>	46
3.3.5.1.	Hardware	46
3.3.5.2.	Software	47
3.3.5.3.	Analysis of Power Consumption	49
3.3.5.4.	Deployment in Test Structure	49
3.3.5.5.	Results	54
3.3.5.6.	Discussion	55
3.3.6.	MICA2-Based Wireless ACM Version 3 – <i>Shake 'n Wake</i>	60
3.3.6.1.	Geophone Selection	61
3.3.6.2.	Shake 'n Wake Design	62
3.3.7.	Hardware	65
3.3.7.1.	Software	67
3.3.7.2.	Operation	69
3.3.7.3.	Analysis of Power Consumption	70
3.3.7.4.	Deployment in Test Structure	72
3.3.7.5.	Results	72
3.3.7.6.	Discussion	76
3.3.8.	Wireless ACM Conclusions	80
Chapter 4.	Techniques for Wireless Autonomous Crack Propagation Sensing	83
4.1.	Chapter Introduction	83

4.1.1. Visual Inspection	84
4.1.2. Other Crack Propagation Detection Techniques	86
4.1.3. The Wireless Sensor Network	87
4.2. ACPS Using Commercially Available Sensors	88
4.2.1. Integration with Environmental Sensor Bus	89
4.2.2. Proof-of-Concept Experiment	93
4.2.2.1. Experimental Procedure	94
4.2.3. Results and Discussion	97
4.3. Custom Crack Propagation Gage	98
4.3.1. Theory of Operation of Custom Crack Propagation Sensor	99
4.3.2. Sensor Design	99
4.3.3. Proof-of-Concept Experiment	103
4.3.4. Results and Discussion	105
4.4. Wireless ACPS Conclusions	107
Chapter 5. Conclusion	109
5.1. Conclusion	109
5.2. Future Work	111
5.2.1. Wireless Autonomous Crack Monitoring	111
5.2.2. Wireless Autonomous Crack Propagation Sensing	112
References	113
Appendix A. Experimental Verification of <i>Shake 'n Wake</i>	117
A.1. Transparency	118

A.2. Verification of Trigger Threshold	119
A.2.1. Physical Meaning of Trigger Threshold	123
A.3. Speed	124
A.4. Discussion	127
A.4.1. Upper Frequency Limit: Shake 'n Wake Response Time	128
A.4.2. Lower Frequency Limit: Geophone Output Amplitude	129
A.5. Appendix Conclusion	129
Appendix B. Data Sheets and Specifications	131
B.1. MICA2 Data Sheet	132
B.2. String Potentiometer Data Sheet	134
B.3. MDA300CA Data Sheet	137
B.4. MIB510CA Data Sheet	138
B.5. Stargate Data Sheet	139
B.6. Alkaline Battery Data Sheet	141
B.7. Lithium Battery Data Sheet	143
B.8. GS-14 Geophone Data Sheet	145
B.9. HS-1 Geophone Data Sheet	148
B.10. UC-7420 Data Sheet	151
B.11. Bus Resistor Data Sheet	154
B.12. Conductive Pen Data Sheet	156
B.13. "Bridge Paint" Data Sheet	158



## List of Tables

2.1	Comparison of the attributes of three types of crack width sensors	12
3.1	Distribution of MICA2-based wireless ACM Version 2 packets over the parents to which they were sent	58
3.2	ACM-related commands added to <i>xcmd</i> by Version 3 of the MICA2-based wireless ACM software	70
3.3	Results of filtering Version 3 wireless ACM potentiometer readings	78
4.1	Change in $\bar{e}Ko$ ADC steps for first rung break for each combination of bus resistor and current-sense resistor values	101
A.1	Summary of functional ranges for Shake 'n Wake event detection at level 2	129



## List of Figures

2.1	Flow of data from sensors to users, after Kosnik (2007)	7
2.2	Sketch of a view of a crack to illustrate the difference between crack width and crack displacement (change in crack width), redrawn after Siebert (2000)	7
2.3	Plan view of an ACM system installed in a residence, after Waldron (2006)	9
2.4	Photographs of three types of crack width sensors: <b>(a)</b> LVDT, after McKenna (2002) <b>(b)</b> eddy current sensor, after Waldron (2006) <b>(c)</b> string potentiometer, after Ozer (2005)	10
2.5	Different directions of crack response, after Waldron (2006)	11
2.6	Photograph of a triaxial geophone with quarter for scale	13
2.7	Layout of miniature geophones such that wall strains can be measured, after McKenna (2002)	14
2.8	Photographs of (a) indoor and (b) outdoor temperature and humidity sensors, after Waldron (2006)	15
2.9	Resistance measured between points A and B decreases as crack propagates	20
2.10	Two types of commercially available crack propagation patterns shown with a quarter for scale	22

2.11	Screen shots of <b>(a)</b> long-term correlation of crack width and humidity from <b>Mode 1</b> recording <b>(b)</b> crack displacement waveforms from <b>Mode 2</b> recording	23
3.1	Example of a multi-hop network: green lines represent reliable radio links between motes, after Crossbow Technology, Inc. (2009b)	28
3.2	Photograph of a string potentiometer with quarter for scale, after Jevtic et al. (2007b)	32
3.3	Photograph of a fully mounted string potentiometer, after Ozer (2005)	33
3.4	Photograph of a Crossbow MICA2 mote with quarter for scale	34
3.5	Photograph of a Crossbow MIB510CA serial gateway with MICA2 (without batteries) installed, after Ozer (2005)	35
3.6	Photograph of a Crossbow MDA300 with quarter for scale, after Dowding et al. (2007)	36
3.7	Photographs of Version 1 of the MICA2-based wireless ACM system, after Ozer (2005): <b>(a)</b> base station (in closet) <b>(b)</b> node (on ceiling monitoring crack)	40
3.8	Temperature and crack displacement measurements by wireless and wired ACM systems in test house over two month period, after Ozer (2005)	43
3.9	Alkaline battery voltage decline of a mote running <i>MDA300Logger</i> , after Ozer (2005)	44
3.10	The Stargate Gateway mounted to a plastic board	47

3.11	Current draw profile of a mote running the modified XMDA300 software for Mode 1 recording: the periodic sampling window is shown in the dashed oval in the inserted figure, demonstrating intermittent operation compared to ongoing operation; after Dowding et al. (2007)	50
3.12	Distribution of sensor nodes throughout test structures	51
3.13	MICA2-based wireless ACM Version 2 nodes located <b>(a)</b> in the basement, <b>(b)</b> on the sun porch, <b>(c)</b> in the apartment, and <b>(d)</b> over the garage	52
3.14	A typical mote in a plastic container	53
3.15	A string potentiometer measuring the expansion and contraction of a plastic donut	53
3.16	Plot of each mote's battery voltage versus time	54
3.17	Plot of temperature versus donut expansion over a period of <b>(a)</b> 200 days and <b>(b)</b> one week	56
3.18	Plot of each Version 2 wireless ACM mote's temperature versus time	57
3.19	Plot of each Version 2 wireless ACM mote's humidity versus time	57
3.20	Plot of each Version 2 wireless ACM mote's parent versus time	58
3.21	Traditional wired ACM system's determination of threshold crossing	60
3.22	<b>(a)</b> GeoSpace GS 14 L3 geophone <b>(b)</b> GeoSpace HS 1 LT 4.5 Hz geophone	62
3.23	The Shake 'n Wake sensor board, after Jevtic et al. (2007a)	64
3.24	Simplified Shake 'n Wake reference circuit diagram	65
3.25	Photograph of a Version 3 wireless ACM node	66

3.26	Photograph of the base station of Version 3 of the wireless ACM system, including UC-7420, MIB510CA, cellular router, power distributor, and industrially-rated housing	67
3.27	Photograph of a Version 3 wireless ACM node with string potentiometer and HS-1 geophone with mounting bracket installed on a wall	68
3.28	Current draw of <b>(a)</b> wireless ACM Version 2 mote with no Shake 'n Wake, after Dowding et al. (2007) <b>(b)</b> Version 3 mote with Shake 'n Wake	71
3.29	Layout of nodes in Version 3 test deployment	73
3.30	Version 3 wireless ACM nodes located <b>(a)</b> on the underside of the service stairs <b>(b)</b> over service stair doorway to kitchen, and <b>(c)</b> on the wall of the main stairway – <b>(d)</b> the base station in the basement	74
3.31	Plots of <b>(a)</b> temperature <b>(b)</b> humidity <b>(c)</b> battery voltage and <b>(d)</b> parent mote address recorded by Version 3 of the wireless ACM system over the entire deployment period	75
3.32	Plots of <b>(a)</b> temperature <b>(b)</b> humidity <b>(c)</b> crack displacement and <b>(d)</b> Shake 'n Wake triggers recorded by the Version 3 of the wireless ACM system over the 75-day period of interest	76
3.33	Comparison of battery voltage versus time for the Version 2 and Version 3 wireless ACM systems	77
3.34	Plot of three separate sets of crack width data as recorded by Mote 3 of the Version 3 wireless ACM system	78

3.35	Plots of <b>(a)</b> humidity and <b>(b)</b> temperature versus filtered crack displacement recorded by the Version 3 wireless ACM system over the 75-day period of interest	79
4.1	Fatigue crack at coped top flange of riveted connection, after United States Department of Transportation: Federal Highway Administration (2006)	85
4.2	Fatigue crack marked as per the BIRM, after United States Department of Transportation: Federal Highway Administration (2006)	85
4.3	<b>(a)</b> ēKo Pro Series WSN including base station, after Crossbow Technology, Inc. (2009a) <b>(b)</b> Individual ēKo mote with a 12-inch ruler for scale	87
4.4	Cartoon of a crack propagation pattern configured to measure the growth of a crack: resistance is measured between points A and B.	88
4.5	Crack propagation patterns <b>(a)</b> TK-09-CPA02-005/DP (narrow) <b>(b)</b> TK-09-CPC03-003/DP (wide)	89
4.6	Crack propagation resistance versus rungs broken for <b>(a)</b> TK-09-CPA02-005/DP (narrow) <b>(b)</b> TK-09-CPC03-003/DP (wide), after Vishay Intertechnology, Inc. (2008)	90
4.7	Schematic of the EEPROM mounted in the watertight connector assembly, after Crossbow Technology, Inc. (2009c)	91
4.8	Watertight ESB-compatible cable assembly, after Switchcraft Inc. (2004)	91
4.9	Diagram of sensor readout circuit, adapted from Vishay Intertechnology, Inc. (2008)	92

4.10	Schematic of compact test specimen: $W=3.5$ in, $B=0.5$ in, after for Testing and Materials (2006)	94
4.11	Test coupon with <b>(a)</b> narrow gage and <b>(b)</b> wide gage installed	94
4.12	Photograph of experiment configuration for pre-manufactured crack propagation gages	95
4.13	Test coupons with crack propagated through <b>(a)</b> narrow gage and <b>(b)</b> wide gage affixed with elevated-temperature-cured adhesive	96
4.14	Photograph of glue failure on wide gage affixed with room temperature-cured adhesive: the indicated region shows the glue failed before the gage.	96
4.15	Data recorded by eKo mote during tests of Coupons A and B	97
4.16	Schematic of a custom crack propagation gage; crack grows to the right, 3 V DC is applied between A and B, sensor output is measured between C and B.	100
4.17	Photograph of a commercially available bus resistor, after Bourns (2006)	100
4.18	Predicted change in output voltage of custom crack propagation sensor with rungs broken	102
4.19	Photograph of an engineer applying a custom crack propagation gage	104
4.20	Photograph of coupon with attached custom crack propagation gage	104
4.21	Coupon with custom gage after all rungs broken	105
4.22	Custom crack gage output versus time <b>(a)</b> unfiltered, and <b>(b)</b> with 0.1 hertz low-pass filter	106

A.1	Shake 'n Wake transparency test apparatus	119
A.2	Shake 'n Wake transparency test results for HS-1 geophone	120
A.3	Shake 'n Wake trigger threshold test apparatus	121
A.4	Shake 'n Wake Level 2 trigger threshold test results for HS-1 geophone at 5 hertz	121
A.5	Shake 'n Wake Level 2 trigger threshold test results for GS-14 geophone at 5 hertz	122
A.6	Summary of Shake 'n Wake level 2 trigger threshold voltages	123
A.7	Summary of Shake 'n Wake level 2 trigger threshold velocities	125
A.8	20 hertz sinusoidal input signal with rise time of 12.5 milliseconds	126
A.9	Scope readout indicating the mote can execute user code within 89 $\mu$ s of a signal of interest, after Jevtic et al. (2007b)	128

## CHAPTER 1

### **Introduction**

Autonomous Crack Monitoring (ACM) and Autonomous Crack Propagation Sensing (ACPS) are two autonomous structural health monitoring techniques performed on two different types structures. This thesis describes the use of Wireless Sensor Networks (WSNs) to greatly reduce the cost and installation effort of these systems, and to make practical their use in situations where the use of wired versions would be impossible.

ACM is a structural health monitoring technique that measures and records the changes in widths of cracks and time-correlates these changes to causal phenomena in and around the structure, autonomously making available the data and analyses via a securely-accessible Web page. Developed as a tool to support regulation and litigation in quarrying, mining, and construction, an ACM system is typically installed for a period of months or years in a residential structure, during which time it records continuously and publishes autonomously to the Web changes in the widths of cosmetic cracks in walls, ambient environmental conditions, ground vibrations, air overpressure, and internal household activity. This data is then used to determine the effect of the blasting or other vibratory activity on cyclical widening and narrowing of cosmetic cracks.

ACPS is a structural health monitoring technique that measures and records the propagation of existing cracks in structures, not only automatically making available the data via a securely-accessible Web page but also alerting stakeholders via e-mail, telephone, text message, or pager, should cracks extend beyond some pre-determined length. Developed for use on steel bridges, ACPS is designed to supplement federally mandated crack inspection procedures, which suffer

from poor repeatability and low frequency of occurrence, with precise, objective, and repeatable information on the condition of cracks.

This thesis will discuss the challenges of advancing of long-term structural health monitoring systems from the wired to the wireless domain. It will describe the design, development, and deployment of three iterations of a wireless ACM system built on a commercially available wireless sensor network (WSN) platform and examine three case studies in which wireless ACM systems were installed in residential structures. It will then discuss the design of an ACPS system based on both commercially available and custom-designed sensors and detail laboratory proof-of-concept experiments to demonstrate the system.

Chapter 2 describes the fundamentals of the monitoring of cracks. It will discuss the motivation for ACM and ACPS, describe exactly what physical phenomena they measure, and provide an example of the output of a traditional wired ACM system. It will consider the various types of sensors and address their suitability for monitoring cracks using both wired and wireless systems. Finally, Chapter 2 will discuss the different recording *modes* used by crack monitoring systems. These modes specify sampling rates and conditions that must be implemented by the data logger on which the monitoring system is built. The monitoring systems' utilization of one or both of the recording modes will directly constrain the choice of WSN platform on which to build the system.

Chapter 3 describes in detail hardware and software techniques employed to move an ACM system from the wired to the wireless domain. Challenges regarding power consumption and sampling mode will be examined. Chapter 3 will discuss the selection of the optimal sensors and WSN hardware to implement wireless ACM. It will then discuss three versions of the wireless ACM system, examining each system's design criteria, hardware and software advancements,

and performance in test deployments. Discussion focuses on issues of battery life, multi-hop mesh networking, practicalities of system installation, and the invention of a new device to allow commercially available hardware to better perform ACM functionality.

Chapter 4 will describe the design and development of an ACPS system using a WSN adapted from the agriculture industry. Special attention is given to commercially available and newly invented crack propagation sensors to make more practical the use of ACPS on bridges. Also described is the integration of sensors with the existing WSN system. Finally, Chapter 4 will summarize several laboratory experiments in which the WSN, the commercially available sensors, and the newly invented sensor, were tested.

Chapter 5 presents conclusions and recommends future work.

Appendix A describes a set of experiments to verify the functionality of the newly invented hardware first discussed in Chapter 3.

Appendix B contains manufacturer data and specification sheets for the commercially available sensors, wireless sensor networks, batteries, and electronics mentioned throughout the thesis.

A separate document, *Wireless Sensor Networks for Monitoring Cracks in Structures: Source Code and Configuration Files* (Kotowsky, 2010), contains all of the source code and configuration files used to implement the various systems described in the thesis. Only code that was modified from the original manufacturer code is included.



## CHAPTER 2

### **Fundamentals of the Monitoring of Cracks**

#### **2.1. Overview of Autonomous Crack Monitoring**

Autonomous Crack Monitoring (ACM) systems grew out of increasing public concern that construction and mining activities cause structural damage to nearby residences in the form of cracking of interior wall finishes. ACM systems can satisfy the need of mine operators, construction managers, homeowners, and their lawyers to quantify exactly how much, if any, damage the vibration-inducing activity causes to a residence.

The purpose of ACM systems, first described in Siebert (2000) as Autonomous Crack Comparometers, is to compare the effects of long-term weather-induced changes in crack width with changes induced by nearby construction activity, blasting activity, wind gusts, thunder claps, or common household activity, and publish this comparison to a Web site for review. This flow of data from physical measurements to a Web site is entirely autonomous and requires no human interaction. In general, if it can be shown that long-term weather-induced changes in crack width far exceed the vibration-induced changes, it can be concluded that the vibration is not, in fact, damaging the structure.

ACM systems were further refined and tested in the work of Louis (2000), McKenna (2002), Snider (2003), Baillot (2004), and Waldron (2006). The ACM systems described in this literature adhere to the general structure of computerized surveillance instrumentation as laid out by Dowding (1996):

- transducers to measure
  - ambient indoor and outdoor temperature
  - ambient indoor and outdoor humidity
  - ground or structural motion at a selected point or points
  - changes in the widths of existing cracks in walls
- centralized data logger to record data from all transducers
- high-quality instrument cable to carry signal from transducers to centrally-located data logger

The ACM system as described above is then connected, usually via the Internet though rarely via the public telephone network, to servers in the lab which automatically collect the readings and make them available on a Web site. Figure 2.1 illustrates the flow of data from the sensors to interested parties. The Internet connectivity of an ACM system also allows for remote reconfiguration of the system operating parameters which is essential for data management of dynamic even recording as discussed in section 2.4.1.2.

## 2.2. Crack Width

Siebert (2000) describes the high resolution with which the change in width of a typical household crack must be measured ( $0.1 \mu\text{m}$  or  $4 \mu\text{in}$ ) to capture fully even its smallest changes. This plays a significant role in the selection of the transducer to measure the crack. It is shown in Chapter 3 the resolution requirements have a different impact on a wireless ACM system than on a traditional, wired ACM system. Only the *change* in crack width is significant, as shown in Figure 2.2.

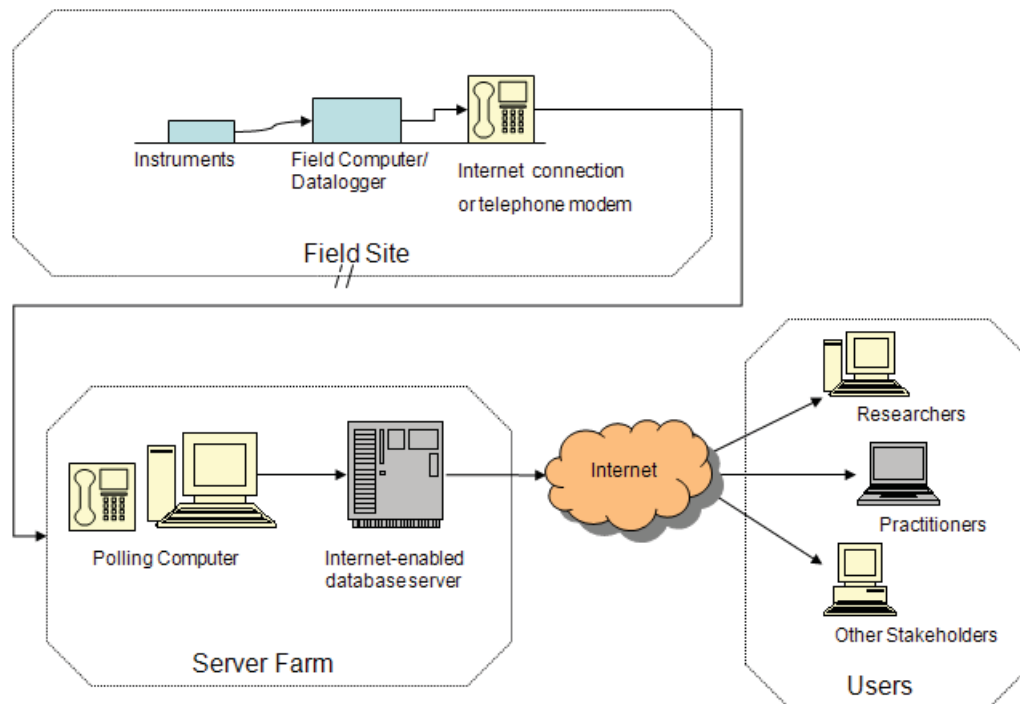


**Figure 2.1:** Flow of data from sensors to users, after Kosnik (2007)

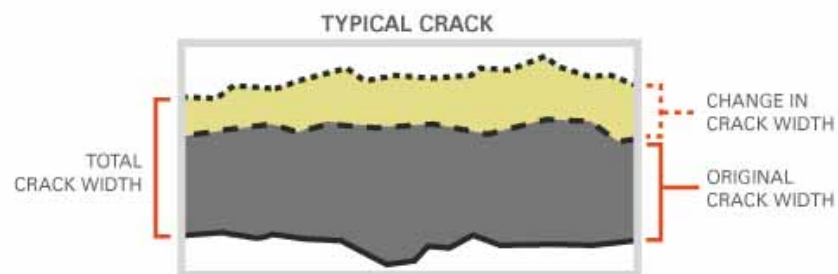


**Figure 2.2:** Sketch of a view of a crack to illustrate the difference between crack width and crack displacement (change in crack width), redrawn after Siebert (2000)

### 2.3. A Wired ACM System

The basic ACM system measures four different physical quantities: particle velocity of the ground on which the instrumented structure rests, changes in widths of cracks within the structure, ambient temperature both inside and outside the structure, and ambient relative humidity

both inside and outside the structure. Measurement on a single time scale of all of these quantities in a given structure lends insight into the effects of both weather and nearby blasting or construction vibration on a structure.

A typical ACM system is designed to record these physical quantities throughout a structure, not just in one particular location. Figure 2.3 shows a scale drawing of a house in which a wired ACM system was installed. Note that sensors are installed both indoors and outdoors, upstairs and downstairs, and separated in some cases by over 20 feet. This type of layout is typical of ACM systems. In the case of the system outlined in Figure 2.3, three engineers and a graduate student spent two full days in the home of a litigant drilling holes through interior and exterior walls, pulling cables through an attic, and gluing sensors to walls. Because this type of system is most often installed in a home or place of business for months or years at a time, minimization of intrusiveness and vulnerability of the ACM system is as crucial as minimization of cost and installation time. This need to minimize simultaneously the cost, the installation time, and the overall disruptiveness of the ACM system leads directly to the necessity of wireless ACM: high quality instrument cable can cost several dollars per foot and must be routed discretely through an occupied structure, avoiding sources of electromagnetic interference and hazardous locations. Cable installation adds significantly to the time, effort, and manpower required to install an ACM system. The existence of cables within an occupied structure also increases the chance of intentional and unintentional damage to the cabling by the structure's occupants.

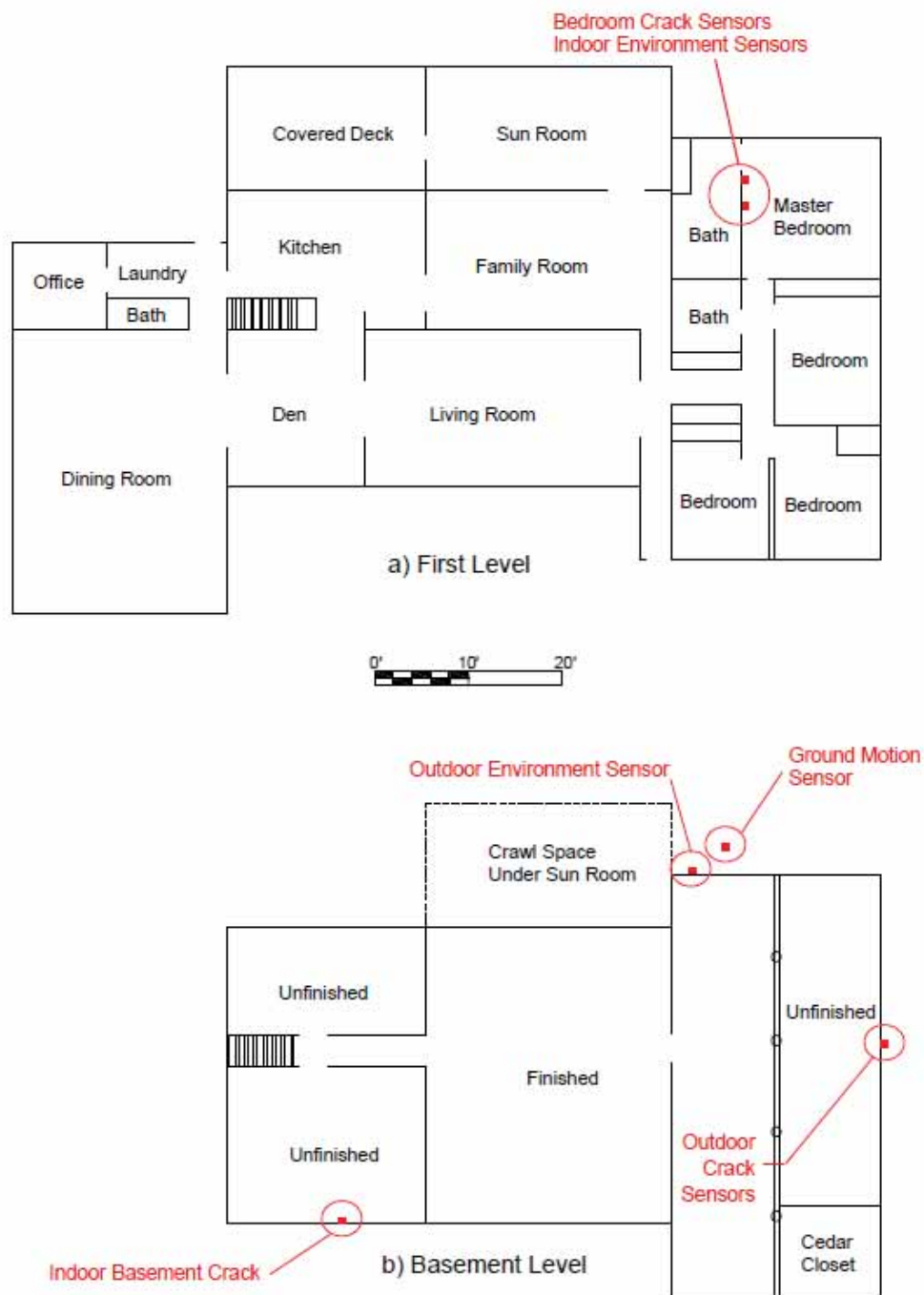


**Figure 2.3:** Plan view of an ACM system installed in a residence, after Waldron (2006)

### 2.3.1. Crack Width Sensors

ACM systems utilize three different types of sensors to measure changes in widths of cracks. Each of these sensors meets the precision and dynamic response characteristics required for ACM (Siebert, 2000; Ozer, 2005). Figure 2.4 shows the three different types of crack width sensors used for ACM: Linear variable differential transformers (LVDTs), eddy current displacement gages, and string potentiometers. Table 2.1 compares the attributes of each type of crack width sensor and can suggest which sensor should be chosen for a given measurement scenario.

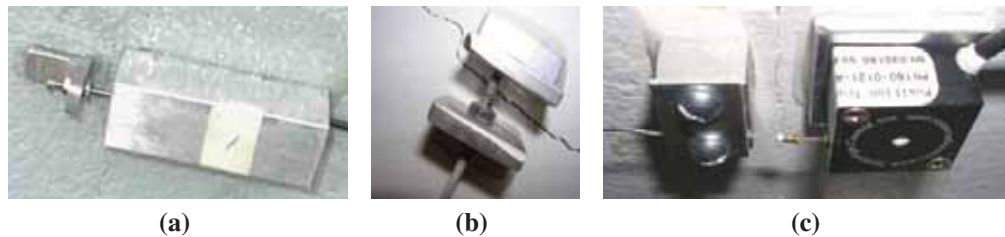


**Figure 2.4:** Photographs of three types of crack width sensors: (a) LVDT, after McKenna (2002) (b) eddy current sensor, after Waldron (2006) (c) string potentiometer, after Ozer (2005)

These three crack sensors that meet the requirements of precision and dynamic response utilize significantly different physical mechanisms to measure the width of a crack. Some sensors physically bridge the crack such that the movement of the crack can have an effect on the functionality of the sensor or the existence of the crack sensor might actually affect the movement of the crack. Other sensors do not physically bridge the crack. Sensor size, the need for signal conditioning electronics, and cost all play a role in determining the optimal sensor for an ACM system.

The ACM strategy of measuring the changes in the widths of cracks to characterize crack response to weather and vibration makes the assumption that the crack moves with a single degree of freedom - opening and closing along a line perpendicular to the crack (i.e. along direction *A* in Figure 2.5). Experience reveals, however that cracks will respond to excitation not only by opening and closing but also by their individual sides moving relative to each other in a directional normal to the plane of the wall in which the crack exists. This motion, known as out-of-plane movement and shown as direction *C* in Figure 2.5, is generally not significant in the characterization of crack response (Waldron, 2006) but can have a significant impact on the proper functionality of crack width displacement sensors. For example: should significant motion occur in directions *B* or *C* in a crack that is monitored by an LVDT, the core of the LVDT may be forced into the side of the sensor casing causing stick-slip behavior or even complete sensor failure. This danger can be circumvented using an eddy current gage.

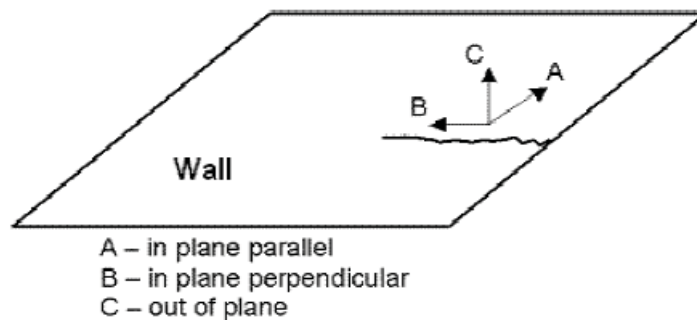


**Figure 2.5:** Different directions of crack response, after Waldron (2006)

Ease of installation and removal also plays a role in sensor selection: the crack sensor must be rigidly (i.e. with minimal creep due to gravity) and robustly (i.e. able to last for the entire duration of the monitoring activity) attached to the wall at the location of a crack. This dictates

the use of a quick-setting epoxy as described in Siebert (2000). The larger the area that needs to be glued, the more difficult and destructive sensor removal will be.

Design of a wired ACM system typically does not need to take into account the power draw of a given sensor type - the system has a power source (typically household 110 V AC service) so large that power considerations are usually ignored in sensor selection. In a wireless system, however, power is a much greater concern, as discussed in Chapter 3 and Chapter 4. Table 2.1 shows the various factors to consider when selecting a sensor for an ACM system.

	<b>LVDT</b>	<b>Eddy Current</b>	<b>Potentiometer</b>
<b>Model:</b>	DC-750-050	SMU-9000	Series 150
<b>Approximate Cost:</b>	\$250	\$1700	\$400
<b>Measuring Range:</b>	$\pm 0.05$ in	0.05 in	1.5 in
<b>Out-of-plane capable:</b>	no	yes	minimally <sup>a</sup>
<b>Physically bridges crack:</b>	yes	no	yes
<b>Footprint:</b>	large	small <sup>b</sup>	small
<b>Power Requirements:</b>	$\pm 15$ V DC, $\pm 25$ mA	7-15 V DC, 15 mA	7 mA at 35 V DC <sup>c</sup>
<b>Warm-up time:</b>	2 minutes	30 minutes	none

<sup>a</sup> The string potentiometer is not designed to measure motions in directions other than along the length of the string, but experience suggests that incidental motion of this type will not damage the sensor.

<sup>b</sup> The sensor itself is smaller than either of the other two types of sensors, however, the eddy current displacement sensor requires signal conditioning electronics to be placed on the wall near the sensor. The enclosure for the electronics does not, however, need to be fastened as securely (i.e. with epoxy) as the sensor itself, so removal of the sensor and its accompanying electronics will likely do less damage to paint and plaster than the other two displacement sensors.

<sup>c</sup> The power draw of the string potentiometer is directly proportional to its input voltage; the total resistance of the string potentiometer is  $5000\Omega$

**Table 2.1:** Comparison of the attributes of three types of crack width sensors

### 2.3.2. Velocity Transducers

ACM systems make use of velocity transducers to measure two different physical phenomena: particle velocity in the soil on which the structure is built, and the motion of the structure itself.

#### 2.3.2.1. *Traditional Buried Geophones*

Particle velocity in the soil, the traditional mechanism by which mining industry regulators restrict the effect of blasting vibration at locations away from the blast site (Dowding, 1996), is measured using a large triaxial geophone, shown in Figure 2.6, buried in the ground near a structure of interest. When a blast wave propagates through the soil, the geophone generates a sinusoidal output that is observed by the ACM system at 1000 samples per second. The ACM data logger will use this sensor's output to trigger high-frequency recording of all relevant sensors in the system.



**Figure 2.6:** Photograph of a triaxial geophone with quarter for scale

### 2.3.2.2. Miniature Geophones

In wired ACM systems, smaller geophones can be used to measure the actual motion of the structure. These smaller geophones are single-axis devices and are therefore smaller than the geophone in Figure 2.6. These transducers measure velocity versus time which can then be integrated to reveal displacement versus time. If the transducers are installed at the top and bottom of a wall section, as shown in Figure 2.7, the recorded velocity measurements can be used to calculate the strains in the walls.

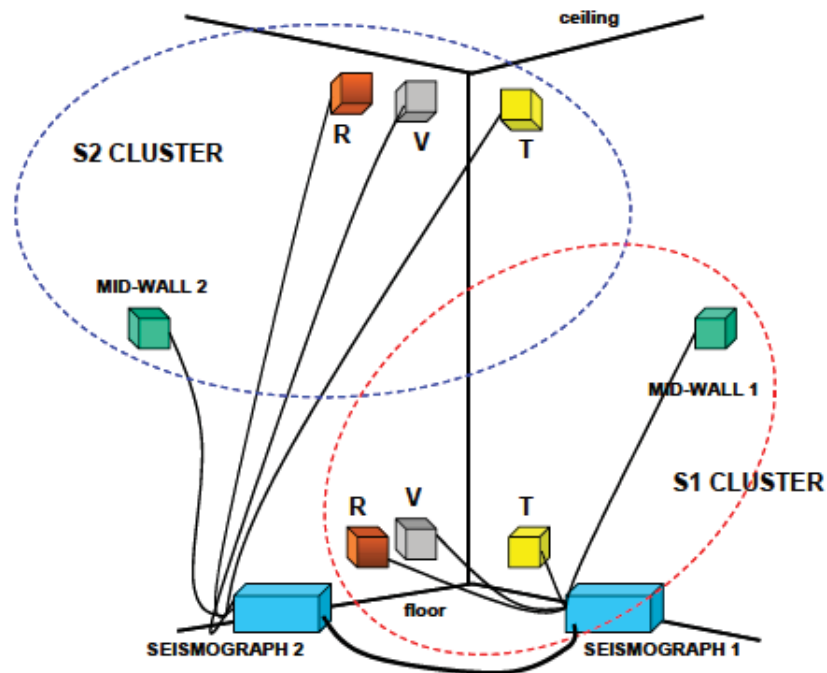


**Figure 2.7:** Layout of miniature geophones such that wall strains can be measured, after McKenna (2002)

In a wireless ACM system, these same miniature geophones can serve the purpose of providing signal by which to alert wireless nodes to the occurrence of a significant vibratory event.

Instead of relying on a centrally-installed geophone buried in the soil near the structure, a wire-less system can utilize a geophone at every node to measure local vibration.

### 2.3.3. Temperature and Humidity Sensors

Indoor and outdoor temperature and humidity sensors, such as those shown in Figure 2.8, are utilized to record long-term trends in temperature and humidity both inside and outside an instrumented structure. The outdoor gage supplies useful information about the passage of weather fronts and seasonal weather trends. The indoor gage supplies relevant information about the activity of the furnace or air conditioning system in the house. Both data streams can be correlated to crack response as discussed in section 2.4.1.1.

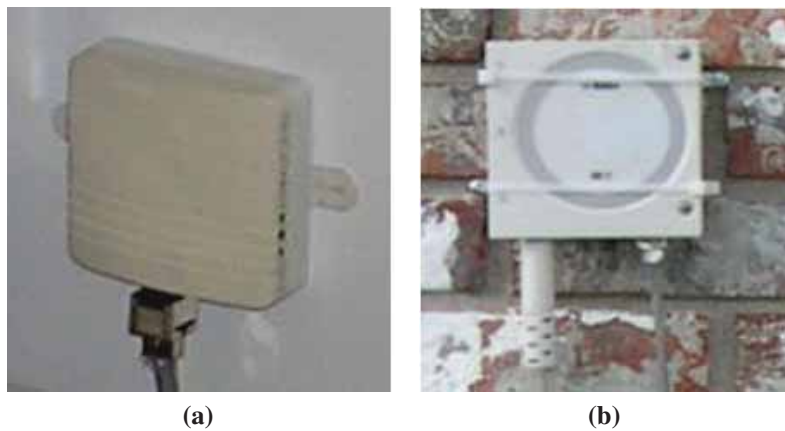


**Figure 2.8:** Photographs of (a) indoor and (b) outdoor temperature and humidity sensors, after Waldron (2006)

## 2.4. Types of Crack Monitoring

Crack behavior in response to vibration or environmental effects can manifest itself through a number of different physical changes in the crack. The crack can elongate, open (i.e. widen)

and close (see direction *A* in Figure 2.5), shear along the axis of the crack (see direction *B* in Figure 2.5), or move out-of-plane (see direction *C* in Figure 2.5). Measurement of each of these types of motion can lend insight into their causes.

#### **2.4.1. Width Change Monitoring**

ACM systems are largely concerned with measurements of changes in crack widths. Though the most serious crack activity to a homeowner might be extension or propagation of the crack rather than opening or closing of the crack, it is reasonable to assume the driving force behind any elongation will, in fact, be the same driving force behind widening and contracting.

Two types of phenomena exist that tend to cause changes in crack width (and therefore possible elongation or growth of a crack). The first type, so-called *long-term* effects, are those that must be measured over the periods of hours, days, months, and years in order to realize their effect on crack behavior. The other type, so-called *dynamic* effects, are the motions in cracks induced by vibration, blasting, slamming of doors, leaning against walls, and other common household activities. These phenomena tend to be short-lived (i.e. fewer than fifteen seconds in duration) and must be observed at a high frequency to realize their true effect on cracks. Additionally, these dynamic phenomena cannot be expected to occur on a predictable schedule, therefore an ACM system must be constantly aware of its sensor inputs to determine whether such an event is occurring. A wired ACM system is able to measure both long-term and dynamic events.

#### 2.4.1.1. *ACM Mode 1: Long-term*

Effects that can be observed using only hourly measurements include changes in temperature and humidity as driven by weather or the utilization of in-home heating and cooling systems or kitchen appliances such as ovens and stoves. Measuring these effects more frequently than a few times per hour will yield no new information about the cracks as temperature and humidity changes are slow produce changes in crack width. To capture accurately these phenomena and their effects on cracks, every hour the system will measure ambient indoor and outdoor temperature, ambient indoor and outdoor humidity, and the current widths of all cracks. Though ideally only one sample per sensor per hour is necessary to observe these long-term effects, it is often common practice to measure average short bursts of high-frequency measurements (e.g. sample one thousand samples for one second and average) to attempt to filter out any noise or electromagnetic interference that may be introduced due to long cable runs.

This long-term, periodic measurement of temperature, humidity, and crack sensors is known as *Mode 1* logging and is the simpler of the two modes in which an ACM system operates. It should be noted that readings from geophones are ignored in Mode 1 logging because slow periodic readings from a geophone yield no useful physical information.

#### 2.4.1.2. *ACM Mode 2: Dynamic*

Physical phenomenon other than temperature and humidity can have effects on cracks in the walls of structures; the very motivation behind the development of ACM systems is to characterize the effects of construction vibration and blasting on houses. These types of events have two characteristics that make them ill-suited for recording in Mode 1. First, they can occur at any time – one cannot assume that even the most organized construction or mining

operation will have a precise enough schedule of their daily activities that a system can be pre-programmed to record at the appropriate times. Secondly, these types of events require high frequency sampling to capture their true nature. Siebert (2000) indicates that these types of dynamic phenomena can last for three to fifteen seconds and must be recorded at one thousand samples per second to fully resolve all high-frequency motion.

In order to capture the entire dynamic event, some of which may occur at a time before the peak of the input signal exceeds the trigger threshold, ACM systems utilize buffering to avoid losing the pre-trigger data. At any given time, an ACM system has a buffer (typically one half to a full second) of data sampled one thousand times per second stored in its memory. If a threshold crossing condition does not occur, the data is discarded. If a crossing does occur, however, then the pre-trigger data is concatenated to the post-trigger data to form a single time history that clearly shows the point at which the trigger threshold was crossed.

The issue of *when* a dynamic event should be recorded is non-trivial. The occurrence of a random event is determined by the data logger continuously measuring the output of a geophone (or geophones) and using its microprocessor to compare the current geophone output to the pre-programmed threshold value. If the threshold value is set too low, the system will be overloaded with data that then must be transmitted back to the lab. If the value is set too high the system will fail to record an event of interest. For this reason, remote reconfiguration of the triggering threshold is critical for any ACM system. The best practice is to set the threshold relatively low during system installation and testing. Should that threshold prove to generate too much data or record events of little interest, the threshold is then slowly raised until an adequate balance is reached.

This high-frequency, randomly-occurring, remotely-configurable monitoring of both geophones and crack sensors is known as *Mode 2* logging and is more complex to implement than Mode 1. It should be noted that readings from temperature and humidity gages are ignored in Mode 2 as high-frequency sampling of their data yields no useful physical information.

### 2.4.2. Crack Extension Monitoring

Though ACM systems focus on measuring changes in the width of the cracks under the assumption that crack extension cannot occur without crack widening, crack propagation sensors allow for direct measurement of the extension of a crack. Crack propagation sensors are generally made up of a series of metallic traces of known electrical resistance. A sensor can be affixed to the tip of a crack such that if the crack propagates, one or more of the metallic traces will break which will change the resistance measured across the terminals of the sensor. Figure 2.9 shows how such a sensor might function.

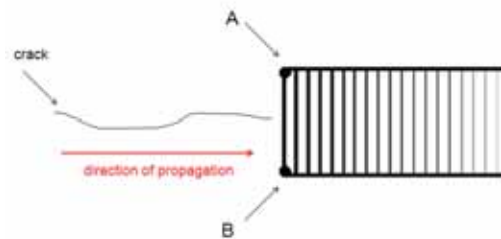


**Figure 2.9:** Resistance measured between points A and B decreases as crack propagates

This type of sensor has advantages and disadvantages over the crack width measurement strategy of measuring crack activity. The obvious advantage of such a crack propagation sensor is that it will directly measure the crack behavior in which a homeowner is interested: the extension of a crack. A traditional crack propagation sensor is also typically an order of magnitude less costly than a typical crack width measurement sensor described in Section 2.3.1 above.

#### 2.4.2.1. *Traditional Crack Propagation Patterns*

Traditional crack propagation gages are designed to be chemically bonded to a substrate that has crack or is predicted to crack. The gages, shown in Figure 2.10 are made up of a high-endurance K-alloy foil grid backed by a glass-fiber-reinforced epoxy matrix (Vishay Intertechnology, Inc., 2008). Though these gages are proven to be useful in the measurement of cracking in materials such as steel or ceramic, their usefulness for measuring cracks in residential structures is diminished due to the fact that the glass-fiber-reinforced epoxy backing is much stronger than the drywall or plaster to which it would be affixed as part of an ACM system (Marron, 2010). Additionally, it is not difficult to imagine that a propagating crack may alter its direction before breaking the rungs of the crack propagation gage which would render the gage ineffective. Chapter 4 describes a method in which these sensors can be applied to steel bridges to track progression of existing cracks.

#### 2.4.2.2. *Custom Crack Propagation Patterns*

To overcome the two main difficulties inherent in using a commercially available crack propagation sensor for either an ACM system or a system designed to measure cracks in steel, a new type of crack propagation sensor is proposed in this thesis: a custom crack propagation pattern. This pattern, detailed in Chapter 4, can be made in whatever shape is necessary for capturing any possible direction of crack growth. It also uses the wall (or steel) to which it is mounted as its substrate so the problem of mismatched material strengths between the substrate and the sensor backing is eliminated.

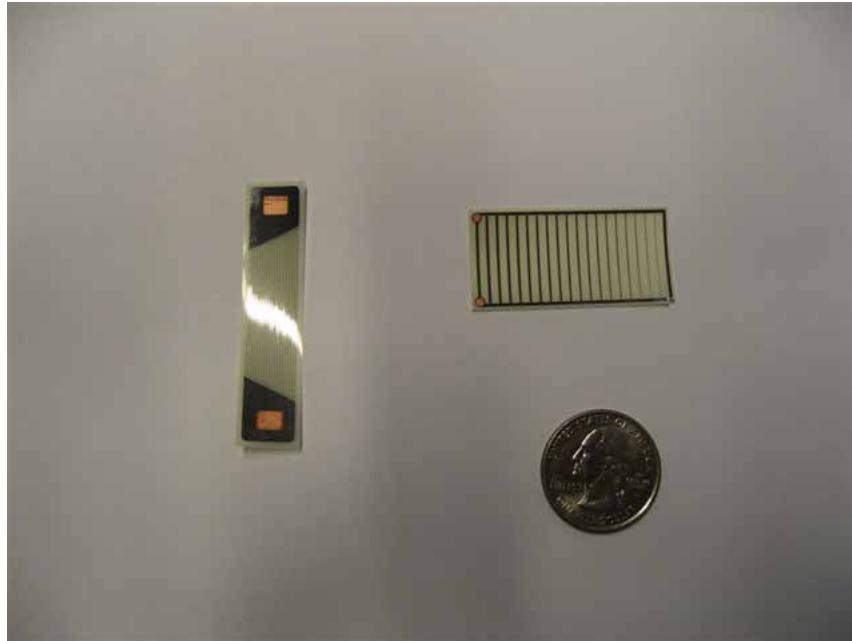


**Figure 2.10:** Two types of commercially available crack propagation patterns shown with a quarter for scale

## 2.5. Examples of the output of an ACM system

The following images are taken from the live Web interface of an ACM system. Figure 2.11a shows the long-term correlation between humidity and crack displacement as captured with Mode 1 recording. Figure 2.11b shows typically recorded crack displacement waveforms during a dynamically triggered event as captured with Mode 2 recording.

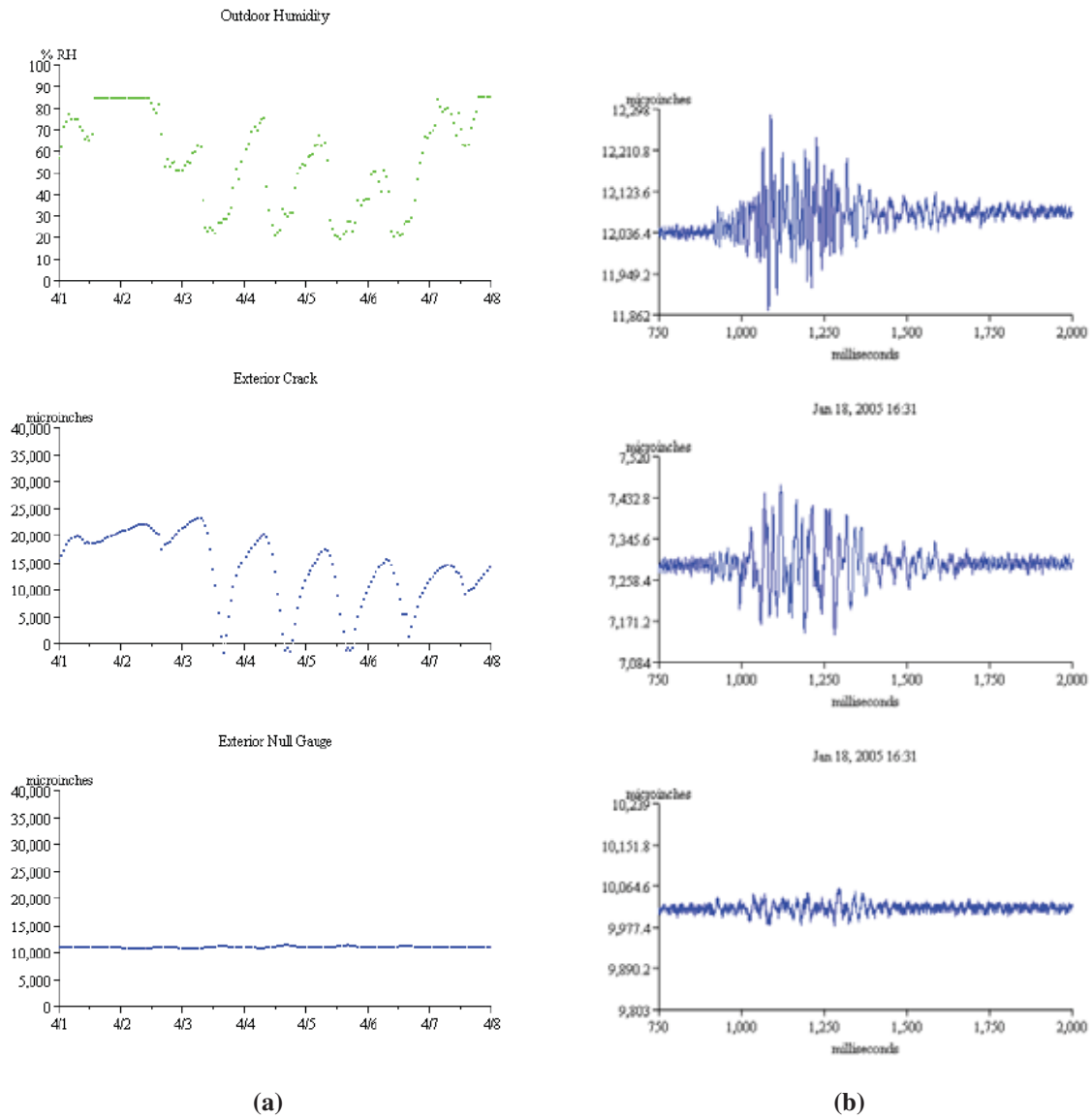


**Figure 2.11:** Screen shots of (a) long-term correlation of crack width and humidity from **Mode 1** recording (b) crack displacement waveforms from **Mode 2** recording

## 2.6. Chapter Conclusion

This chapter has shown that for the purposes of monitoring crack activity as caused by vibration, mining, or weather, different types of sensors may be used to measure crack displacement. Choice of sensor type is determined by constraints on the availability of power, precision excitation, and physical space for sensor installation. By combining Mode 1 and Mode 2 recording, the effects of long-term changes in temperature and humidity can be compared to the dynamic effects of vibration and household activity. Both modes are essential to the true quantification of the effects of vibration on residential structures.

This chapter has also shown that direct monitoring of crack elongation or propagation does not require as sophisticated a data logger as does the monitoring of crack width changes with respect to vibration, though it does require specialized crack propagation patterns.

Regardless of the chosen sensor and the makeup of a crack measurement system, the installation of any wired system is labor-intensive and expensive: high-quality instrument wires must be run through the monitored structure: typically an occupied residence in the case of ACM and an active highway bridge in the case of ACPS. The need to minimize installation time, cut down on the cost and labor of installing wires, and minimize intrusiveness to the user(s) of a structure over the course of the monitoring project clearly demonstrates the utility of wireless monitoring systems. Chapters 3 and 4 will examine the construction of such systems.

## CHAPTER 3

# Techniques for Wireless Autonomous Crack Monitoring

### 3.1. Chapter Introduction

The ever decreasing size and increasing performance of computer technology suggest that an expensive, labor-intensive, and residentially intrusive wired Autonomous Crack Monitoring (ACM) system may be replaced by a similarly capable, easier to install, yet less expensive and intrusive wireless ACM system based on existing, commercially available wireless sensor networks. The implementation of a wireless ACM system with all the functions of a standard ACM system (i.e. Mode 1 and Mode 2 recording capability), no requirement for an on-site personal computer for system operation, a small enough footprint such that it will not disturb the resident of the instrumented structure, a sensor suite that can be operated with minimal power use, and system operation for at least six months without a battery change or any other human intervention, is fraught obvious and non-obvious challenges.

#### 3.1.1. Wireless Sensor Networks

Wireless sensor networks (WSNs) consist of a network of nodes, or “motes,” that communicate with one or more base stations via radio links. Most WSNs transmit in the low-power, license-free ISM (industrial, scientific, and medical) band, typically between 420 and 450 megahertz. In general, motes are designed to be low-cost, relatively interchangeable, and in many cases, redundantly deployed.

#### 3.1.1.1. *Motes*

Each mote is made up of a processing unit, a radio transceiver, a power unit, and a sensing unit. The two main components within the sensing unit are an analog-digital converter (ADC) and software-switchable power sources to activate and deactivate sensors. The sensors, ADCs, and switchable power supplies are either integral to the mote itself or added by means of an external sensor board that is physically attached to the mote. In none of the WSNs described in this thesis does any data processing occur on the motes themselves – all data is transmitted back to the base station before any data processing might occur. For more detail on motes and their components, see Ozer (2005). In the remainder of this document, a “mote” shall refer to the actual processor/radio board device while a “node” shall refer to the combination of mote, sensor board(s) external to the mote, and sensors deployed at a specific location in a structure.

#### 3.1.1.2. *Base Station*

At minimum, the base station is responsible for receiving by radio all of the transmissions that originate from within the wireless sensor network then relaying this data through some other communication mechanism back to interested parties. In most cases, though, the base station of a WSN contains the majority of intelligence of the system. More sophisticated base stations have provisions for on-board data storage and analysis and provision of a control interface by which a remote user might reconfigure the WSN after it has been deployed in the field. Some base stations provide a Web-based interface for control of the network, provide the ability to process and analyze data, and make available the ability to send alerts to interested parties. Some WSN systems require this base station to be connected to a personal computer; others support direct connection to the Internet.

### 3.1.1.3. *Wireless Communication*

Each mote is equipped with a radio that allows it to send and receive data to and from both other motes and the base station. In the simplest possible WSN, each mote transmits its data directly to the base station whenever data is available. If site conditions change such that radio communication between the base station and the mote is no longer possible, that mote's data is no longer available.

More sophisticated WSNs make use of *multi-hop* or *mesh networking* with *self-healing* capabilities. In this scenario, each mote has the capability of transmitting and receiving data to and from any mote within its radio range. This ability not only extends the physical range of the network (i.e. motes can be deployed beyond the transmission distance to the base station) but provides alternate paths for the data to travel should an intermediary mote become damaged or deplete its energy source. Figure 3.1 shows an example of a WSN with multi-hop capabilities.

This chapter examines both simple and sophisticated base stations, rudimentary and advanced power management strategies, and single and multi-hop network topologies.

### **3.1.2. Challenges of Removing the Wires from ACM**

The first and most obvious challenge to the creation of a wireless ACM system is power – more specifically: the fact that each mote is powered by a battery pack, sometimes supplemented with a solar panel, and not by direct connection to household power lines. Because a main motivator in the transition from wired to wireless ACM is to minimize disruption to the resident of the instrumented structure, frequent visits to change batteries or the use of large, high-capacity battery packs, are unacceptable strategies to extend system longevity. Instead, the design of a wireless



**Figure 3.1:** Example of a multi-hop network: green lines represent reliable radio links between motes, after Crossbow Technology, Inc. (2009b)

ACM system's hardware and software must prioritize minimization of size but maximization of system longevity using an energy source no larger than 2-3 standard AA batteries.

The second and relatively obvious challenge is that due to the fact that motes run on batteries, it is impractical to continuously buffer data in order to monitor the readings from sensors *before* a significant sensor reading triggers the system to record at a high frequency. Since there is no way to know in advance when such a sensor reading will be needed, it becomes necessary to continuously check the data against a known threshold. This continuous sample-compare-buffer-discard cycle utilized by traditional ACM systems is impractical for any system based

on a WSN since WSNs achieve their longevity by “sleeping,” or operating in an extremely low-power mode, for the large majority of their deployed life. In this sleeping mode, sensors cannot be read, radio signals cannot be sent or received, and each mote is powered off with the exception of a low-power timer that instructs it when to “wake up,” or resume a fully-functional operating state, in order to take its next scheduled reading.

The third and somewhat less obvious challenge inherent to the transition to wireless ACM is quality of the sensor excitation and analog-to-digital conversion capabilities of the motes. In a state-of-the-art wired ACM system, power is supplied to the sensors by an independent  $\pm 15$  V DC regulated power supply capable of supplying 0.3 A of regulated current and powered by standard 110 V AC (SOLA HD, 2009). Analog-to-digital conversion in the state-of-the-art wired ACM system is performed by a 16-bit analog-to-digital converter (ADC) with software-configurable gain to allow for maximum use of the 16-bit resolution over the expected output range of the sensor (SoMat, Inc., 2010). The wireless ACM systems examined in this chapter have far less sophisticated power supplies and ADC units; extra effort is required to achieve the repeatable, high-precision, high-frequency measurements required by ACM. In some cases, a single WSN cannot meet all of these requirements in addition to the requirement of a six-month operational lifetime with no human interaction.

Additionally, physical robustness of a wireless ACM system is not guaranteed – it depends completely on the manufacturer and model of the WSN upon which the wireless ACM system is built. In the case of certain types of WSNs, the end-user is responsible for fabricating an enclosure to protect the delicate electronics of the system components.

Finally, and perhaps most importantly, few commercially available WSNs are designed for end-user deployment – especially end users who do not possess expertise in computer science

or computer engineering. The hardware that composes a wired ACM system relies far less upon the user to configure the internals of the system and instead allows a focus on exactly what is desired to measure and the exact mechanism of measurement.

This chapter examines the process of selecting a WSN for use in a wireless ACM system, selection of appropriate sensors for use with each type of WSN, challenges in configuration and deployment of the systems, and the fabrication of new hardware and software techniques to enable a wireless ACM system to more closely duplicate the functionality of its wired counterpart.

### **3.2. Crack Displacement Sensor of Choice**

Regardless of the which WSN is to be used as a wireless ACM system, changes in crack width must be measured. Section 2.3.1 enumerates three different sensors that have been qualified by previous researchers to adequately measure expected crack changes. Table 2.1 summarizes the differences between the operating characteristics of the three candidate sensors for a wireless ACM system.

The LVDT has the advantage in terms of sensor cost, and in a situation in which out-of-plane motion is not expected, the LVDT shows promise for the wireless ACM application, especially since casual observation does not reveal a significant difference in power draw between the three sensors. The eddy current gage has a clear advantage in footprint size and crack motion flexibility, and it even seems to draw less current than the LVDT. Closer inspection of the sensor characteristics, however, reveals that the string potentiometer emerges as the clear choice for a wireless ACM application.

The string potentiometer's maximum power draw is 7 mA at 35 V DC. However, since the potentiometer is a purely resistive ratiometric device, any voltage up to the manufacturer-specified maximum of 35 V DC (Firstmark Controls, 2010) may be used to excite the sensor. Thus, by using a lower voltage to power the device, the power consumption of the device can be lowered significantly below that of the LVDT or the eddy current sensor.

Even if one concedes that since ACM only measures the width of a crack once per hour, or even for a fifteen second dynamic window, the sensor will be powered off most of the time and thus not have a significant impact on overall power draw, one must consider the warm-up time of each device. The LVDT and eddy current gages both use complex and temperature-dependant signal conditioning electronics to achieve their specified precision. This means that immediately after the sensors are powered on, one must wait a certain amount of time before an accurate reading can be taken. For the LVDT, this time is an average of 2 minutes (Puccio, 2010) while the eddy current sensor can take up to 30 minutes (Speckman, 2010) to achieve its specified precision. Though the measurement of crack width takes only a fraction of a second, the warm-up times of the LVDT and eddy current sensors would draw several orders of magnitude more power than would a string potentiometer that requires no warm-up time to take a precise measurement. Thus, the string potentiometer is the clear choice for measurements of crack width in wireless ACM applications.

The string potentiometer, pictured in Figure 3.2, is a three-wire ratiometric displacement measurement sensor with a stroke length of 1.5 inches. At a position of zero inches (i.e. when the potentiometer cable is fully retracted into its housing), the resistance measured between the white output lead and black ground lead is  $0\Omega$  and the resistance measured between the white output lead and red DC input lead is  $5000\Omega$ . At any cable position between fully-retracted and

fully-extended, the resistance measured between the white and black leads is proportional to the distance the cable has been pulled out of its housing. To operate the sensor, a known DC voltage is placed across the red and black leads and the voltage between the white and black leads is measured. The distance of cable extension is the ratio of output voltage to the input voltage times 1.5 inches. Technical specifications of the string potentiometer may be found in Appendix B.2.

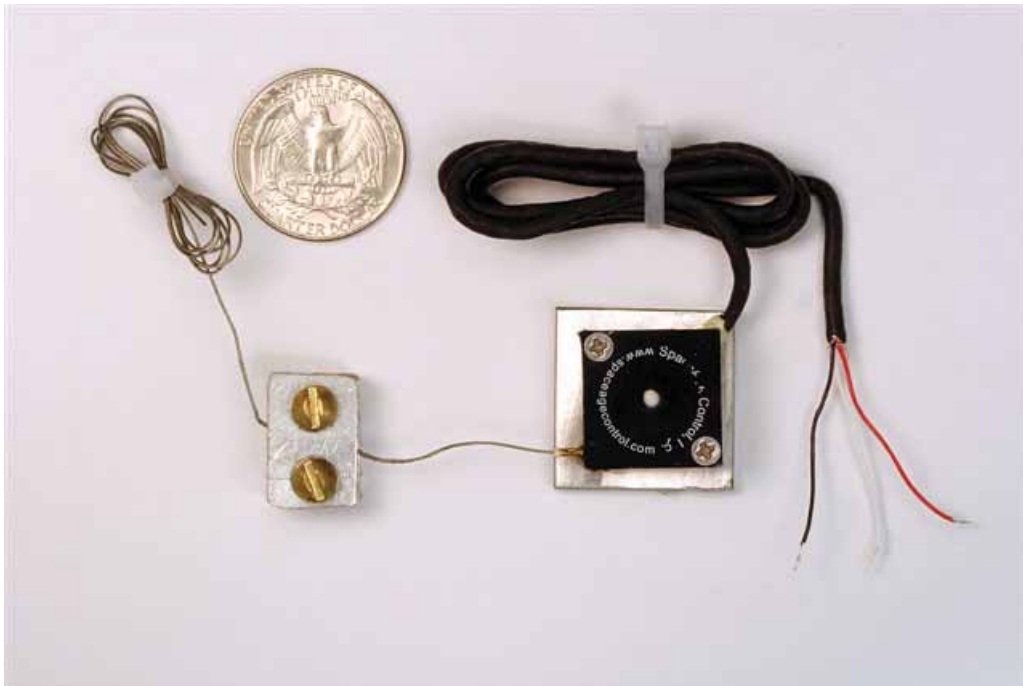


**Figure 3.2:** Photograph of a string potentiometer with quarter for scale, after Jevtic et al. (2007b)

Installation of the string potentiometer is accomplished using two simply fabricated aluminum mounting accessories. The first, a square aluminum plate with countersunk holes, is screwed into the bottom of the string potentiometer then glued to a wall on one side of a crack. The plate prevents epoxy from entering the housing of the potentiometer. It also provides a

uniform gluing surface to ensure a robust installation. The second part of the mounting fixture, a small aluminum block with two drilled and tapped holes to accept a very thin aluminum plate with two corresponding holes, is glued to the opposite side of the crack from the potentiometer and grasps the measurement string. The block is sized such that the string remains parallel to the wall. This type of fixture is preferable to a hook or a post because there is no possibility for the string to slip or turn. Figure 3.3 shows a fully mounted string potentiometer.



**Figure 3.3:** Photograph of a fully mounted string potentiometer, after Ozer (2005)

### 3.3. WSN Selection

The WSN platform selected for the initial migration of ACM to the wireless domain was the MICA2 wireless sensor network manufactured and sold by Crossbow Technology Inc. and powered by TinyOS 1.x software. The MICA2 system's small size, flexible software, ability to operate without a PC on site, large user base, relatively low cost, and a catalog of add-on sensor

boards made it the ideal choice to begin to develop a wireless ACM system. Figure 3.4 shows a MICA2 mote with a quarter for scale.

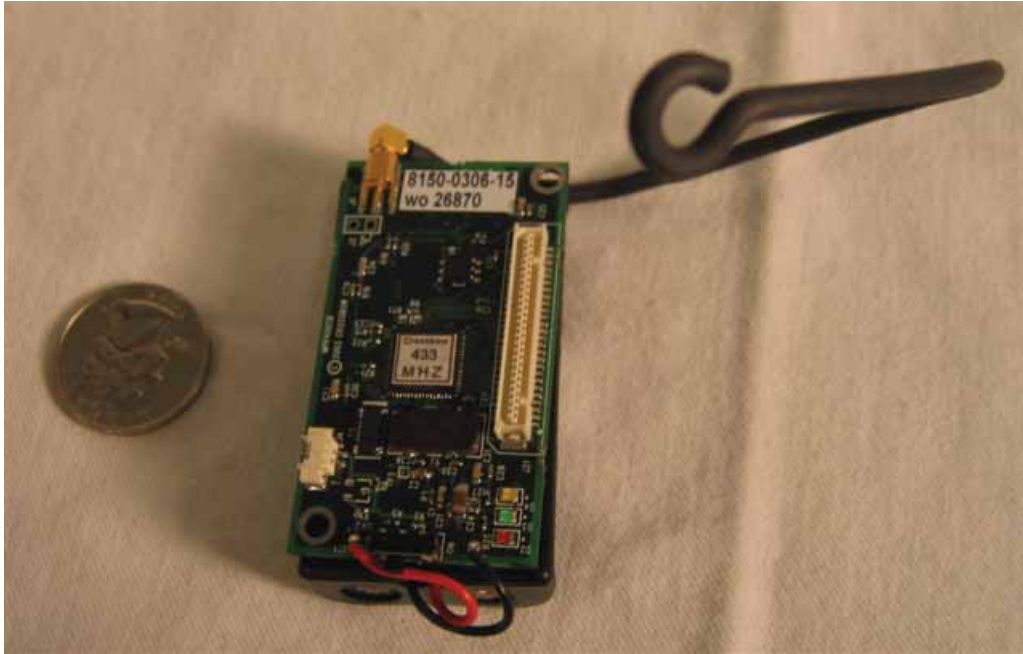


**Figure 3.4:** Photograph of a Crossbow MICA2 mote with quarter for scale

### 3.3.1. The Mote

The MICA2 mote, Crossbow model number MPR400CB “is a third generation mote module used for enabling low-power, wireless, sensor networks (Crossbow Technology, Inc., 2007a).” The MICA2 features an industry-standard ATmega128L low-power microcontroller which is powerful enough to run sensor applications while maintaining radio communication with the base station and other motes. It also features a 10-bit ADC and a 51-pin connector and support for several digital communication protocols for connecting to other Crossbow- and third-party-manufactured sensor boards. Finally, it features a multi-channel radio with a nominal 500-foot

line-of-sight transmission range. The MICA2 arrives from the manufacturer configured to use two standard AA-cell batteries.

The MICA2 mote is designed to operate with a Crossbow MIB510CA Serial Gateway. This device, pictured in Figure 3.5 serves the dual purposes of acting as a programming board to load software onto a MICA2 and acting as part of a base station that will, when paired with an appropriately-programmed MICA2 mote, receive data from the wireless network and relay them via RS-232 to either a local embedded field computer or directly over the Internet back to the lab.



**Figure 3.5:** Photograph of a Crossbow MIB510CA serial gateway with MICA2 (without batteries) installed, after Ozer (2005)

### 3.3.2. Sensor Board Selection

Though the MICA2 mote itself features an internal 10-bit ADC, it has no ability to measure temperature or humidity, nor does it have a convenient way to physically wire a sensor into its ADC;

note that Figure 3.4 shows no screw terminals or ADC connectors of any kind. Additionally, the use of a 10-bit ADC on a sensor with a 1.5 inch full-scale range yields a maximum resolution of  $1465 \mu\text{in}$  – far too coarse for the expected crack width changes outlined in Section 2.2. The MDA300CA sensor board solves all of these problems.

The MDA300CA, pictured in Figure 3.6, is a general-purpose measurement device that can be integrated with a MICA2 mote. It is designed to be used in applications that require low-frequency measurements for agricultural monitoring and environmental controls. The MDA300CA adds significant sensor functionality to the MICA2 board, such as a higher resolution ADC and precision sensor excitation.



**Figure 3.6:** Photograph of a Crossbow MDA300 with quarter for scale, after Dowding et al. (2007)

In addition to its ability to measure ambient temperature and humidity without any additional hardware, the MDA300CA provides two additional capabilities:

### 3.3.2.1. *Precision Sensor Excitation*

Because the string potentiometer is a ratiometric sensor, its output is linearly proportional to its input at any given instant. In order to record a precise and accurate reading from such a sensor, the data logger must either record simultaneously the input to and the output from the potentiometer or provide as an input to the potentiometer a precisely regulated voltage that is guaranteed to be constant at a known value whenever the sensor is read. The MDA300CA does the latter by providing a 2.5 V DC regulated excitation voltage to the potentiometer.

### 3.3.2.2. *Precision Differential Channels with 12-bit ADC*

The MDA300CA has several different channels with which it can read analog signals with 12-bit resolution – four times more resolution than the MICA2's internal ADC. Four of the MDA300CA's channels are precision differential channels with a sensor front-end gain of 100 which yields an input range of  $\pm 12.5$  mV with a constant programmable offset such that a sensor with a minimum output of 0 V DC can still take advantage of the full 25 mV range. With a 2.5 volt precision excitation and the front-end gain, the MDA300CA is capable of resolving 0.0061 millivolts, or approximately 3.7  $\mu\text{in}$  of displacement using the string potentiometer. This is within the specification laid out in Section 2.2. The active sensor range of the potentiometer in the 25 mV window is 15,000  $\mu\text{in}$  – 30% of the range of the eddy current gages used in the traditional wired ACM systems (see Table 2.1) but still acceptable for ACM (Ozer, 2005). It is important to note that although the MDA300CA is theoretically capable of resolving 3.7  $\mu\text{in}$  of movement from a string potentiometer, this assumes an environment free of all electromagnetic interference and ambient vibration.

### **3.3.3. Software and Power Management**

The MICA2 and MDA300CA, and MIB510CA compose the hardware of the wireless sensor network. Specialized software runs on each individual MICA2 mote to control sensing, manage transmission of data, maintain the connectivity of the mesh network if necessary, and regulate power consumption to maximize system longevity. When software alone cannot meet all system design specifications, hardware solutions can be employed, as in Section 3.3.6, to make the wireless ACM system more useful.

### **3.3.4. MICA2-Based Wireless ACM Version 1**

The first iteration of the wireless ACM system had a modest design goal: Implement Mode 1 data recording while maximizing system longevity. Version 1 did not attempt to implement multi-hop mesh networking or sophisticated power management. It was deployed in a occupied single-family home near an active limestone quarry. A traditional wired ACM system was already installed in the home and the deployment location (an already-monitored crack in the ceiling) was chosen to corroborate the wireless sensor readings with those taken with the established wired system.

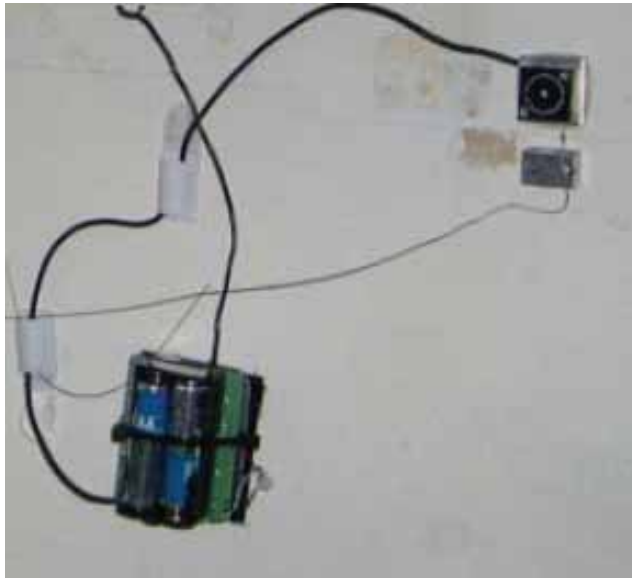
#### *3.3.4.1. Hardware*

Version 1 consisted of two MICA2 motes each equipped with an MDA300CA sensor board and a single string potentiometer. An aluminum plate was attached with screws to the bottom of each MDA300CA so that the entire mote could be affixed to the ceiling using hook-and-loop fastener, as shown in Figure 3.7b, instead of epoxy. A nylon cable tie secured each MICA2 to the MDA300CA because the motes were not designed to be inverted and the 51-pin connector

could not support the weight of a MICA2 and two AA batteries. The string potentiometer and its cable clamp were affixed to the ceiling using the quick-setting epoxy used by Siebert (2000). The MIB510CA with another MICA2 mote installed were located only a few feet away in a nearby closet and attached directly to the Internet via a commercially available serial-to-Internet Protocol gateway.



(a)



(b)

**Figure 3.7:** Photographs of Version 1 of the MICA2-based wireless ACM system, after Ozer (2005): (a) base station (in closet) (b) node (on ceiling monitoring crack)

#### 3.3.4.2. *Software*

The application software written for Version 1 of the MICA2-based wireless ACM system was known as *MDA300Logger*. The application itself and the utility applications and libraries required to make it operational are based on the example application *SenseLightToLog* included with the MICA2 development kit from Crossbow. The separate publication Kotowsky (2010) contains all of the modified source code that was used to change *SenseLightToLog*.

#### 3.3.4.3. *Operation*

The *MDA300Logger* application directed each mote onto which it was installed to act as an independent data logger that could be instructed to start and stop logging, change sampling rate, and transmit data. A single MICA2 mote was programmed with application *TOSBase* (an application provided by the manufacturer and used without modification) and inserted into the MIB510CA base station. Instead of connecting the base station directly to a PC, the base station was connected to a serial-to-Internet Protocol gateway that was then attached to the test house resident's consumer-grade cable modem. Using that gateway, a PC in the lab could issue commands directly to each mote over the Internet.

Once the motes were installed and the Internet connection established, the user would simply use the PC to connect to each mote and instruct it to begin logging at an arbitrary interval (e.g. once per hour). To conserve power, the *MDA300Logger* application would instruct the mote to shut down five minutes after it completed taking its data readings. This five minute period of full power would give the remote user a window in which he could retrieve a mote's data, change a mote's sampling interval, or command the mote to stop logging. The user had to

maintain a careful record of when each mote was started and stopped such that it would know exactly when the motes would be powered on and available to respond to commands.

An additional piece of software, the *XSensorMDA300* software package included with the development kit, was used to center the string potentiometer. An extra MICA2 mote would be programmed with this calibration software and inserted into the MDA300CA already mounted near the crack. When activated, this calibration mote would transmit its readings several times per second so a PC plugged into the base station could view the real-time output of the string potentiometer. With this live display in hand, the user could then center the string potentiometer in the middle of its range, tighten down the screws, and replace the calibration mote with a mote programmed with *MDA300Logger*.

#### 3.3.4.4. *Deployment in Test Structure*

Ozer (2005) performed detailed analysis of the data that was collected using Version 1 of the wireless ACM system. His work concluded that for during its entire operational period, lasting from November 18<sup>th</sup>, 2004 through January 16<sup>th</sup>, 2005, the wireless ACM system based on *MDA300Logger* performed similarly to a wired ACM system monitoring the same crack over the same time period. Figure 3.8 shows that both systems measured the same general trends in temperature and crack displacement over the two-month period.

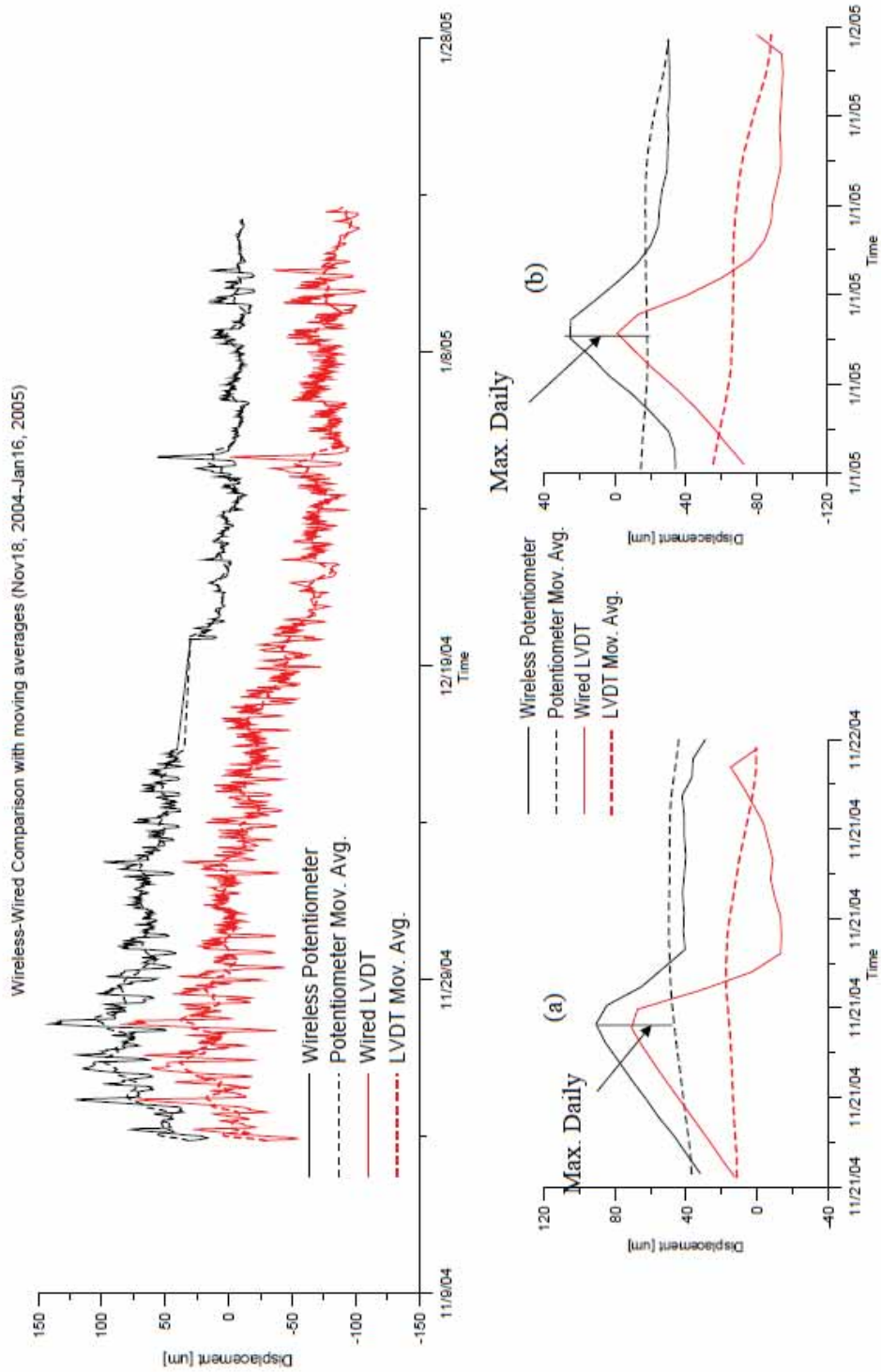


**Figure 3.8:** Temperature and crack displacement measurements by wireless and wired ACM systems in test house over two month period, after Ozer (2005)

From November 2004 through January 2005, the system took data once per hour. Because of the provision of the communication window for the issuance of new commands, each mote was fully powered-on and awaiting instructions for a full five minutes out of every hour – a duty cycle of just over 8%. It is no surprise, then, that the system consumed all of its available battery power in only one month (the batteries were changed in late December of 2004). Figure 3.9 shows the decline of the alkaline AA battery voltage over the time of deployment until it was no longer sufficient to support logging and data collection halted. More detailed analysis of power consumption can be found in Ozer (2005).

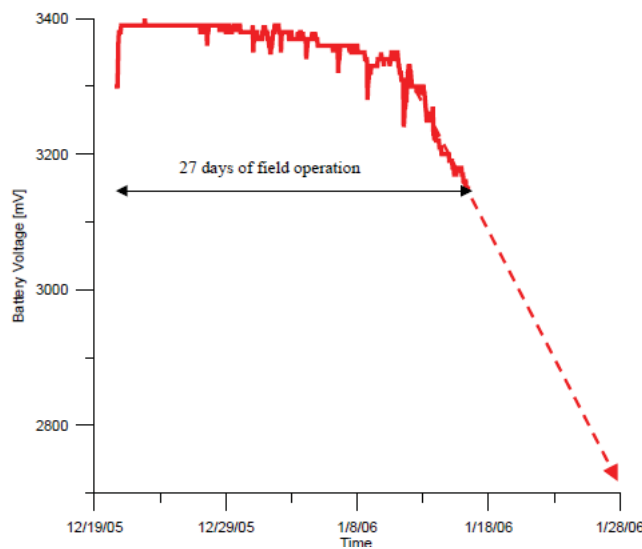


**Figure 3.9:** Alkaline battery voltage decline of a mote running *MDA300Logger*, after Ozer (2005)

#### 3.3.4.5. Results

Version 1 of the MICA2-based wireless ACM system was largely successful. It showed that the MICA2 combined with the MDA300CA and a string potentiometer could perform Mode 1 data

recording on par with a state-of-the-art wired ACM system. In spite of these positive results, however, several improvements would still be necessary to achieve a fully-functional Mode 1 system before a Mode 2 system could be developed:

- Power management must be improved: the minimum target deployment life of a wireless ACM system is six months but the *MDA300Logger* system lasted only one.
- Data retrieval is difficult: a user of *MDA300Logger* must remember when data was last uploaded to know when the next window will be available. Should the motes' clocks drift, the window might become difficult to find.
- The *MDA300Logger* system has no ability to route data through other motes. In complex or RF-noisy residential environments, or in structures where the base station may not be within radio range of all of the motes, multi-hop routing will be necessary.

### 3.3.5. MICA2-Based Wireless ACM Version 2 – *XMesh*

Based on the newly-released *XMesh*-enabled example applications developed by the WSN manufacturer, Version 2 made use of largely the same hardware but an entirely different software design to better implement Mode 1 logging. The design goal of Version 2 was to create wireless ACM system that:

- increased system operation lifetime from one month to at least six months
- provided a more convenient operator interface
- formed a self-healing mesh network to increase both the range and the reliability of the wireless ACM system

#### 3.3.5.1. *Hardware*

Like Version 1, Version 2 consisted of several MICA2 motes equipped with MDA300CA sensor boards and string potentiometers. The only hardware difference between Version 1 and Version 2 was the replacement of the base station, which in Version 1 simply relayed packets between a PC in the lab and the individual wireless motes, with an embedded computer. This computer, called a *Stargate Gateway* and sold by Crossbow, is a fully functional GNU/Linux computer featuring an Ethernet port, a CompactFlash slot, and a connector for a single MICA2 mote. Because the Stargate did not ship with an enclosure, it was mounted to a plastic board as shown in Figure 3.10. Technical specifications of the Stargate may be found in Appendix B.5.

Attached to household 110 V AC power, the Stargate and the mote that was attached to it were always powered-on and listening for data from the remote motes. The data was recorded to the CompactFlash card where it was stored until the Stargate automatically transmitted the



**Figure 3.10:** The Stargate Gateway mounted to a plastic board

data back to the lab via the house’s high-speed Internet connection and standard Internet file transfer protocols.

#### 3.3.5.2. *Software*

After the deployment and validation of Version 1 of the MICA2-based wireless ACM system, the WSN manufacturer released to the public a set of software libraries, *XMesh*, designed to simplify power and network management of their WSNs. WSN application software written using these software libraries automatically has the ability to create and maintain a self-healing, multi-hop mesh network of motes. The *XMesh* libraries also provide advanced power management of the sensor network as a whole to maximize system longevity.

The manufacturer also supplied a sample application, *XMDA300*, and a set of drivers for the *MDA300CA* to demonstrate its functionality. This example software and the supplied hardware drivers were modified to implement Mode 1 recording. Full source of all modified files can be

found in the separate publication Kotowsky (2010). It should be noted that the mote attached to the base station ran the same software as did all of the remote motes. The XMDA300 software, when installed on a mote with an identification number of zero, will automatically function as a base station mote.

The original XMDA300 application was obtained from the manufacturer's publicly accessible Concurrent Versions System repository in April of 2005. The majority of the modifications took place in the main application control code, *XMDA300M.nc*, as the general strategy of the application was changed. As written, the application would start the SamplerControl module, part of the MDA300CA driver software, and allow the driver to dictate the interval at which samples are taken. Because the available intervals were not long enough to implement Mode 1 recording, *XMDA300M.nc* was modified such that it has its own timer that starts and stops the SamplerControl module, thereby putting the MDA300CA into its lowest power state when not sampling.

The main application will start the MDA300CA, instruct it to get samples quickly, wait for one set of readings to be completed, send those readings up the network, then completely shut down the MDA300CA until the next sample should be read. If the MDA300CA driver itself were responsible for managing the interval timings, the mote would never enter its lowest power mode, severely limiting the operational lifetime. The application was built using the same development tool chain by which the original XMDA300 application was built. The software utilizes low-power listening mode, the second-lowest power mode that XMesh is able to provide (Crossbow Technology, Inc., 2007e).

To facilitate ease of installation, when the motes are first turned on, the first sixty readings are sent out once per minute. This allows the multi-hop mesh network to form (or fail to form)

within several minutes so that the installer has time to reconfigure the network if necessary. Without this modification, several hours would be required to determine whether a network layout would be functional.

#### *3.3.5.3. Analysis of Power Consumption*

To calculate the power draw of a mote using the ACM-modified version of XMDA300, a simple ammeter circuit was implemented by placing a 10-ohm resistor in series with the positive terminal of the battery on the mote. By reading the voltage across this resistor, the current draw of the mote can be calculated, recorded and compared to the total theoretical power capacity of a pair of lithium AA batteries in series: 3000 mAh at 3 V DC (Energizer Holdings (2010b); Appendix B.7). Figure 3.11 shows the current draw profile of a single mote.

The current readings were recorded at 10 hertz and averaged to determine the average current used by the mote during a period of 18 hours. The average current draw when the mote is sampling once per hour is 325  $\mu$ A. Since the total current capacity of the battery pack is 3000 mAh, the total estimated lifespan is estimated to be approximately 384 days, assuming the first hour of higher-frequency sampling is ignored.

#### *3.3.5.4. Deployment in Test Structure*

A deployment test of Version 2 of the MICA2-based wireless ACM system was conducted in a century-old historic house near the Northwestern campus. The objective of the test was to determine the degree of difficulty of the installation of the system, the effectiveness of the XMesh routing layer to create and maintain a low-power multi-hop network, and a projection for the true system deployment lifetime before batteries must be changed.

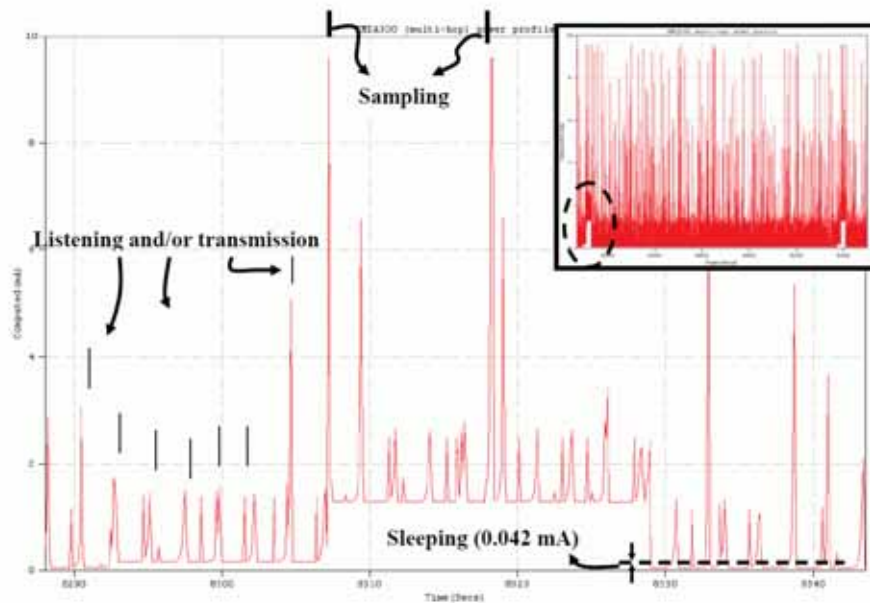


**Figure 3.11:** Current draw profile of a mote running the modified XMDA300 software for Mode 1 recording: the periodic sampling window is shown in the dashed oval in the inserted figure, demonstrating intermittent operation compared to ongoing operation; after Dowding et al. (2007)

Sensor nodes were deployed throughout two structures, as shown in Figure 3.12. In the main building, shown on the right, the Stargate base station was installed in the first floor office such that it could be connected to the building's high-speed Internet connection. Additional sensor nodes were placed on each floor of the main structure: one in the basement (Figure 3.13a), one on a sun porch on the second floor (Figure 3.13b), and one near a window in the third floor apartment (Figure 3.13c). To increase the likelihood that the XMesh routing protocol would form a multi-hop network, a node was placed on the second floor of the structure's detached garage (Figure 3.13d) some sixty feet away from the main building. Neither the sun porch nor the garage had any insulation or climate control systems to keep their temperatures from being affected by the outdoor temperature.

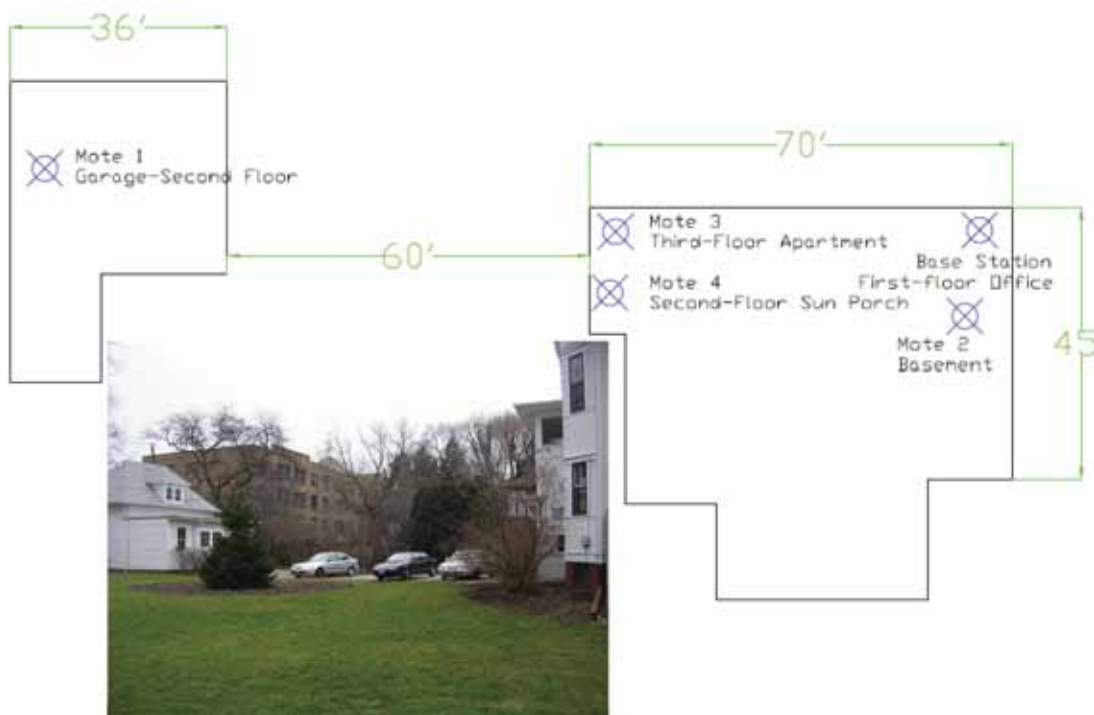


**Figure 3.12:** Distribution of sensor nodes throughout test structures

Because qualification of the string potentiometer had already been completed during the deployment of Version 1 in parallel with a wired ACM system, the node with the string potentiometer was not configured to measure a crack but instead was configured in the manner of a “donut qualification test” as described in Baillot (2004). In this this configuration, instead of measuring the change in width of a crack in a wall, the string potentiometer measures the thermal expansion and contraction of a plastic ring, or “donut,” as shown in Figure 3.15. The node measuring the donut was placed on the sun porch to ensure exposure to maximum temperature differences and therefore achieve the largest possible expansion and contraction of the donut.

Finally, alkaline batteries were used in the deployment test instead of lithium batteries. Although alkaline batteries have less capacity than lithium batteries, especially when operating in



**Figure 3.13:** MICA2-based wireless ACM Version 2 nodes located (a) in the basement, (b) on the sun porch, (c) in the apartment, and (d) over the garage

colder temperatures (Energizer Holdings, 2010a), their voltage output decreases over time such that the remaining battery life might be estimated. The voltage output of lithium batteries tends to stay steady over time then drop rapidly at the end of their working capacity (Energizer Holdings, 2010b). It was therefore expected that the total service life of the wireless sensor network might decrease from the ideal estimate of 384 days to 150-200 days.



**Figure 3.14:** A typical mote in a plastic container



**Figure 3.15:** A string potentiometer measuring the expansion and contraction of a plastic donut

### 3.3.5.5. Results

Version 2 of the MICA2-based wireless ACM system was deployed in the test structure from March 2006 through November 2006. Figure 3.16 shows a plot of the voltage of the batteries versus days of deployment. Mote 2, the mote deployed in the basement, depleted its batteries the most quickly after approximately 140 days of deployment. Mote 4, the mote deployed on the sun porch, fared next best with a lifetime of approximately 210 days. After approximately 250 days, when the system was removed from the test structure, neither Mote 1 nor Mote 3 had depleted its batteries.

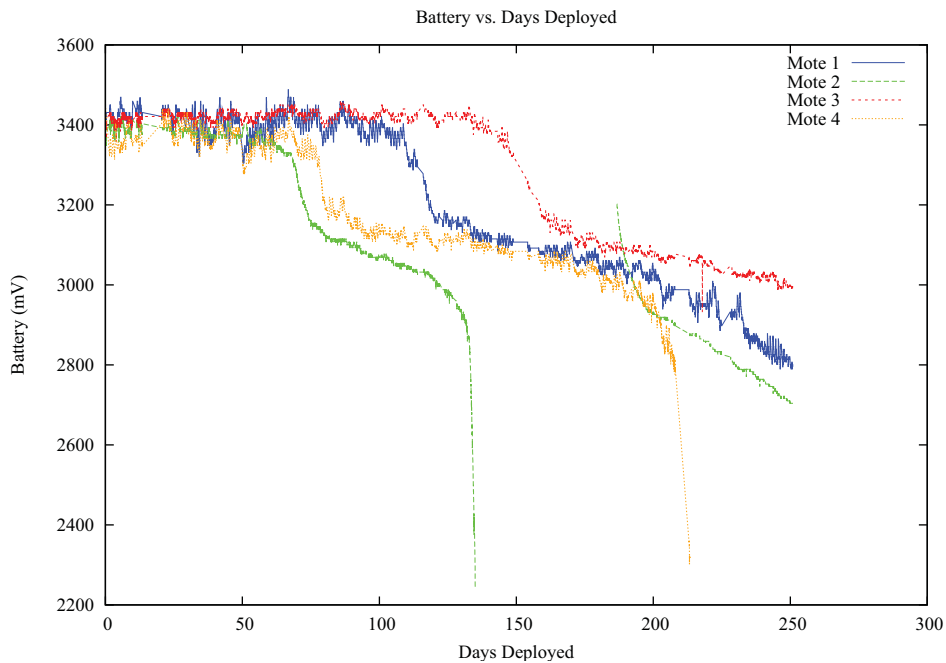


**Figure 3.16:** Plot of each mote's battery voltage versus time

Figure 3.17 compares the expansion and contraction of the donut with the ambient temperature. The mote with the donut was placed on the sun porch which was minimally insulated and had no climate control.

Figures 3.18 and 3.19 compare the ambient temperature and humidity, respectively, recorded by each mote over the deployment period. Motes 1 and 4 were deployed in environments highly influenced by outdoor temperature, Motes 2 and 3 were deployed in climate-controlled indoor spaces.

Along with the battery, temperature, humidity, and potentiometer readings it takes periodically, each mote also sends back the identity of its parent mote in the XMesh routing tree at the time the data point is taken. The first ACM packet, i.e. a packet that contains sensor data rather than XMesh status data, of the monitoring period came from Mote 2 at 12:00 AM on March 23<sup>rd</sup> 2006. Between that time and the time that the last data packet was received from Mote 2, the first mote to deplete its batteries, at 11:42 PM on August 4<sup>th</sup> 2006, 37,268 ACM packets were received by the base station. Of these packets, 71.8% were received directly from the mote that recorded the data – the packet “hopped” only once. Mote 1, the mote in the garage, sent most of its data back via either Mote 3 or Mote 4, however it transmitted 16.9% of its packets directly to the base station. Table 3.1 shows the detailed listing of motes’ parents between the start of monitoring and the depletion of the first mote’s batteries.

#### 3.3.5.6. *Discussion*

Figure 3.17 indicates that Mote 4 recorded expansion and contraction of the plastic donut that correlated closely with temperature changes. This demonstrates that the XMesh-based ACM software can perform Mode 1 recording.

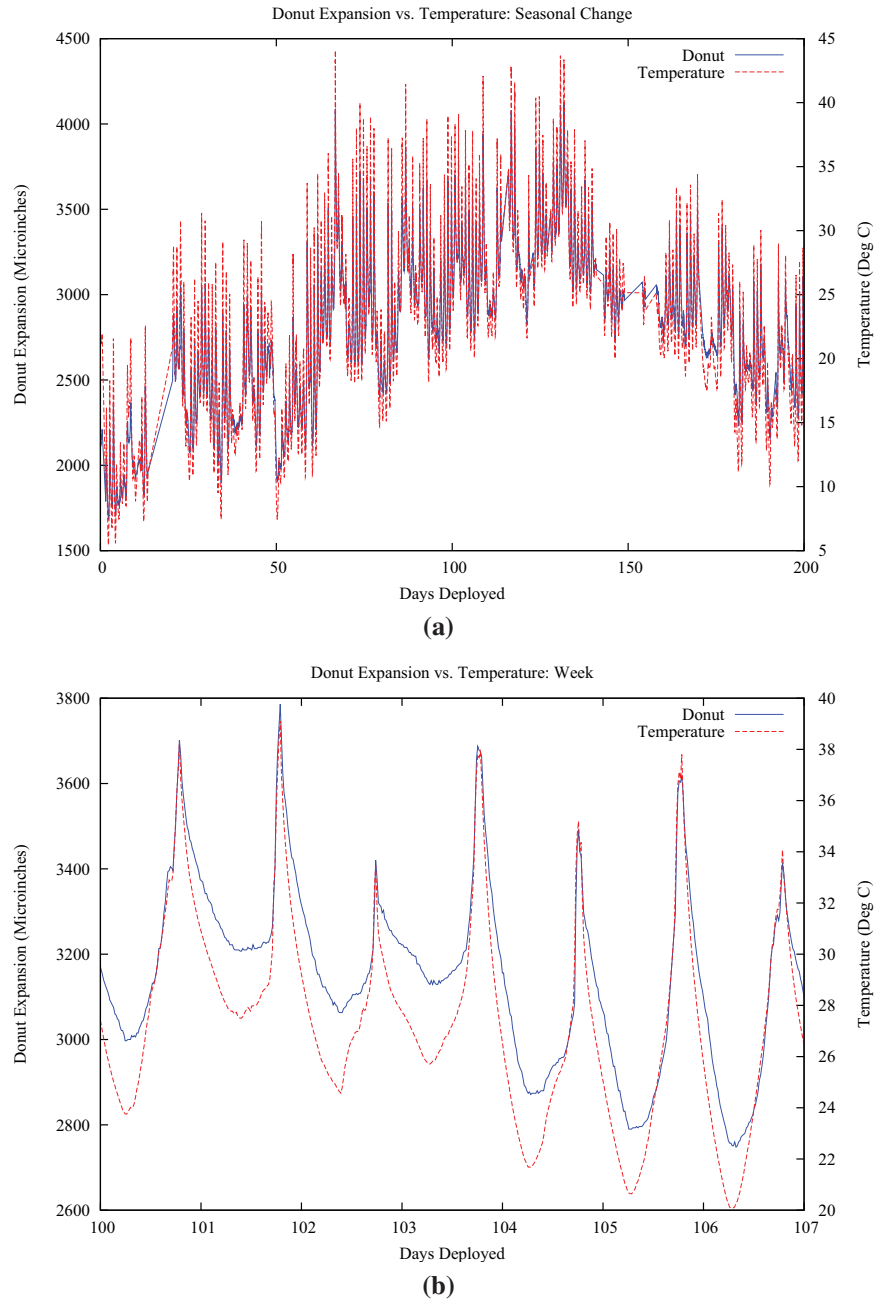


**Figure 3.17:** Plot of temperature versus donut expansion over a period of (a) 200 days and (b) one week

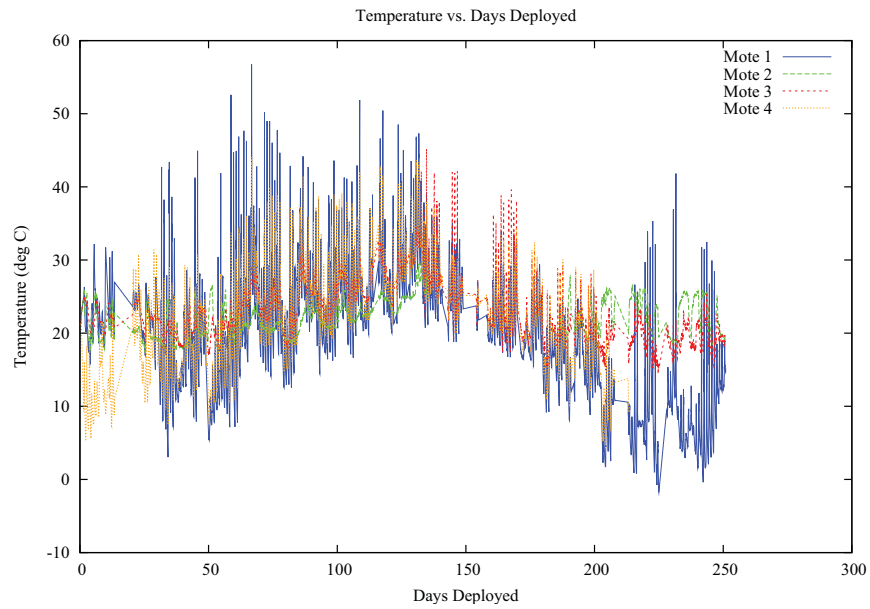


**Figure 3.18:** Plot of each Version 2 wireless ACM mote's temperature versus time

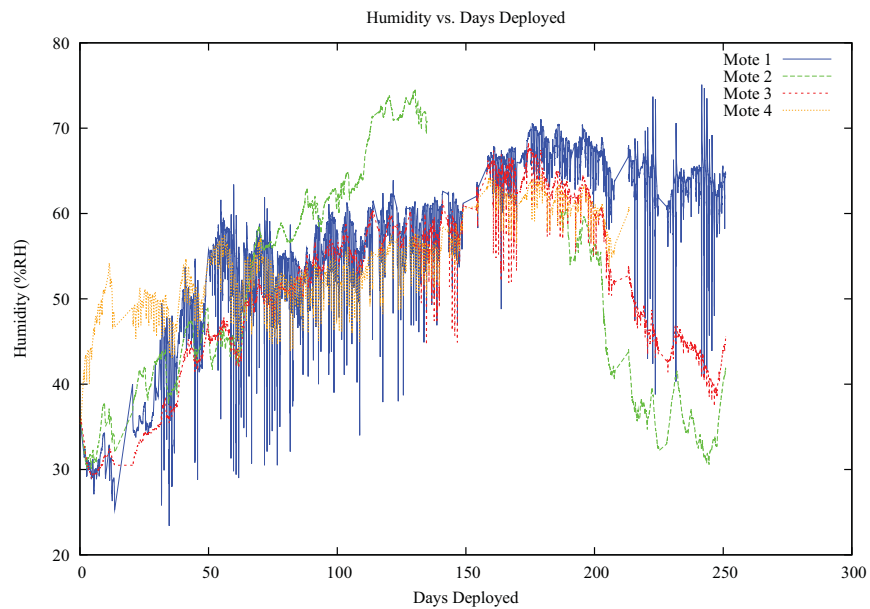


**Figure 3.19:** Plot of each Version 2 wireless ACM mote's humidity versus time

		Transmitting Mote				
		Mote 1	Mote 2	Mote 3	Mote 4	Total
Parent Mote	Base	1519 (17%)	8583 (91%)	8481 (90%)	8174 (87%)	26,757 (72%)
	Mote 1	–	854 (9%)	854 (9%)	853 (9%)	2561 (7%)
	Mote 2	37 ( $\approx 0\%$ )	–	102 (1%)	81 (1%)	220 (1%)
	Mote 3	5440 (61%)	4 ( $\approx 0\%$ )	–	309 (3%)	5753 (15%)
	Mote 4	1977 (22%)	0	0	–	1977 (5%)
Total		8973	9441	9437	9417	37,268

**Table 3.1:** Distribution of MICA2-based wireless ACM Version 2 packets over the parents to which they were sent

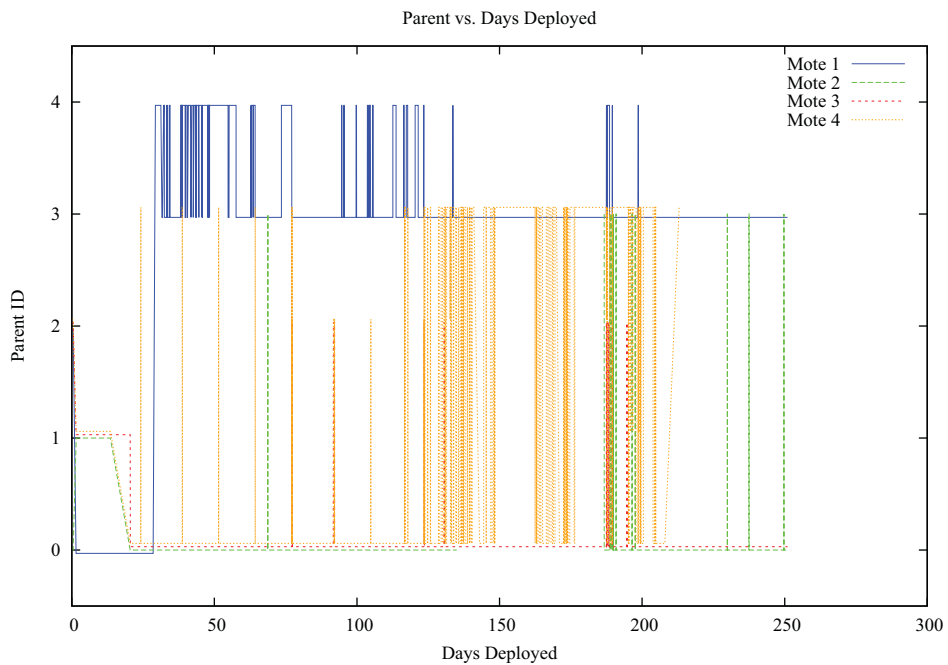


**Figure 3.20:** Plot of each Version 2 wireless ACM mote's parent versus time

Figure 3.16 shows that Mote 2, the mote in the basement directly underneath the room with the base station, depleted its battery more quickly than any other mote. Although Mote 2 is physically closer to the base station than any of the other motes, Table 3.1 reveals that only 1% of packets from other motes were transmitted first through Mote 2 on their way to the base station. Figure 3.20 also shows that Mote 2 did not act as a parent mote for longer than Mote 3 did. Because only 28% of the total ACM packets transmitted went through an intermediary mote on their way to the base station and because Mote 3, after having been a parent mote for 15 times more packet transmissions as Mote 2, did not deplete its batteries, it is unlikely that overuse as an intermediary mote caused Mote 3 to drain its batteries faster than the other motes.

Because alkaline batteries powered the motes, motes at lower temperatures would likely have less battery longevity than motes at higher temperatures. Figure 3.18 shows ambient temperatures recorded by each mote over the total deployment period. It is clear that the ambient temperatures recorded by Mote 2 were not higher or lower than the temperatures recorded by the other three motes, so it is unlikely that temperature played a role in the early battery depletion.

The only physical quantity that has any correlation with the early depletion of the batteries attached to Mote 3 is ambient relative humidity. Figure 3.19 shows that the ambient relative humidity measured in the basement of the main structure is significantly higher in the period between days 100 and 150 than that measured by the other motes. This increased humidity may have led to corrosion of the battery or the mote's battery terminals which would have adversely affected battery life. In future deployments, any negative effect of increased relative humidity could be negated by placing the motes in sealed enclosures and applying silicone to the battery terminals.

### 3.3.6. MICA2-Based Wireless ACM Version 3 – *Shake 'n Wake*

Mode 2 recording requires an ACM system to have the ability to determine whether a vibratory event has occurred and is of sufficient magnitude to be deemed an event of interest. Traditional wired ACM systems make this determination by sampling continuously the output of a geophone at a high frequency, typically one thousand times per second, and comparing the sampled value to a predetermined threshold value. Should the sampled value exceed the trigger threshold, the ACM system begins recording at one thousand samples per second from the geophone and all crack displacement sensors. Figure 3.21 shows this process.

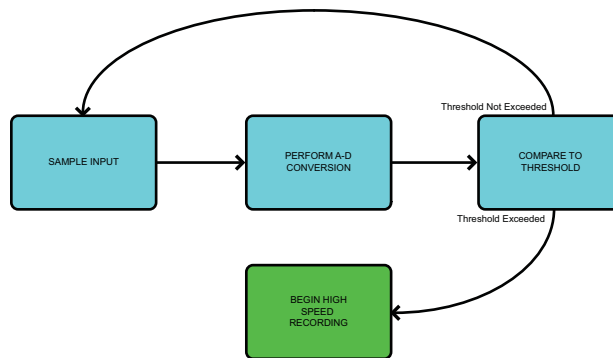


**Figure 3.21:** Traditional wired ACM system’s determination of threshold crossing

This process of continuous digital comparison, while possible to implement using a wireless sensor network, is not practical if the system is to operate for months without replacing or recharging its batteries. The continuous process of sampling, converting the signal to a digital value, and comparing that signal with a stored threshold value requires constant attention from

the control processor, signal conditioners, and analog-to-digital conversion circuitry. Implementation of Mode 2 recording with a WSN therefore required the design and fabrication of a new hardware device to process the input from a geophone and determine whether or not it has detected an event of interest, all without overtaxing the limited energy supply of a typical mote. This new hardware device, *Shake 'n Wake*, was conceived with the following design criteria:

- (1) It must not significantly increase the power consumption of a mote.
- (2) It must not contaminate the output signal of its attached sensor.
- (3) Its trigger threshold must be predictable and repeatable.
- (4) It must wake up the mote in time to record the highest amplitudes of the motion of interest.

Each of these criteria were proven to have been met by the Shake 'n Wake design. The results of the experiment to verify criterion 1 are detailed in Section 3.3.7.3. The rest of the results of the experimental verification are detailed in Appendix A.

#### 3.3.6.1. *Geophone Selection*

Though the Shake 'n Wake will operate with any type of sensor that produces a voltage output, a passive, or self-powered, sensor is necessary to realize practical power savings. A geophone, a passive sensor that produces output voltage using energy imparted to it by the very motion that it measures, is an ideal sensor to pair with the Shake 'n Wake. Two geophones were experimentally tested with the Shake 'n Wake: a GeoSpace GS-14-L3 28 Hz  $570\Omega$  geophone, pictured in Figure 3.22a and a GeoSpace HS-1-LT 4.5 Hz  $1250\Omega$  geophone, pictured in Figure 3.22b. Response spectra for these geophones are supplied as Appendices B.8 and B.9, respectively.

To maximize the signal-to-noise ratio of the output of the geophones, shunt resistors were not installed at the geophone output terminals.



**Figure 3.22:** (a) GeoSpace GS 14 L3 geophone (b) GeoSpace HS 1 LT 4.5 Hz geophone

McKenna (2002) showed that the dominant frequencies of the walls and ceilings in a wide variety of residential structures are between 8 and 15 hertz. The HS-1 geophone has a minimum defined non-shunted response frequency of approximately 1.5 hertz and is therefore well-suited to measuring the expected structural response. The GS-14 geophone, with a minimum defined non-shunted response frequency of 12 hertz, is not as well suited but its smaller size makes it more attractive for installation in an occupied residential structure.

#### 3.3.6.2. *Shake 'n Wake Design*

The Shake 'n Wake board, shown in Figure 3.23, implements the same modular design and is the same size as the commercially available sensor boards manufactured by Crossbow. It can therefore be attached to any MICA-based wireless sensor mote by way of its standard 51-pin

connector. Shake 'n Wake implements the hardware portion of the Lucid Dreaming strategy for event detection in energy constrained applications introduced by Jevtic et al. (2007a).

Because of the single-ended design of the low-power analog comparator on which the Shake 'n Wake hardware is based, the device cannot inspect both the positive and negative portions of any geophone output waveform using a single comparator. To avoid ignoring either half of an input waveform, the Shake 'n Wake board has two comparators and provides the user with two sensor input connectors: CN3 and CN4. The output leads from the geophone are wired simultaneously to CN3 and CN4, but the connectors have opposite polarities. This wiring ensures that both the positive and negative portions of the geophone output will be considered in determining whether the triggering threshold is crossed.

CN3 passes its input signal directly to a comparator that compares the positive portion of the input waveform to the user-specified threshold while ignoring the negative portion; CN4 passes the inversely polarized input signal to a second, identical comparator which compares the negative portion of the input waveform to the threshold while ignoring the positive portion. The same user-supplied threshold is applied to both signals. Either connector can be disabled using the jumper switches J1 and J2. Jumper J3 provides the ability to select the interrupt controller address on the MICA2's processor over which the Shake 'n Wake can communicate the occurrence of a threshold crossing, thus ensuring compatibility with other sensor boards that might also need to interrupt the mote's processor (Jevtic et al., 2007a).

The voltage input threshold at which the Shake 'n Wake board will wake up the mote's main control processor can be set in software by the user both before and after deployment of the mote. The variability of the trigger threshold is achieved by using a programmable potentiometer with a 32-position electronically reprogrammable wiper which is placed in series

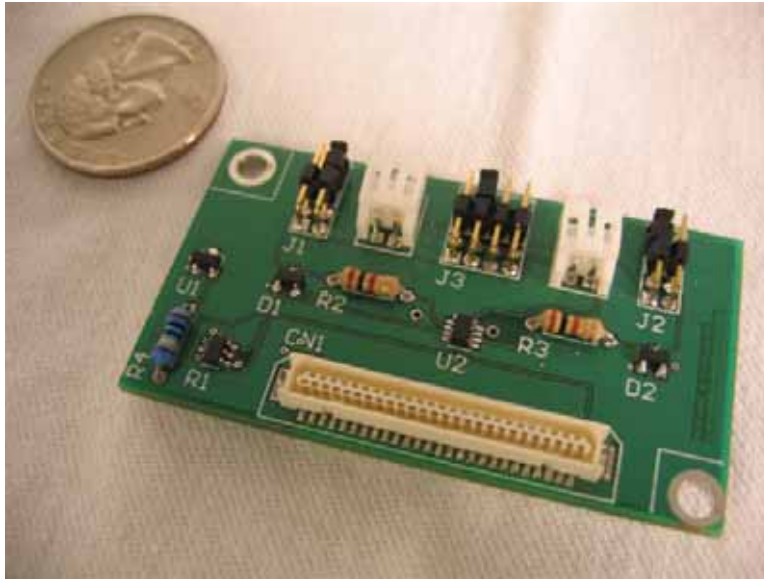


**Figure 3.23:** The Shake 'n Wake sensor board, after Jevtic et al. (2007a)

with a precision 1.263 V DC reference and a 1 M $\Omega$  precision resistor (Jevtic et al., 2007a). Figure 3.24 shows a simplified diagram of the voltage comparison circuitry.  $V_{comp}$ , the reference voltage to which the geophone output is compared, is directly determined by the position of the wiper,  $x$ , which is an integer between 0 and 31, inclusive. Thus, the threshold voltage to which the input voltage is compared is:

$$V_{comp} = 3.558 * x$$

where  $V_{comp}$  is the threshold voltage (in millivolts) and  $x$  is the setting (0-31) of the potentiometer.

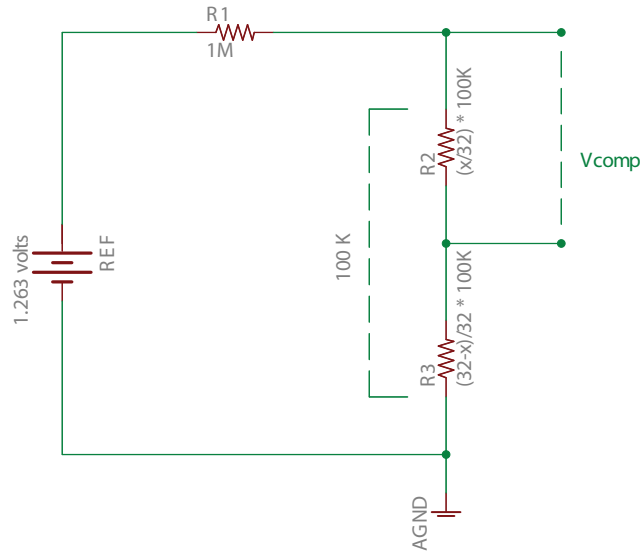


**Figure 3.24:** Simplified Shake 'n Wake reference circuit diagram

### 3.3.7. Hardware

Like Versions 1 and 2, Version 3 consisted of several MICA2 motes equipped with MDA300CA sensor boards, string potentiometers, and two AA batteries. Version 3 nodes also included a single Shake 'n Wake board and a geophone. Figure 3.25 shows a photograph of a fully-assembled Version 3 node.

The base station was significantly changed from the base station used with Version 2. First, the Stargate was replaced with a commercially available Moxa UC-7420 RISC-based GNU/Linux embedded computer. The Stargate was found to be too physically fragile for practical use without the creation of a fully-customized enclosure. The UC-7420 ships from the factory in a rugged metal enclosure designed for industrial use. Because the UC-7420 was not designed to connect to a mote via the mote's 51-pin connector, an MIB510CA serial interface

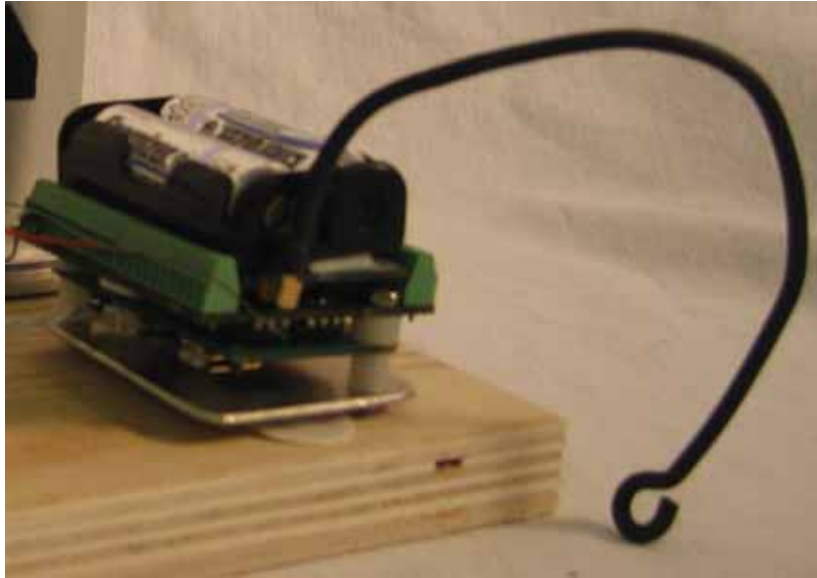


**Figure 3.25:** Photograph of a Version 3 wireless ACM node

board was used to connect the base mote to one of the serial ports on the UC-7420. Detailed specifications of the UC-7420 can be found in Appendix B.10.

Second, instead of relying on a locally available Internet connection to connect back to the laboratory, the Version 3 base station includes a 3G cellular router and antenna. The inclusion of the cellular router allows placement of the base station at any location in an instrumented structure as long as that location has available cellular signal and 110 V AC power. Figure 3.26 shows a photograph of the base station.

Physical installation of Version 3 of the MICA2-based wireless ACM system is an extension of Versions 1 and 2: the MICA2/MDA300CA/string potentiometer combination is mounted to the wall in the same manner as in Version 1. The geophone, as it needs to be coupled closely with the wall or ceiling to be monitored, requires rigid attachment to the wall using epoxy, but the mote and sensor boards may be fastened to the wall only hook-and-loop fasteners. The HS-1

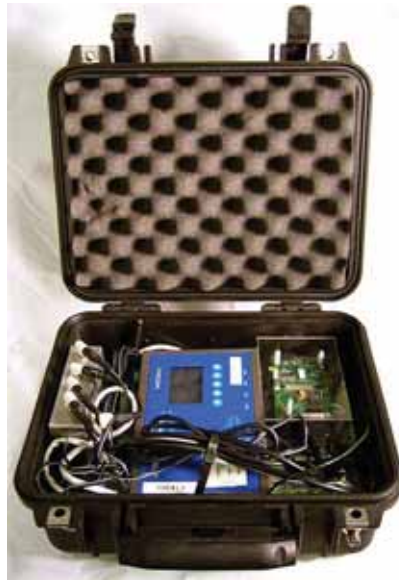


**Figure 3.26:** Photograph of the base station of Version 3 of the wireless ACM system, including UC-7420, MIB510CA, cellular router, power distributor, and industrially-rated housing

geophone features a threaded protrusion for ease of installation on mechanical equipment, so installation was made easier through the fabrication of an aluminum bracket that could accept the protrusion and provide a flat surface for the epoxy-wall interface. Figure 3.27 shows a Version 3 wireless ACM node installed on a wall with a string potentiometer over a crack and an HS-1 geophone in a mounting bracket.

#### 3.3.7.1. *Software*

The software portion of Version 3 of the MICA2-based wireless ACM system is an extension of the software of Version 2 with two significant additions: the ability to allow a hardware interrupt from an external device to bring the mote out of low-power sleep mode and the ability for each mote to receive and relay commands broadcast from the base station. These two new features

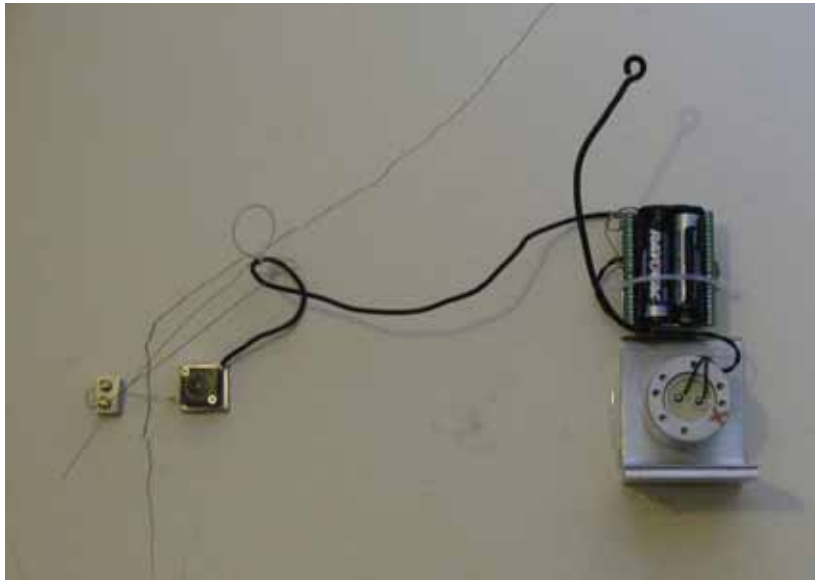


**Figure 3.27:** Photograph of a Version 3 wireless ACM node with string potentiometer and HS-1 geophone with mounting bracket installed on a wall

allow a MICA2 mote to interact with the Shake 'n Wake hardware and for a user to change the Shake 'n Wake triggering threshold, node sampling rates, and node identification numbers while the system is deployed.

Implementation of Version 3 required modification and cross-compilation for the UC-7420 of the *xlisten* and *xcmd* applications provided with the Crossbow MICA2 system. *xcmd*, the application that allows a PC to send commands to the wireless sensor network, was modified to allow the sending of ACM-related commands to modify sampling rates, accelerate the formation of the mesh network, and change the triggering threshold of the Shake 'n Wake devices. *xlisten*, the application that allows a PC to read data coming back from the network, was modified to understand threshold-crossing messages and messages acknowledging receipt of commands. This modified software can be found in the separate publication Kotowsky (2010).

Implementation of Version 3 also required modification of the software that runs on each MICA2. This modification activates an interrupt request channel on the MICA2 and instructs the mote to send back a “trigger received” message upon activation of that interrupt. The mote will also send back its most recent data readings from the MDA300CA upon receiving a Shake 'n Wake trigger. Additionally, the on-mote code was modified to accept the receiving of and responding to commands from a PC. This modified software can be found the separate publication Kotowsky (2010).

#### 3.3.7.2. *Operation*

The addition of the ability to send commands to the sensor network from the base station substantially changes the installation procedure after the mote and sensors have been attached to the structure. Rather than using a physically separate calibration mote to center the string potentiometer, an engineer can center the potentiometer using only the Version 3 software. Once the motes are powered on, the engineer can connect to the base station using any 802.11-capable PC. He logs into the UC-7420 using secure shell and issues a command to the network to enter *quick-mesh* mode in which the rate of packet transmission is significantly increased such that a mesh network forms in under one minute instead of in 30-40 minutes. The engineer uses the *xlisten* program on the UC-7420 to monitor the network output until he sees that all sensors have acknowledged receipt of the quick-mesh command, then he issues another command to disable quick-mesh mode. He then chooses a mote, issues a command to that mote to sample once per second, and uses the increased sampling rate and his computer to center the string potentiometer in the middle of its active range. He then decreases the sample rate of that mote and moves on to the next node until all potentiometers are centered.

When the motes are first powered on, the trigger threshold on each Shake 'n Wake is set by default to 31, the least sensitive setting. By issuing a command from the base station, either at install-time or at any later time by connecting to the base station over the Internet, the trigger threshold may be adjusted to suit the needs of the site. Table 3.2 details the ACM-related commands that are made available with Version 3 of the MICA2-based wireless ACM software.

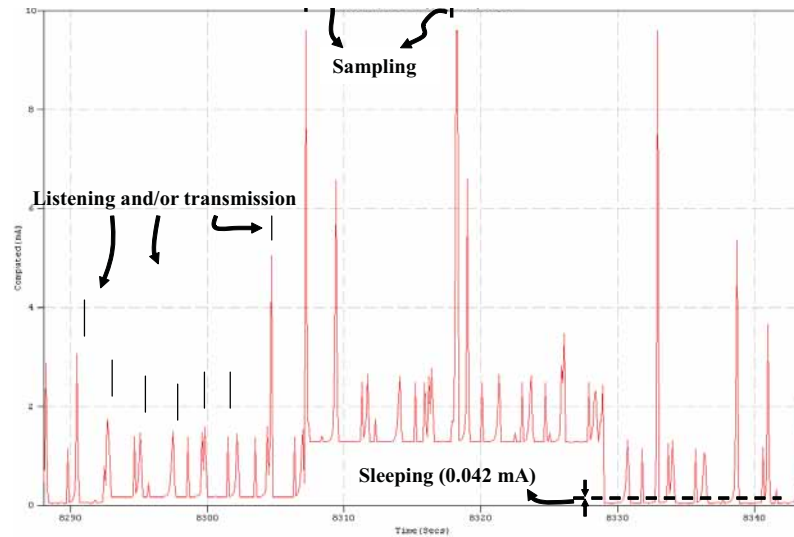
set_rate $X$	$X$ is an integer [1,30]. $X$ specifies frequency, in seconds, of ticks.
set_ticks $X$	$X$ is an integer [1,200]. A sample is taken every $X$ ticks.
set_quick $X$	$X$ is either 0 or 1. If $X$ is 0, the default settings for mesh formation are used. If $X$ is 1, the motes will transmit mesh formation information much more quickly, allowing a mesh to be formed quickly.
set_pot $X$	$X$ is an integer [1,31]. $X = 1$ is the most sensitive.

**Table 3.2:** ACM-related commands added to *xcmd* by Version 3 of the MICA2-based wireless ACM software

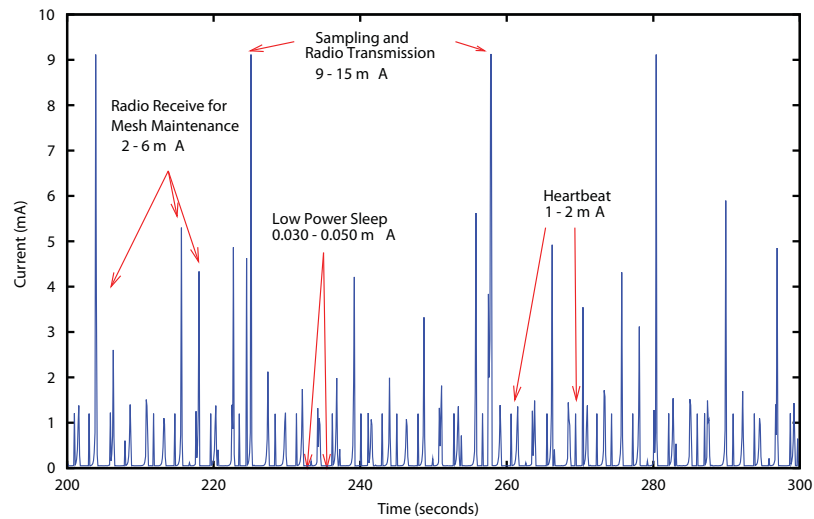
### 3.3.7.3. Analysis of Power Consumption

To analyze the power consumption of a Shake 'n Wake-enabled mote, the simple ammeter circuit and calculations described in Section 3.3.5.3 were utilized. Figure 3.28 shows the current draw of a mote with Shake 'n Wake installed as compared with a Version 2 mote. Figure 3.28b clearly indicates that during the crucial sleep-state of the mote, the current draw varies between 0.03 and 0.05 milliamps – very similar to the sleep-mode current draw of the Version 2 wireless

ACM system without Shake 'n Wake, shown in Figure 3.28a. Thus it can be concluded that the Shake 'n Wake does not draw a significant amount of additional power.



(a)



(b)

**Figure 3.28:** Current draw of (a) wireless ACM Version 2 mote with no Shake 'n Wake, after Dowding et al. (2007) (b) Version 3 mote with Shake 'n Wake

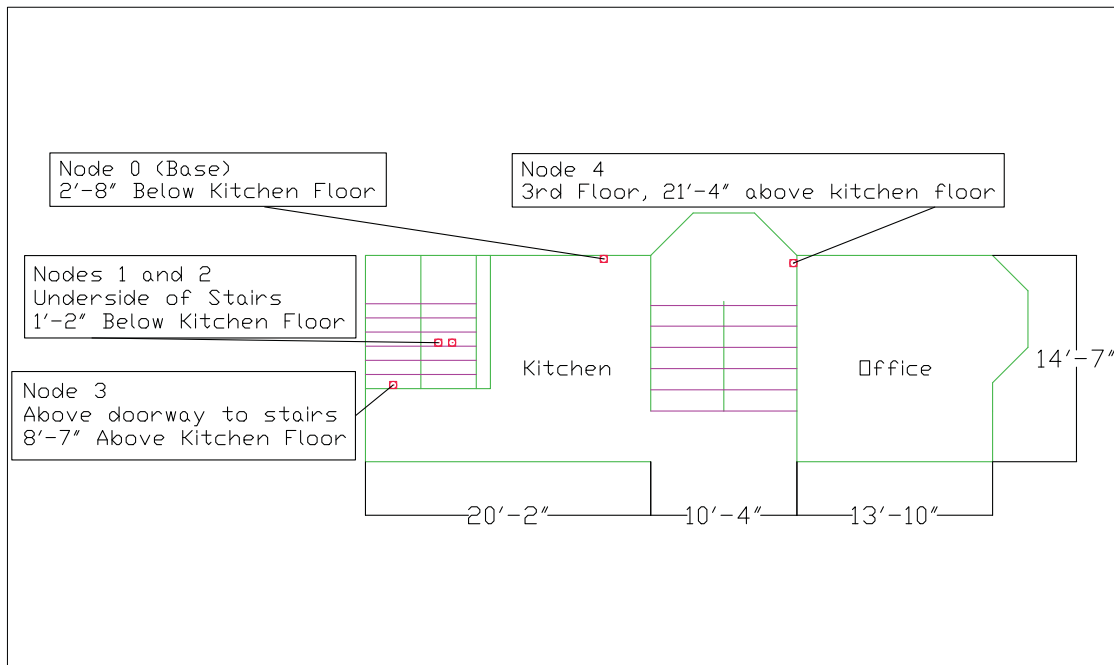
#### 3.3.7.4. *Deployment in Test Structure*

A deployment test of Version 3 of the MICA2-based wireless ACM system was conducted in the main building of the test structures near the Northwestern campus described in Section 3.3.5.4 between September 2007 and February 2008. The objective of the test was to determine the degree of difficulty of the installation of the system, the effectiveness of the Shake 'n Wake in detecting vibration events, and further assurance that Shake 'n Wake does not significantly decrease deployment lifetime of the system.

Sensor nodes were deployed through only one of the structures, as shown in Figure 3.29. Two geophone-only nodes (with no MDA300CA or string potentiometer) were installed on the underside the service stairway leading from the basement to the kitchen, as pictured in Figure 3.30a. One of these nodes was connected to a GS-1 geophone, the other was connected to an HS-1 geophone. Two nodes, each equipped with a MDA300CA sensor board, a Shake 'n Wake sensor board, an HS-1 geophone in a mounting bracket, and a string potentiometer were installed over existing cracks in the structure: one over the doorway leading from the kitchen into the service stairway to the second floor, shown in Figure 3.30b, and one on the wall of the main stairway leading from the second floor to the third floor, shown in Figure 3.30c. These two nodes were installed alongside optical crack measurement devices used for a different project. The base station, shown in Figure 3.30d, was deployed in the basement underneath the kitchen.

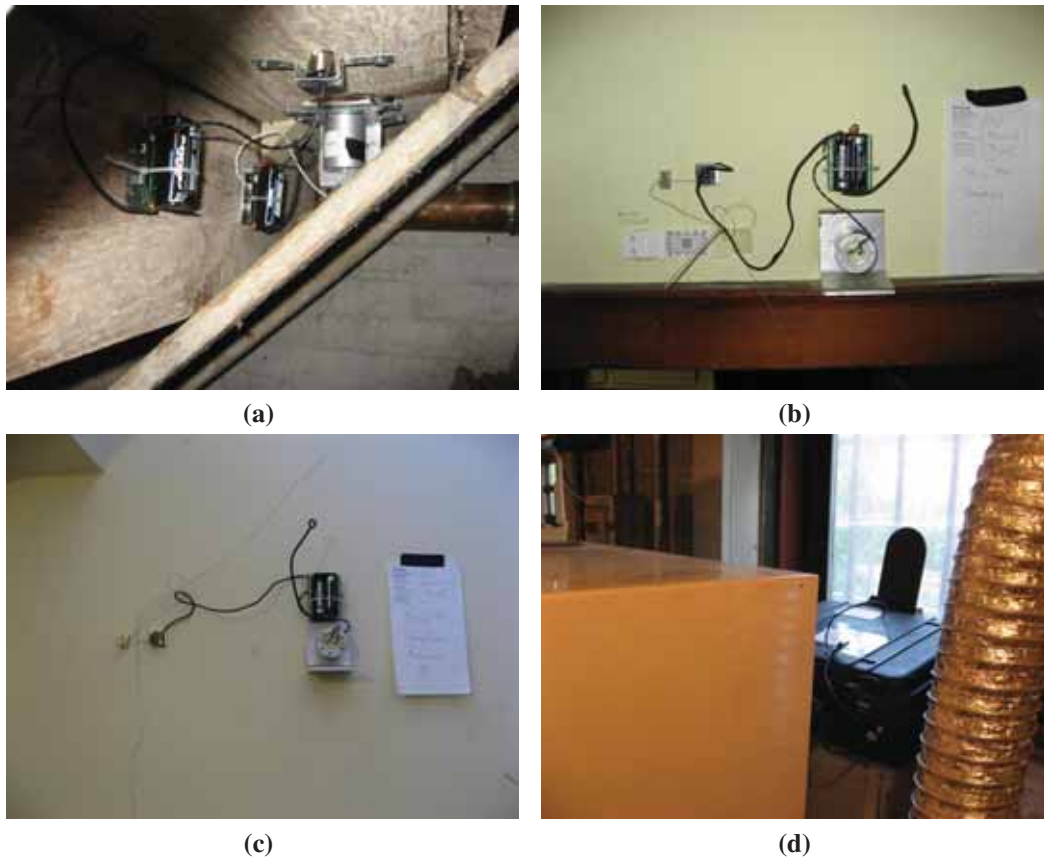
#### 3.3.7.5. *Results*

Figure 3.31 shows plots of temperature, humidity, battery voltage, and parent node over the entire deployment period. Only Nodes 3 and 4 transmit this data – they are the only nodes with an MDA300CA attached. The plots indicate that after approximately 25 days of deployment,



**Figure 3.29:** Layout of nodes in Version 3 test deployment

the system ceased to take data. Later examination indicated that this failure was due to an unforeseen software condition that caused the monitoring to stop prematurely. At approximately day 75, a workaround was implemented: each night, the base station would automatically re-broadcast the correct sampling interval. Data transmission was restored immediately. Mote 4 ceased taking data between days 85 and 115 for a reason that is not yet understood but thought to be an issue with the mesh networking protocol – Figure 3.31d shows that Mote 4 used Mote 3 as an intermediary, which was the only difference between those motes.



**Figure 3.30:** Version 3 wireless ACM nodes located (a) on the underside of the service stairs (b) over service stair doorway to kitchen, and (c) on the wall of the main stairway – (d) the base station in the basement

Diagnostic logs on the base station showed that Motes 1 and 2, the motes underneath the service staircase with no MDA300CA sensor boards, did not reply when the sampling interval workaround was implemented near day 75. The most reasonable explanation for this behavior is that the lack of MDA300CA attached to these motes caused the XMesh power management algorithm to fail causing the batteries to deplete after only two days, approximately the same expected lifetime of a MICA2 with no power management. Figure 3.31d does show that Mote 1 was functioning as a parent mote for Mote 3 before it failed.

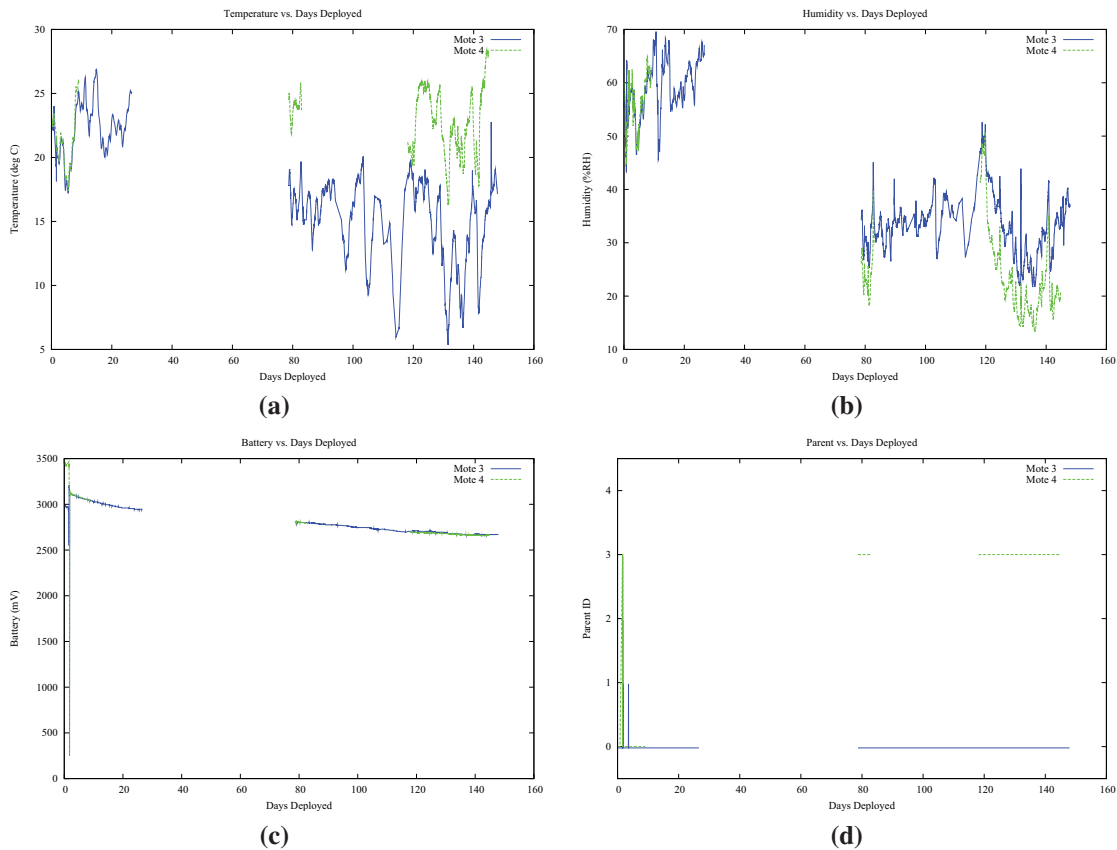


**Figure 3.31:** Plots of (a) temperature (b) humidity (c) battery voltage and (d) parent mote address recorded by Version 3 of the wireless ACM system over the entire deployment period

Figure 3.32 shows the data recorded over the period from day 75, when the base station workaround was implemented, through the time the system was removed from the test structure.

Figure 3.32d shows when a Shake 'n Wake trigger signal was received at Motes 3 or 4.

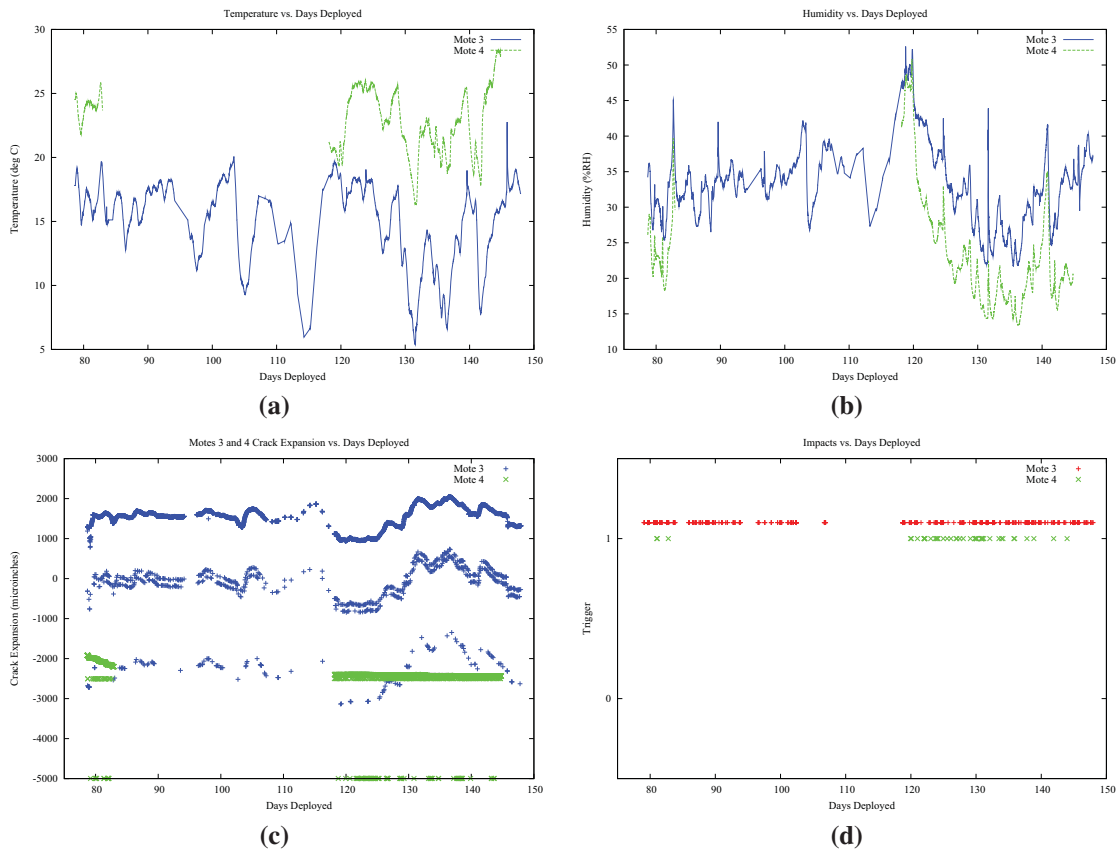


**Figure 3.32:** Plots of (a) temperature (b) humidity (c) crack displacement and (d) Shake 'n Wake triggers recorded by the Version 3 of the wireless ACM system over the 75-day period of interest

### 3.3.7.6. Discussion

Figure 3.31c shows the alkaline battery voltage versus deployment time for Version 3 of the MICA2-based ACM system. Figure 3.33 compares the battery voltage versus time of Versions 2 and 3 of the two MICA2-based wireless ACM systems. The two Version 3 motes with MDA300CA boards installed lasted approximately 150 days. The graph indicates, however, that battery voltage decay curve of the more economical batteries used in Version 3 did not

match those used in Version 2. This evidence, added to the similar current consumption profiles shown in Figure 3.11, indicates that Version 3 can operated for at least six months when high-quality alkaline batteries are used.

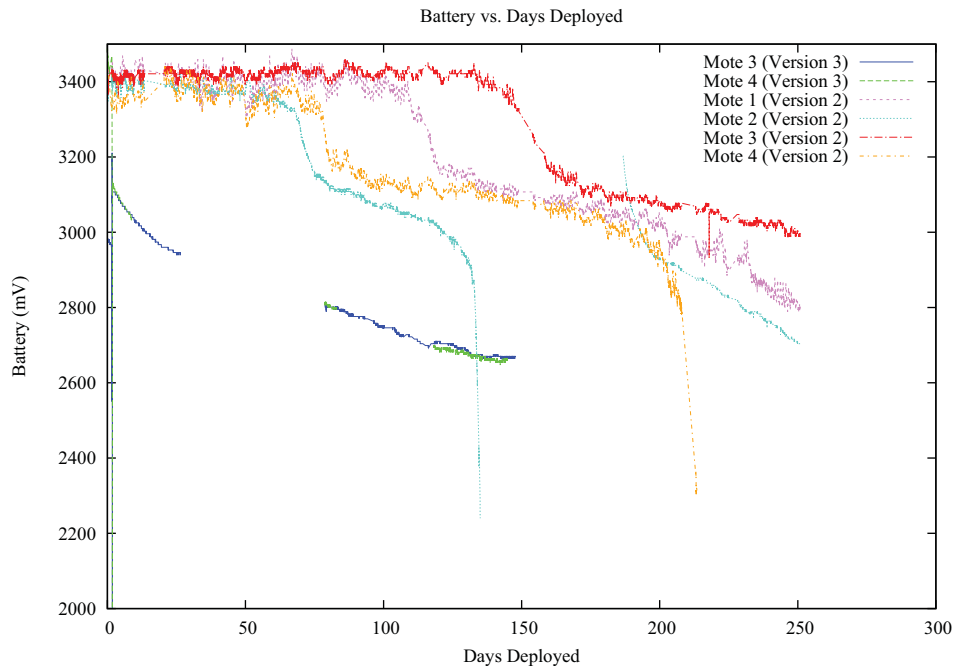


**Figure 3.33:** Comparison of battery voltage versus time for the Version 2 and Version 3 wireless ACM systems

Figure 3.32c shows that the MDA300CA reported what appear to be three different sets of string potentiometer readings, each separated by an approximately 1800  $\mu\text{in}$  pseudo-constant offset. In post processing, it is possible to filter the three sets of data into three regions, as shown in Figure 3.34, under the assumption that each region represents the same physical reading with constant 1800  $\mu\text{in}$  offsets. 84% of the data points fall into the region with an absolute value above 760  $\mu\text{in}$ . The *high* region, as outlined Table 3.3, contains the majority of the recorded

points. Figure 3.35 shows plots of temperature and humidity versus the high region of measured crack width.

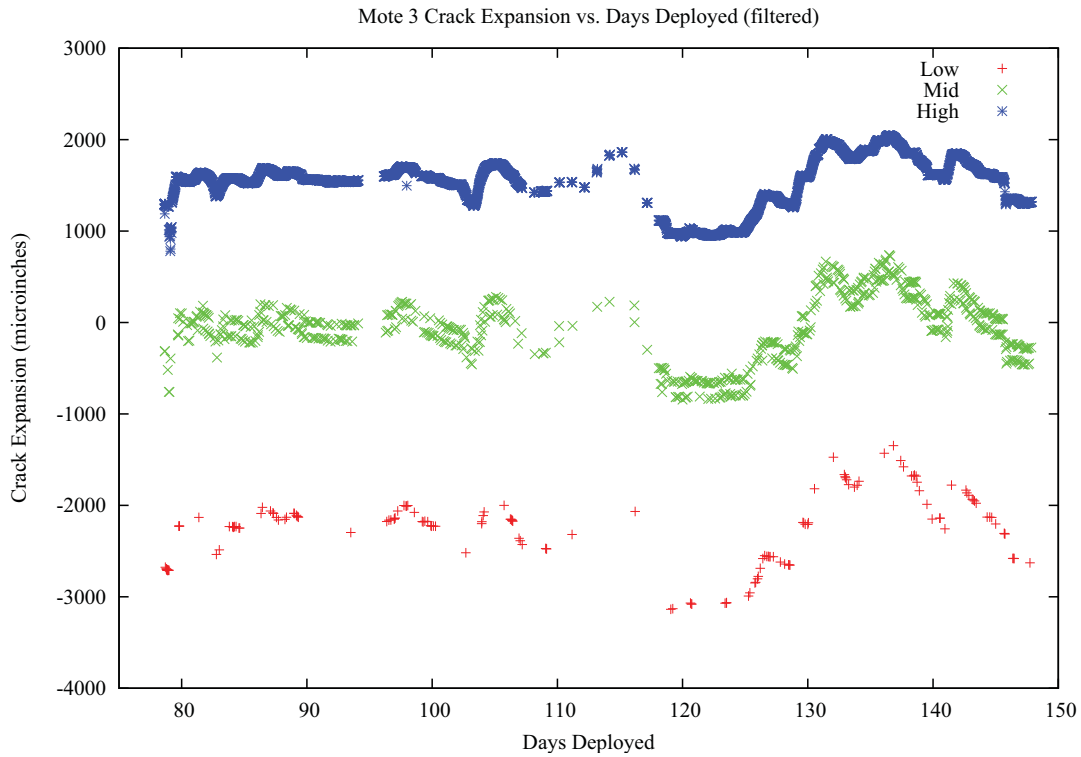


**Figure 3.34:** Plot of three separate sets of crack width data as recorded by Mote 3 of the Version 3 wireless ACM system

	<b>Points Recorded</b>	<b>Percentage</b>	<b>Bounds (mV)</b>	<b>Bounds (<math>\mu\text{in}</math>)</b>
<b>High</b>	4634	84%	$> 1.9\text{mV}$	$> 760 \mu\text{in}$
<b>Mid</b>	736	13%	$1.9\text{mV} > y > -2\text{mV}$	$760 \mu\text{in} > y > -800 \mu\text{in}$
<b>Low</b>	160	3%	$< -2\text{mV}$	$< -800 \mu\text{in}$

**Table 3.3:** Results of filtering Version 3 wireless ACM potentiometer readings

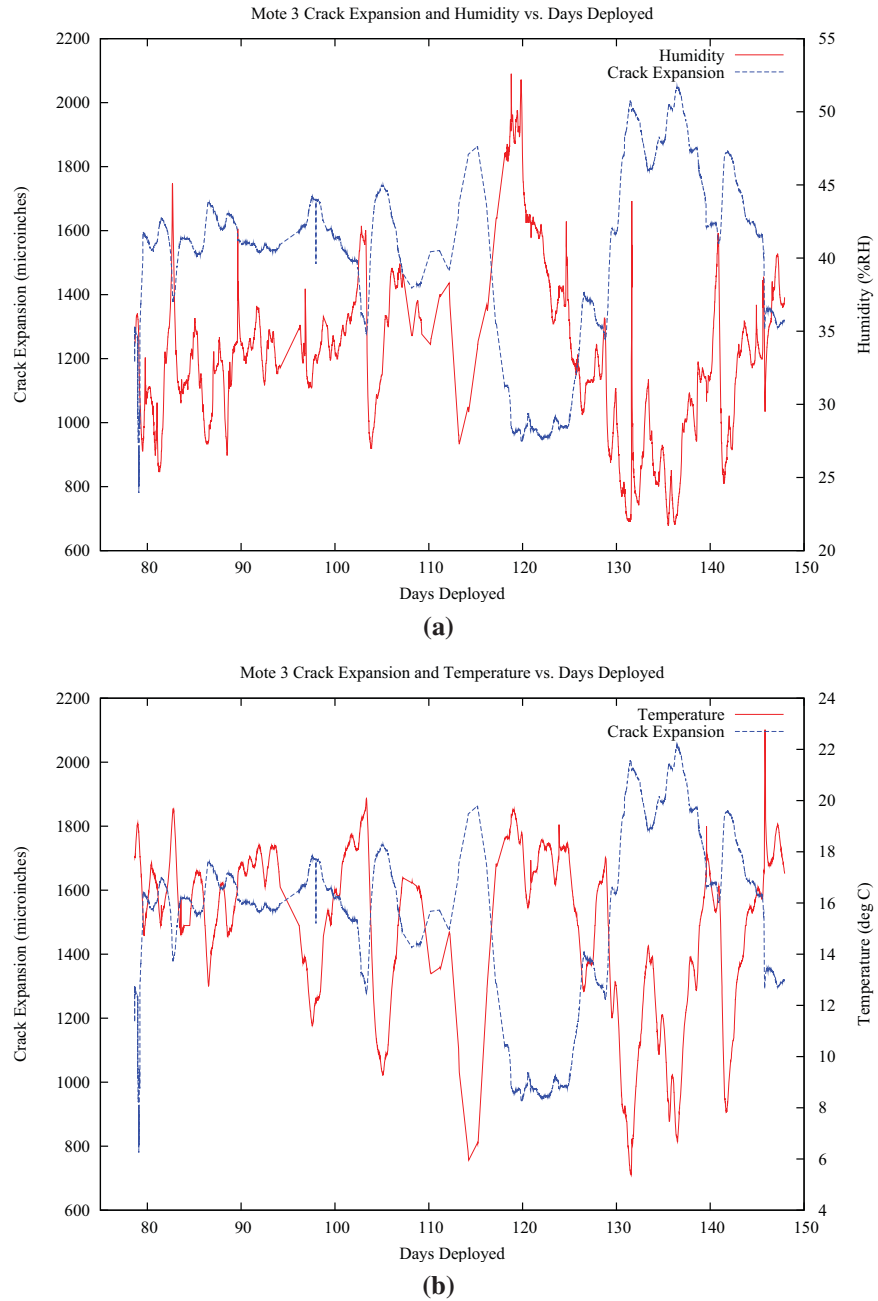


**Figure 3.35:** Plots of (a) humidity and (b) temperature versus filtered crack displacement recorded by the Version 3 wireless ACM system over the 75-day period of interest

### 3.3.8. Wireless ACM Conclusions

This chapter has described three versions of a wireless ACM system built on the MICA2 platform. Version 1 was a proof-of-concept designed to demonstrate the viability of a MICA2-based implementation of ACM by implementing Mode 1 recording. Version 2 incorporated new wireless mesh networking and power management libraries to implement Mode 1 recording with more reliability and system longevity. Version 3 incorporated the design and manufacture of a new sensor board, the Shake 'n Wake, to allow data to be taken at random times rather than scheduled times without sacrificing system longevity. The following conclusions can be drawn:

- The MICA2 WSN platform combined with MDA300CA sensor boards and string potentiometers is capable of performing Mode 1 recording for approximately 30 days. The MDA300CA is essential as the internal ADC on the MICA2 does not have sufficient resolution or front-end gain for the expected potentiometer output.
- Intelligent power management software based on the XMesh routing layer can be used with the MICA2/MDA300CA/potentiometer system to operate a fully functional Mode 1 system for six to twelve months.
- Battery longevity is dependent on the ambient temperature and humidity of the deployment environment.
- A robust, industrially-rated and fully enclosed GNU/Linux embedded computer can be combined with an MIB510CA board to create a reliable and secure Internet-accessible base station that can continue to collect data even while the Internet connection might be off-line. Such a base station can also be used to modify the WSN operating parameters, either automatically or on demand.

- The inclusion of a cellular modem in the base station allows a MICA2-based ACM system to be deployed anywhere with 110 V AC power within radio range of the sensor network.
- Installation time is decreased with the added ability to put the motes into quick-mesh mode to form the initial mesh network. Installation is further simplified by the added ability to individually increase the sampling rate of a mote in order to more easily center the string potentiometer over a crack.
- Shake 'n Wake adds the ability for a MICA2-based wireless ACM mote to respond to a randomly occurring event of interest without sacrificing power.
- A MICA2-based wireless ACM node should not be deployed without a MDA300CA sensor board, even if the node does not need to measure the width of a crack.
- The MDA300CA board and its drivers prevent the MICA2-based ACM system from fully implementing Mode 2 recording, even when paired with Shake 'n Wake, as its drivers do not fully support sampling rates of 1000 hertz.
- Installation of a string potentiometer would be made less difficult if the MDA300CA had a software-programmable front-end gain; the active range of the potentiometer decreases by 99% due to the front-end gain on the MDA300.
- Software incompatibilities between the MDA300CA drivers and the Shake 'n Wake drivers cause the MDA300CA to take readings from the string potentiometer with a DC offset approximately 15% of the time. These anomalous readings can be filtered out in post-processing.
- The Shake 'n Wake hardware design and a software implementation of the Lucid Dreaming strategy for random event detection in energy-constrained systems are not

uniquely compatible with the MICA2-MDA300CA system described in this chapter; they can be ported to any wireless sensor network that allows for direct physical access to the interrupt lines on the control processor and proper access to the low-level software. Unfortunately, many commercially available systems designed for ease of use for novice users do not provide such access, thus Shake 'n Wake/Lucid Dreaming integration must be performed at the factory and not by the end user.

## CHAPTER 4

**Techniques for Wireless Autonomous Crack Propagation Sensing****4.1. Chapter Introduction**

Autonomous Crack Propagation Sensing (ACPS) is a measurement technique designed to record the propagation of slow-growing structural cracks over long periods of time. In contrast to ACM, ACPS, does not seek to directly correlate crack extension to any other physical phenomena; rather ACPS seeks to record quantitatively, repeatably, and accurately the extension of cracks in structures, specifically to supplement regular inspections of bridges. An ACPS system allows structural stakeholders to be alerted to crack extensions with ample time to ensure the safety of the structure and those using it.

Though ACPS techniques can be applied to any structure that exhibits cracking over time, the primary motivation in the development of this technique is to supplement the in-service inspection of fatigue cracks in steel bridges. Fatigue cracks in steel, such as those shown in Figure 4.1, tend to grow slowly over time, and when found during routine inspection of steel bridges, are cataloged according to procedures laid out in the *Bridge Inspector's Reference Manual*, or *BIRM* (United States Department of Transportation: Federal Highway Administration, 2006). These cracks are then re-examined at the next inspection and compared to records to determine whether the crack has grown.

ACPS, especially on bridges, is an ideal application for a wireless sensor network. Running wires across bridges between different points of interest is usually cost-prohibitive and is

often impossible due to superstructure configuration and access restrictions. Since access can be difficult and expensive, it is desirable to minimize installation time and maximize time between maintenance visits, so long-lasting solar-powered nodes are ideal. Furthermore, power management strategies implemented by the manufacturers of existing wireless sensor networks are well-suited to the low sampling rate required by ACPS.

#### **4.1.1. Visual Inspection**

Visual inspection is the most common mechanism by which the growth of cracks is recorded quantitatively. By federal law, every bridge in the United States over 20 feet in length must be inspected at least once every two years by specially trained bridge inspectors. This inspection frequency can be increased based on the design, past performance, or age of the bridge. A key part of these routine bridge inspections is identification of fatigue cracks, or cracks due to cyclic loading, in steel bridge members. These cracks tend to grow slowly over time depending on the volume of truck traffic, load history, weld quality, and ambient temperature (United States Department of Transportation: Federal Highway Administration, 2006).

Fatigue cracks are commonly cataloged by recording the method by which they were discovered, date of discovery, crack dimensions, current weather conditions, presence of corrosion, and other factors that may contribute to the form or behavior of the crack. The BIRM indicates that the inspector should: “Label the member using paint or other permanent markings, mark the ends of the crack, the date, compare to any previous markings, be sensitive to aesthetics at prominent areas. Photograph and sketch the member and the defect.” Figure 4.2 shows an example from the BIRM of how a fatigue crack should be marked.



**Figure 4.1:** Fatigue crack at coped top flange of riveted connection, after United States Department of Transportation: Federal Highway Administration (2006)



**Figure 4.2:** Fatigue crack marked as per the BIRM, after United States Department of Transportation: Federal Highway Administration (2006)

The tracking of crack growth by visual inspection has several drawbacks, the most obvious of which is that documentation of the conditions of cracks can only be updated during inspections which may occur as infrequently as once every two years. Less obviously, photographic records of crack length tend not to be repeatable due to changes in photography angle, ambient light, photographic equipment, and inspector.

#### **4.1.2. Other Crack Propagation Detection Techniques**

Several other techniques exist for the detection, classification, and monitoring of fatigue cracking in structures. Acoustic emission monitoring, as described in Hopwood and Prine (1987) can be used to determine whether a crack is actively growing or has extinguished itself. Stolze et al. (2009) describe a method to detect and monitor the progression of cracks using guided waves. ACPS with wireless sensor networks has several distinct advantages over these structural health monitoring techniques when applied to in-service bridges:

- ACPS is designed to be deployed for months or years on an actively utilized structure. The other techniques are not designed to be used in the field for more than a few days.
- ACPS using commercially available wireless sensor networks is an order of magnitude less expensive than acoustic emission or guided wave equipment.
- ACPS sensors on a wireless network do not require power or signal cables to be installed on a bridge.
- ACPS using a wireless sensor network may not require special software or programming skills.

### 4.1.3. The Wireless Sensor Network

The ēKo Pro Series Wireless Sensor Network (WSN), shown in Figure 4.3, commercially produced by Crossbow Technology, Inc., is specifically designed for environmental and agricultural monitoring. Each ēKo mote is water and dust resistant, capable of operating in wide temperature and humidity ranges, and will operate for over five years with sufficient sunlight (Crossbow Technology, Inc., 2009a). The ēKo base station, which must be connected to 110 V AC power and a network connection, can transmit e-mail alerts when sensor readings cross programmable thresholds. The ēKo WSN's robust design makes it an attractive platform for deployment in the harsh operating environment of an in-service highway bridge. It is equally important to note that an ēKo mote end-user need not manually program the system to function properly, which is attractive to bridge engineers. The ēKo motes record data every thirty seconds for the first hour after activation. Thereafter they record once every fifteen minutes.

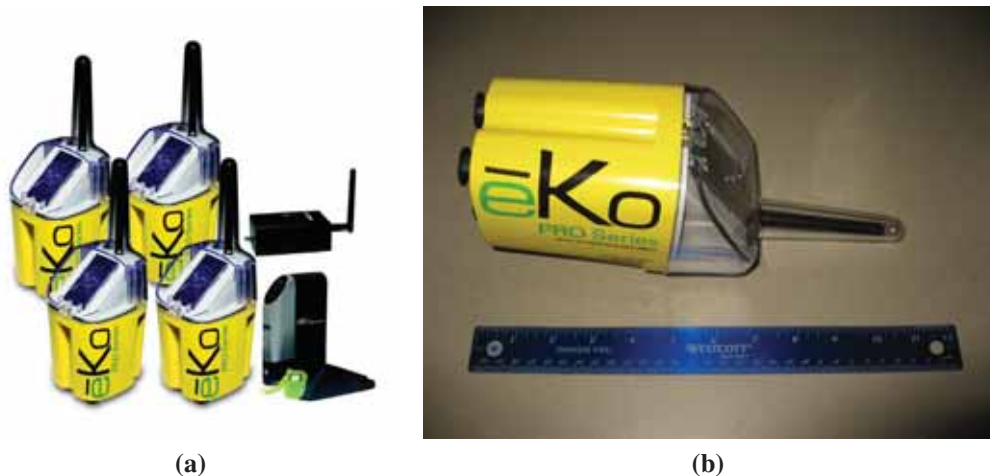


**Figure 4.3:** (a) ēKo Pro Series WSN including base station, after Crossbow Technology, Inc. (2009a) (b) Individual ēKo mote with a 12-inch ruler for scale

## 4.2. ACPS Using Commercially Available Sensors

Direct measurement of the elongation of a crack can be measured with a *crack propagation pattern*, a brittle, paper-thin coupon on which a ladder-like pattern of electrically conductive material is printed. This coupon is glued to the surface of the material at the tip of the crack, as shown in Figure 4.4. When the crack elongates and breaks the rungs of the pattern, the electrical resistance between the sensor's two terminals will change. This resistance is read using an eKo mote to record the distance the crack has propagated.

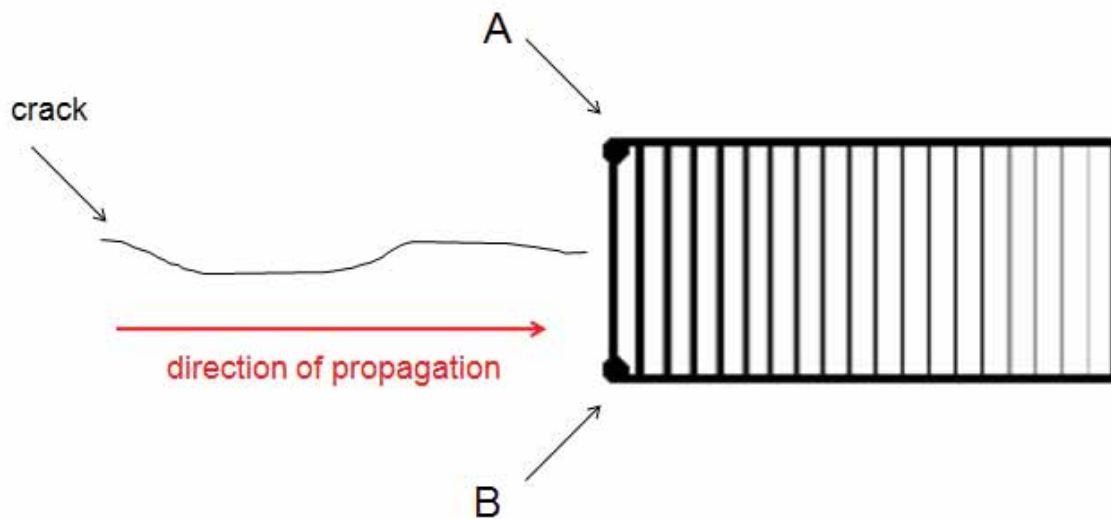


**Figure 4.4:** Cartoon of a crack propagation pattern configured to measure the growth of a crack: resistance is measured between points A and B.

Vishay Intertechnology, Inc. manufactures commercially a series of these crack propagation patterns. Two of these sensors were chosen for use in an ACPS system: the TK-09-CPA02-005/DP, or “narrow gage,” shown in Figure 4.5a and the TK-09-CPC03-003/DP, or “wide gage,” shown in Figure 4.5b. Both sensors allow for the measurement of twenty distinct crack lengths

with their twenty breakable grid lines. The narrow gage's grid lines are spaced 0.02 inches apart, while the wide gage's grid lines are spaced 0.08 inches apart. Additionally, the narrow gage's resistance varies non-linearly with the number of rungs broken, as shown in Figure 4.6a, while the wide gage's resistance varies linearly with number of rungs broken, as shown in Figure 4.6b. This linear behavior occurs because each rung of the wide gage has a resistance specifically designed such that when it is broken, the change in the overall resistance of the sensor is linear, not exponential. The narrow gage's rungs are all approximately the same width and therefore have the same resistance. This behavior becomes significant when signal resolution is considered in Section 4.2.1.

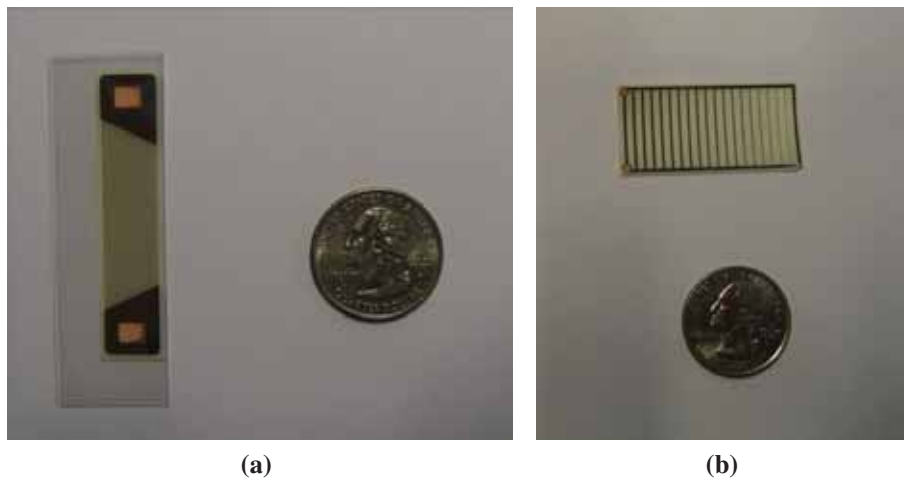


**Figure 4.5:** Crack propagation patterns (a) TK-09-CPA02-005/DP (narrow) (b) TK-09-CPC03-003/DP (wide)

#### 4.2.1. Integration with Environmental Sensor Bus

The eKo Pro Series WSN is designed to be used with sensors that communicate over Crossbow's *Environmental Sensor Bus* (ESB). The ESB protocol (Crossbow Technology, Inc., 2009c)

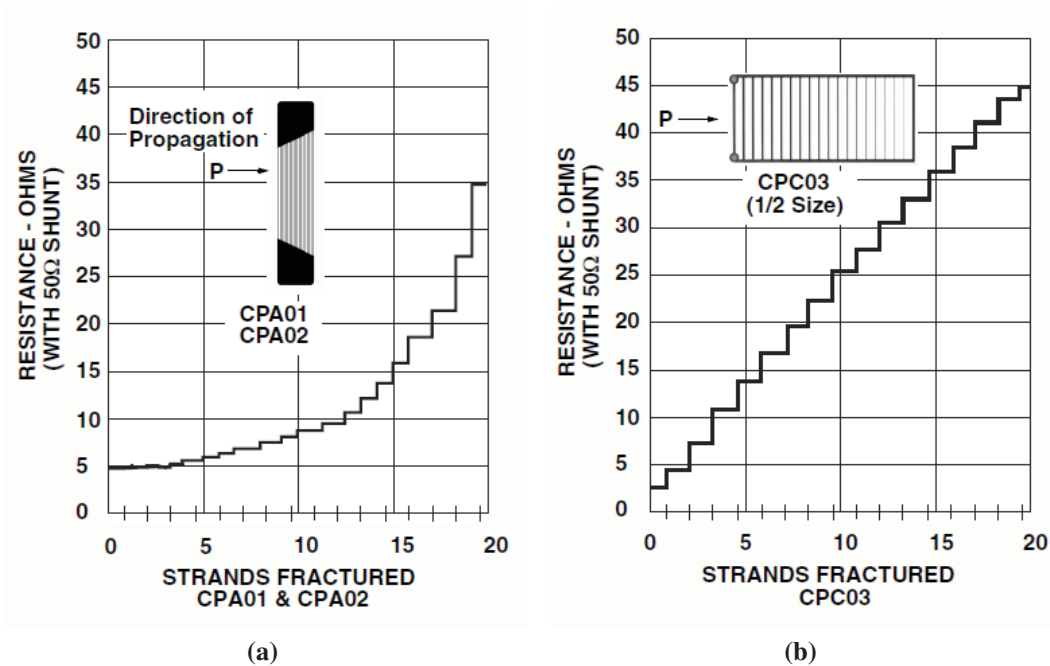


**Figure 4.6:** Crack propagation resistance versus rungs broken for (a) TK-09-CPA02-005/DP (narrow) (b) TK-09-CPC03-003/DP (wide), after Vishay Intertechnology, Inc. (2008)

describes a specific connector type, power supply, and digital interface scheme that must be implemented by the sensor manufacturer if that sensor is to be used with an  $\bar{e}$ Ko mote. The crack propagation patterns are not compliant with the ESB, so a customized interface cable was designed, built, and installed.

The custom interface cable is composed of a Maxim DS2431 1024-Bit 1-Wire EEPROM, a Switchcraft EN3C6F water-resistant 6-conductor connector, a length of Category 5e solid-conductor cable, one  $374\Omega$  precision resistor and one  $49.9\Omega$  precision resistor. The EEPROM was soldered into the water-tight connector housing as shown in Figure 4.7. The EEPROM allows a sensor to respond with a unique sensor identifier when queried by an  $\bar{e}$ Ko mote such that the sensor will be properly identified and configured automatically by any mote to which

it is connected. After the EEPROM was mounted in the connector housing, the individual cable leads were attached and the water-tight cable assembly was completed as shown in Figure 4.8. This cable can be connected to any input port on any  $\bar{e}$ Ko mote once the EEPROM is programmed with the appropriate information to operate the sensor.

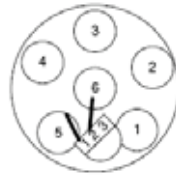


**Figure 4.7:** Schematic of the EEPROM mounted in the watertight connector assembly, after Crossbow Technology, Inc. (2009c)

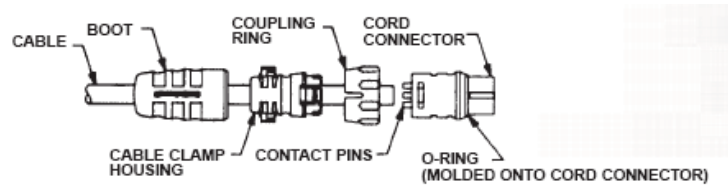


**Figure 4.8:** Watertight ESB-compatible cable assembly, after Switchcraft Inc. (2004)

When fully intact, the narrow and wide crack propagation patterns have a  $5\Omega$  and  $3\Omega$  resistance, respectively, which will increase as their rungs are broken, acting as open circuits when all rungs have been broken. Because the crack propagation patterns are purely resistive sensors and the  $\bar{e}$ Ko mote is only able to record voltages, two precision resistors were used to create a circuit to convert the resistance output into a voltage. The  $49.9\Omega$  resistor was placed in parallel with the two terminals of the crack propagation pattern while the  $374\Omega$  resistor was placed in series with the mote itself. Figure 4.9 shows a schematic of this circuit.

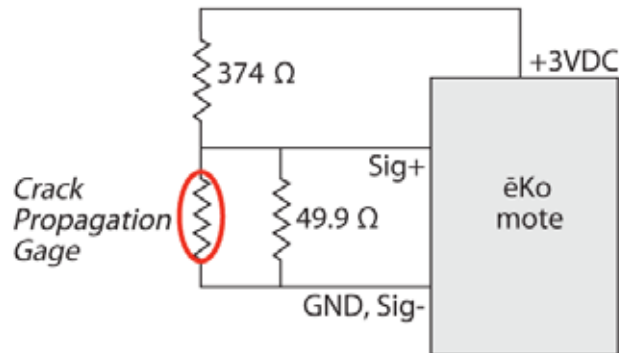


**Figure 4.9:** Diagram of sensor readout circuit, adapted from Vishay Intertechnology, Inc. (2008)

This circuit can be connected to either the narrow or wide gage, and will cause each rung break of a wide pattern to register an increase of approximately 10 millivolts on the ēKo mote. Because the resistance change is so small, the first rung breaks of a narrow sensor will register no measurable voltage difference on the ēKo mote, but the last several rungs broken will register a significantly higher voltage change than the rungs of a wide gage. The circuit was placed within the custom cable so that two exposed leads at the opposite end of the cable from the watertight connector may be soldered to the two terminals of the crack propagation pattern after it has been mounted on the target material.

In addition to the fabrication of the custom ESB interface cable, a customized data interpretation file for each type of crack propagation sensor was created and stored on the ēKo base station. These files, found in the separate document Kotowsky (2010), need only to be created once by the sensor manufacturer and do not need to be created or maintained by the end-user of the ACPS system.

#### 4.2.2. Proof-of-Concept Experiment

A proof-of-concept experiment was designed to test both the effectiveness of the crack propagation gages in measuring fatigue cracking in steel and the eKo motes' ability to reliably and accurately read the sensors. Three 3.5 in by 3.5 in by 0.5 in ASTM E2472 compact tension test coupons A, B, and C, a schematic of which is shown in Figure 4.10, were fabricated from A36 steel. These coupons were placed in a mechanical testing apparatus to apply cyclic tensile forces at their circular attachment points to propagate a crack through the specimens and the gages. Before each coupon was instrumented with a crack propagation pattern, a fatigue crack was initiated in each one under the assumption that any crack to be instrumented in the field would have begun to grow before the sensor is affixed. During the pre-cracking procedure, the relative displacement of the attachment points was cycled between 0.24 inches and 0.0016 inches at a frequency of 10 hertz until a crack was observed to be growing from the tip of the wire-cut notch. Approximately 10,000 cycles were required to initiate crack growth.

Coupon A was instrumented with a narrow crack propagation pattern on one face, as shown in Figure 4.11a. Coupon B was instrumented with a wide crack propagation pattern on one face, as shown in Figure 4.11b. The wide pattern was too long to fit on the test coupon, so the three rungs farthest away from the crack tip were removed before testing. The initial reading would therefore indicate three rungs already having been broken before crack propagation began.

The crack propagation patterns on both Coupons A and B were affixed using the manufacturer's recommended solvent-thinned adhesive cured at a temperature of at least +300 °F. This elevated temperature cure is not practical in the field, so Coupon C was instrumented with a narrow pattern on one face and a wide pattern on the other face using epoxy cured at room temperature to determine if this would have a detrimental effect on ACPS functionality.

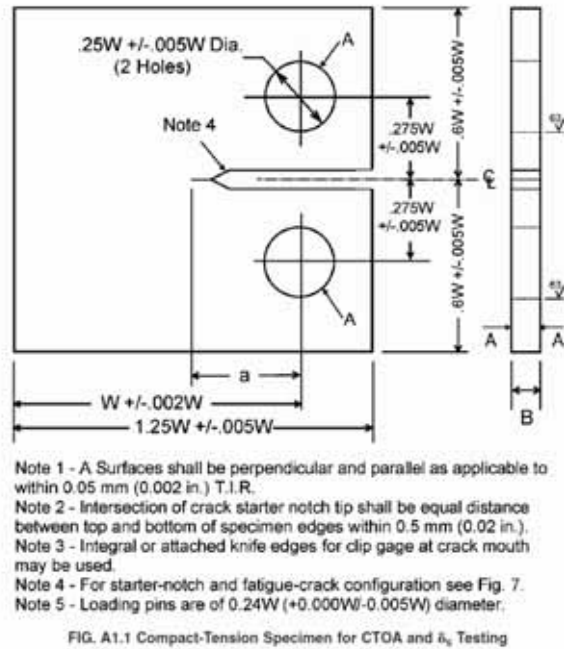


**Figure 4.10:** Schematic of compact test specimen:  $W=3.5$  in,  $B=0.5$  in, after for Testing and Materials (2006)

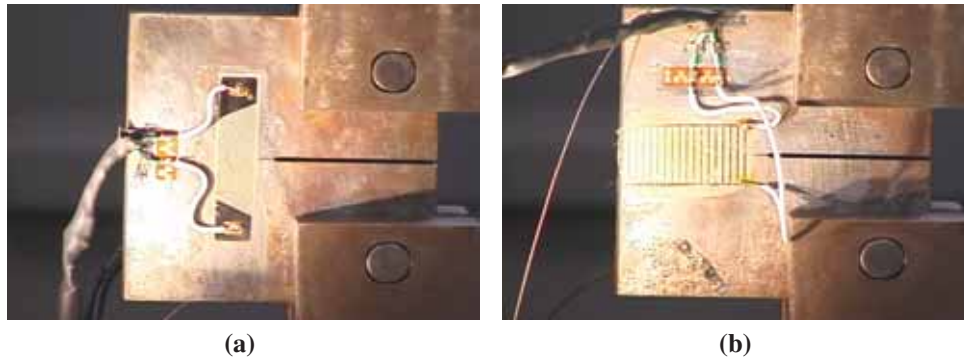


**Figure 4.11:** Test coupon with (a) narrow gage and (b) wide gage installed

4.2.2.1. *Experimental Procedure*

After the fatigue cracking procedure was performed and the gages were affixed to the coupons, each coupon was loaded into the mechanical testing machine and wired to either an eKo mote in

the case of Coupons A and B, or a general-purpose data logger and bench-top power supply in the case of Coupon C. The experiments on coupons A and B were designed to verify functionality of both the gages and the eKo motes, but the experiment on Coupon C was designed solely to verify the performance of the sensor adhesion procedure. Figure 4.12 shows a photograph of the experimental setup.



**Figure 4.12:** Photograph of experiment configuration for pre-manufactured crack propagation gages

During the approximately 80-minute tests, the coupons were cyclically loaded between 0.07 kip and 2.5 kip at decreasing frequencies. The crack in Coupon A propagated through all twenty rungs of the narrow gage, as shown in Figure 4.13a, while the crack in Coupon B propagated through eight rungs of the wide gage, as shown in Figure 4.13b.

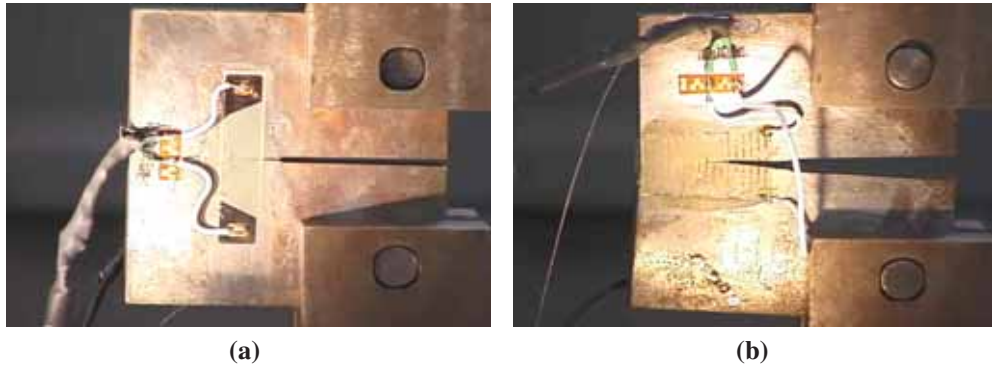


**Figure 4.13:** Test coupons with crack propagated through (a) narrow gage and (b) wide gage affixed with elevated-temperature-cured adhesive

Coupon C was subjected to the same testing procedure as were Coupons A and B, but the testing was aborted when it was observed that the room-temperature-cured adhesive had failed before the gage itself, as shown in Figure 4.14.

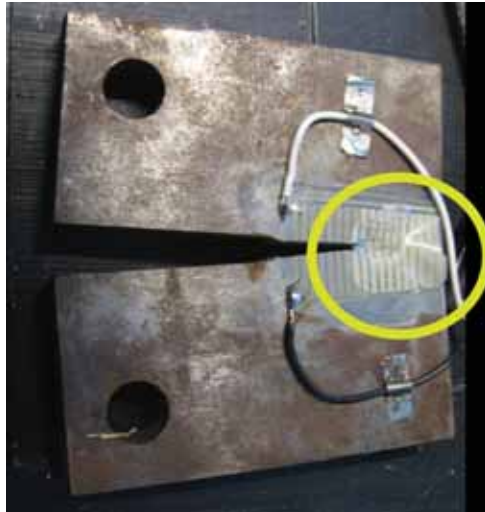


**Figure 4.14:** Photograph of glue failure on wide gage affixed with room temperature-cured adhesive: the indicated region shows the glue failed before the gage.

### 4.2.3. Results and Discussion

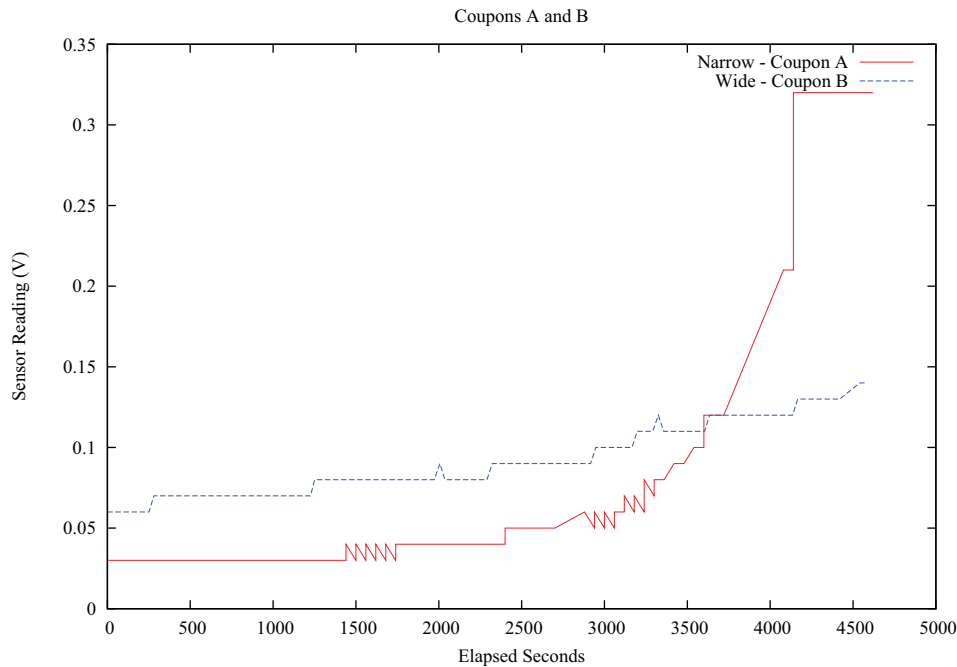


**Figure 4.15:** Data recorded by  $\bar{e}Ko$  mote during tests of Coupons A and B

Figure 4.15 shows the data recorded by an  $\bar{e}Ko$  mote during tests of Coupons A and B. The wide gage showed a linear change of voltage versus number of broken rungs. Eight rung-breaks are easily identifiable. The narrow gage showed a non-linear change of voltage versus number of broken rungs. Figure 4.13a clearly indicates that all twenty rungs have been broken by the crack, but Figure 4.15 only shows ten discernible increases in voltage. This result is not unexpected: the 10-bit analog-to-digital conversion unit and the 3 V DC precision excitation voltage on the  $\bar{e}Ko$  mote combine to limit the minimum-viewable change in voltage output of any sensor to approximately 3 mV. This resolution is suitable for measuring a rung-break on the wide gage but it is not suitable for measuring the breakage of the first 10-12 rungs of the narrow

gage. Figure 4.6a shows that the resistance change exhibited by a narrow gage for the first 10-12 rung-breaks is significantly lower than that for the last 8-10 rung-breaks, therefore the voltage change exhibited by the readout circuit will also be lower for the first 10-12 rung-breaks.

Two times over the course of the test, the  $\bar{e}Ko$  mote read momentary jumps in the voltage output of the wide gage and its readout circuit. This same phenomenon was observed eleven times with the narrow gage. This behavior is explained by noting that for any voltage input to the  $\bar{e}Ko$  mote's analog-to-digital conversion unit that falls on or near one of the 3 mV thresholds, a small amount of electromagnetic interference is capable of increasing or decreasing the voltage of the observed signal such that it could appear to have fallen into either of the two adjacent conversion regions. It is also possible that since the crack, and therefore the conductive portions of the gage, were loaded cyclically, intermittent contact may occur just before or after a rung had been broken.

Figure 4.14 shows that the adhesive cured at room temperature was not able to withstand the cyclic strains imposed by the fatigue test. The lightly colored region indicated in Figure 4.14 shows where the adhesive holding the gage to the steel coupon has released and allowed air to fill the gap between the coupon and the substrate of the crack propagation gage. Once the brittle substrate of the gage separates from the surface on which it is mounted, the gage will not only fail to reflect accurately the position of the crack tip beneath it, but it will become extremely fragile and likely to fail due to some other physical phenomenon than crack propagation.

### **4.3. Custom Crack Propagation Gage**

An implicit assumption made in the use of crack propagation gages such as those described in Section 4.2.2 is that the engineer has a priori knowledge at the time of sensor installation of

the direction in which the crack is going to propagate. In cases where such knowledge does not exist, several of these mass-produced gages would be necessary to track the crack in all of its possible propagation directions. Additionally, the results of the experiment on Coupon C in Section 4.2.2 indicated that for the best results, an impractical installation method involving elevated-temperature-cured adhesive must be employed to utilize these gages.

A solution to both of these problems is a so-called *custom crack propagation gage*. This type of gage is drawn, rather than glued, near the crack to be monitored, using commercially available conductive material. This material, combined with a more sophisticated network of signal conditioning resistors, creates a gage that can be any shape or size.

#### **4.3.1. Theory of Operation of Custom Crack Propagation Sensor**

The basic principles on which custom crack propagation gages function are similar to their pre-fabricated counterparts: an existing crack in a structure grows, propagating over time through one or more rungs of the sensor. As each rung breaks, the resistance of the entire sensor increases by a known value. Using a precision excitation voltage and precision resistors of a known value, each rung break can be observed by an  $\bar{e}Ko$  mote or any other data logger as an increase in voltage. Figure 4.16 shows a schematic of a custom crack propagation gage.

#### **4.3.2. Sensor Design**

Figure 4.16 indicates that the design calls for several resistors wired in parallel. Though this could be implemented with individual precision resistors, pre-manufactured bus resistors, an example of which is shown in Figure 4.17, provide a simpler and more reliable implementation. Each bus resistor has ten pins. One of the pins, designated by a mark on the resistor housing, is

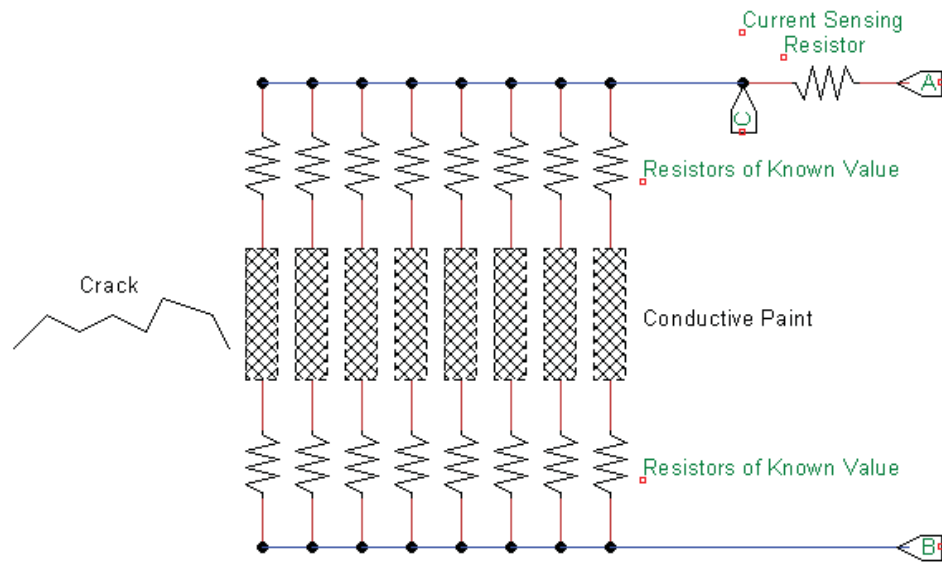


**Figure 4.16:** Schematic of a custom crack propagation gage; crack grows to the right, 3 V DC is applied between A and B, sensor output is measured between C and B.

the *common* pin. The measured resistance between each of the other nine pins and the common pin is always identical, regardless of what is connected or not connected to any of the other pins. This resistor configuration is ideal to simplify fabrication and deployment of a custom crack propagation sensor.



**Figure 4.17:** Photograph of a commercially available bus resistor, after Bourns (2006)

The values of the bus resistors and the current-sense resistor must be selected such that each rung-break may be reliably detected by an  $\bar{e}Ko$  mote's 10-bit analog-to-digital converter and 3 V DC precision excitation voltage. Because the combined resistance of resistors wired in parallel is equal to the reciprocal of the sum of the reciprocals of each resistor's value, the change in resistance of the entire sensor will be smallest for the first rung break and increase non-linearly for each subsequent rung break. The change in resistance, and therefore voltage output, for the first rung break must be maximized while ensuring that the current draw of the sensor never exceeds 8 mA, the maximum current output of the  $\bar{e}Ko$  mote's precision excitation voltage. Table 4.1 shows, for each possible combination of available bus resistor and current-sense resistor, the analog-digital conversion steps for the first rung break. Ohm's Law indicates that the fully-intact resistance of the gage would need to be less than  $375\Omega$  before the sensor would draw more than 8 mA at 3 V. None of the resistor combinations listed in Table 4.1 can combine to form a gage with an intact resistance of  $375\Omega$  or less.

		Bus Resistor Value				
		1K $\Omega$	10K $\Omega$	100K $\Omega$	220K $\Omega$	470K $\Omega$
CS Resistor Value	49.9 $\Omega$	17	2	0	0	0
	374 $\Omega$	29	14	2	1	0
	1K $\Omega$	19	25	5	2	1
	11K $\Omega$	2	18	26	17	10
	20K $\Omega$	1	11	30	24	16
	49.9K $\Omega$	1	5	26	30	26

**Table 4.1:** Change in  $\bar{e}Ko$  ADC steps for first rung break for each combination of bus resistor and current-sense resistor values

Table 4.1 shows that two resistor combinations yield the largest possible analog-to-digital step change for breakage of the first rung. The larger resistor combination, the 220K $\Omega$  bus resistors and the 49.9K $\Omega$  current-sense resistor were chosen because the larger resistors will draw less current from the same voltage supply. Full specifications of the 220K $\Omega$  bus resistor can be found in Appendix B.11. Figure 4.18 shows the theoretical change in sensor output voltage as each of its nine rungs break. It is important to note that the predicted behavior of the voltage output as the rungs break is non-linear. This is, like in the case of the narrow gage in Section 4.2.2, due to the fact that equivalent resistance of resistors in parallel is equal to the reciprocal of the sum of the reciprocals of all of the resistors' values.

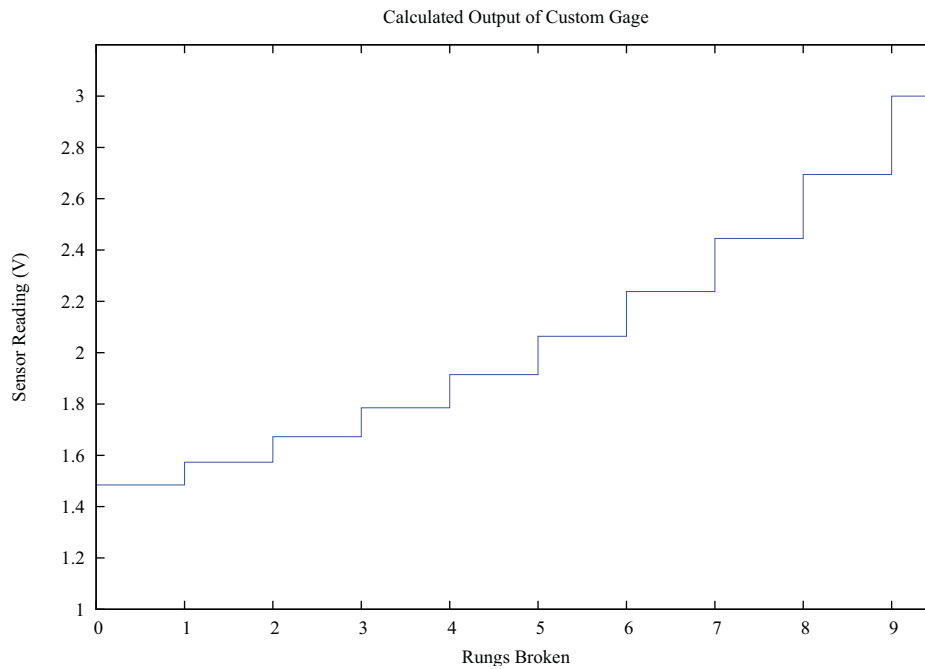


**Figure 4.18:** Predicted change in output voltage of custom crack propagation sensor with rungs broken

The rungs of the crack propagation gage can be any conductive material. For the sensor prototype, a CircuitWorks Conductive Pen, the full technical details of which can be found in Appendix B.12, was used to connect the individual rungs on the two sides of the custom crack propagation sensor. The pen draws a highly conductive silver trace which sets and cures in approximately thirty minutes (ITW CHEMTRONICS, 2009).

While the commercially manufactured crack propagation patterns in Section 4.2.2 were designed to be glued to bare steel, the custom crack propagation gages must be affixed to a non-conductive material for proper functionality. In a field deployment of this sensor, which would likely be on an in-service steel highway bridge, the existing bridge paint system would insulate the conductive traces from the conductive steel substrate. Sherwin-Williams MACROPOXY 646 Fast Cure Epoxy paint was chosen to most closely simulate existing bridge paint (Hopwood, 2008). Industrially-rated quick-setting epoxy adhesive was used to affix the bus resistors to the steel before application of the conductive traces. Sensor application was performed at room temperature. Figure 4.19 shows an engineer applying the gage to a test coupon.

### **4.3.3. Proof-of-Concept Experiment**

A single A36 steel coupon, identical to the coupons used in the experiments in Section 4.2.2, was painted with the simulated bridge paint. Two custom crack propagation sensors were then affixed to the coupon, one on either side. Figure 4.20 shows the test coupon with a custom crack propagation gage installed. Because of the small size of the coupon relative to the size of the sensor, not all pairs of terminals were connected with conductive paint. As such, it was expected that the output of the sensor would behave as though it started with several rungs broken.

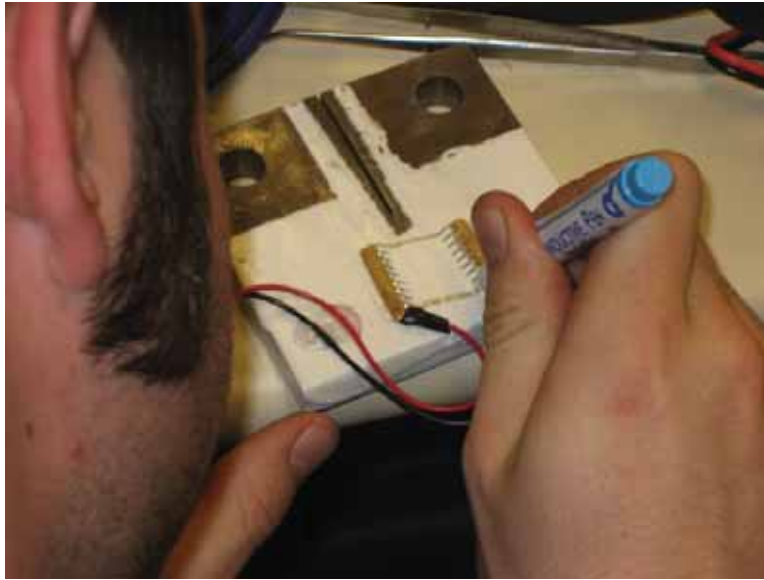


**Figure 4.19:** Photograph of an engineer applying a custom crack propagation gage

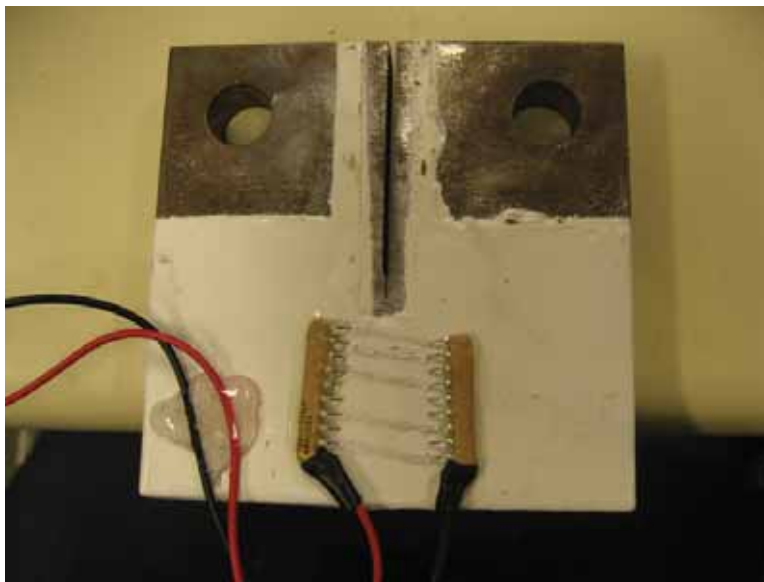


**Figure 4.20:** Photograph of coupon with attached custom crack propagation gage

The experimental procedure to test the custom crack propagation gage was also identical to the one detailed in Section 4.2.2: The coupon was fatigued with no sensors or paint until the crack propagation was initiated. Then, cyclic tension between 0.07 kip and 2.5 kip at 10 hertz was applied to the specimen until failure.

#### 4.3.4. Results and Discussion

After approximately one hour of fatigue testing, the crack propagated through the entirety of the region covered by the custom crack gage. Figure 4.21 shows that all four painted rungs are cleanly broken. Figure 4.22a shows a plot of the gage output versus time. Because this data was taken with a wired data logger, it is more susceptible to the electromagnetic interference generated by the test apparatus. Figure 4.22b shows the results of the application of a 0.1 hertz low-pass Butterworth filter to the data. The data clearly show four distinct rung-breaks.



**Figure 4.21:** Coupon with custom gage after all rungs broken

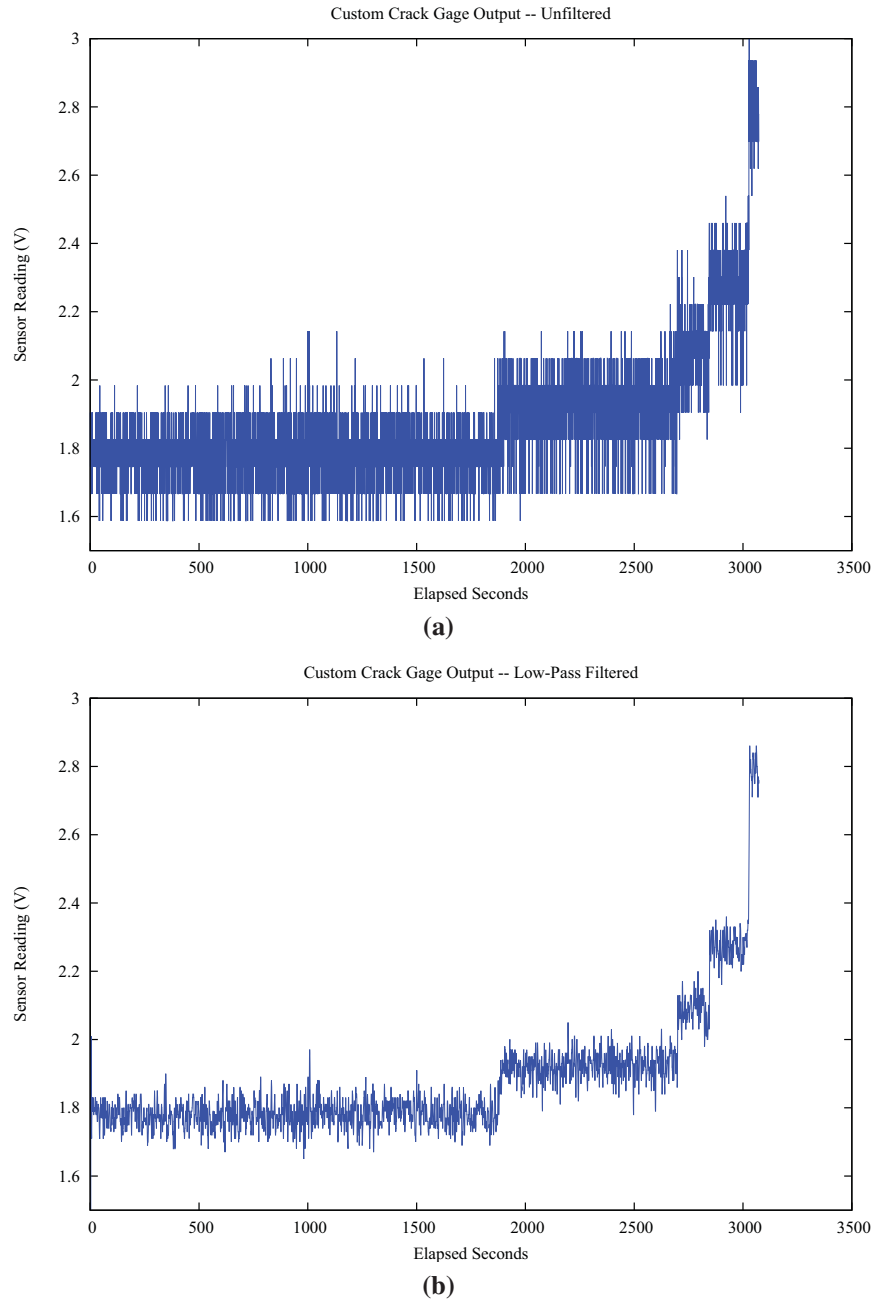


**Figure 4.22:** Custom crack gage output versus time (a) unfiltered, and (b) with 0.1 hertz low-pass filter

#### 4.4. Wireless ACPS Conclusions

This chapter has introduced Autonomous Crack Propagation Sensing (ACPS) and evaluated two types of commercially available crack propagation gages and a newly invented crack propagation gage for ACPS. It has also examined the potential of the Crossbow ēKo Pro Series Wireless Sensor Network for use in ACPS. The following conclusions can be drawn:

- The ēKo Pro Series Wireless Sensor Network is suitable for use in ACPS provided care is taken to accommodate its limited on-board analog-to-digital conversion hardware.
- Both types of the evaluated commercially available crack propagation pattern may be used for ACPS, however, each has its disadvantages: The TK-09-CPA02-005/DP can track crack tip position with a finer resolution, however, its non-linear output causes the first 40-50% of its rung breaks to be undetectable by an ēKo mote. The remaining 50-60% of its rung breaks, however, are easily detected. The TK-09-CPC03-003/DP, conversely, is a larger gage with coarser resolution for crack to position. This gage's linear output characteristics enable each of its individual rung breaks to be detected by the ēKo mote.
- When applied to bare steel using the manufacturer-specified elevated-temperature-cured adhesive, both types of traditional crack propagation patterns are capable of functioning as ACPS sensors using ēKo motes. When applied with a more field-practical room-temperature-cured adhesive, the adhesive has been shown to fail before the gage can break. These gages are therefore only usable in field conditions where elevated-temperature-curing adhesive can be employed.
- Customized crack propagation gages made from conductive ink and commercially available bus resistor networks can track crack propagation and conform to the ēKo

motes' strict analog specifications. These gages can be applied at room temperature without adversely affecting sensor functionality. Customized crack propagation gages allow for a single gage to track the propagation of a crack whose direction of propagation might be unknown or difficult to characterize.

## CHAPTER 5

### **Conclusion**

#### **5.1. Conclusion**

The preceding chapters have described the fundamentals of two wireless systems of autonomous monitoring of cracks: Autonomous Crack Monitoring (ACM) and Autonomous Crack Propagation Sensing (ACPS). ACM systems correlate the changes in the widths of cosmetic cracks in residential structures with nearby vibration and with environmental effects to determine causal relationships. ACPS systems use crack propagation sensors affixed to steel bridge members to track the propagation of existing cracks, alerting stakeholders to any growth. Wired versions of these systems are expensive to install and intrusive to the users of the structures they monitor. As wireless sensor networks (WSNs) decrease in size and cost and increase in capability and longevity, migrating ACM and ACPS systems from the wired to the wireless domain will drastically decrease the time and cost of system installation as well as the disruption to the users of instrumented structures. Chapter 2 described the sensors and components that make up ACM and ACPS systems.

Chapter 3 described the challenges associated with moving an ACM system from the wired to the wireless domain: sensor optimization, minimization of power consumption, and dynamic event detection. Chapter 3 introduced the commercially available MICA2 WSN platform and described three versions of a wireless ACM system built upon it, each with its own test deployment case study.

The three test deployments in Chapter 3 showed that with the proper power and network management software components, the MICA2-based wireless ACM system is well-suited to Mode 1 recording (periodic, single-point measurements taken from all sensors in a structure) over a period of six to twelve months before a battery change is necessary. The test deployments showed that with the invention of the *Shake 'n Wake* hardware expansion board for the MICA2 WSN platform, Mode 2 recording (high-frequency recording whenever an event of interest is detected) can be partially implemented without sacrificing battery longevity. Though *Shake 'n Wake* made possible low-power event detection, limitations in the existing software drivers for the data acquisition board in the MICA2-based system prohibited triggered, high-frequency sampling of all sensors.

Chapter 4 introduced the ēKo Pro Series WSN, a commercially available product designed for the agriculture industry but with capabilities that lend themselves well to ACPS: five-month battery lifetime, integrated solar panels to extend the battery lifetime to five years, a simple web-based interface that requires no programming by the user, and rugged outdoor-rated housing. Though no sensors have been manufactured to allow the ēKo system to perform ACPS monitoring, its implementation of the Environmental Sensor Bus (ESB) allows a third party sensor manufacturer can create a custom interface such that a non-ēKo sensor may be used with any ēKo mote.

Chapter 4 described two types of crack propagation sensors that were made compatible with the ESB and made to function with the ēKo motes. The first type, commercially manufactured resistive crack patterns, are designed to be glued directly to steel in which a crack has formed. The second type, a custom crack propagation gage, is designed to be drawn on to a painted section of steel in which a crack has formed.

Chapter 4 described a series of experiments in which both types of commercially available sensors were integrated with ESB circuitry and attached to steel compact tension specimens. The pre-manufactured test coupons were functional and performed as designed when affixed to the coupons using elevated temperature curing adhesive, but the first several rung-breaks of the narrow gage were not recorded by the eKo mote due to their small voltage changes. The gages attached to the coupon with room temperature curing adhesive were also functional but prematurely de-bonded from the steel and ceased to function as the experiment progressed. Two custom gages were drawn on a painted coupon at room temperature and performed as designed.

Since elevated temperature curing conditions are difficult to achieve on an in-service highway bridge, and since the propagation direction of a crack, and therefore the proper orientation in which to install a pre-manufactured gage, may not be known at the time of installation, the paint-on gage is more practical for field use than either of the pre-manufactured gages.

## **5.2. Future Work**

### **5.2.1. Wireless Autonomous Crack Monitoring**

Autonomous Crack Monitoring will continue to be a useful technique in litigation and regulation of the mining and construction industries; reductions in cost, installation time, and intrusiveness, made possible by implementing ACM using a WSN, will only make the technique more useful. The MICA2 platform is now several years old and is not a focus of active hardware development, therefore future wireless ACM work should be implemented on a different WSN platform, such as the Microstrain V-Link, the Crossbow Imote, or the Moteware Irene platforms. The Shake 'n Wake design can be modified to work with any WSN platform that allows for direct physical and software access to the processor's interrupt lines.

### **5.2.2. Wireless Autonomous Crack Propagation Sensing**

Autonomous Crack Propagation Sensing has been proven in the lab and now must be qualified in the field. The custom crack propagation patterns must be tested for overall field durability over long periods of time. Additional experiments may be necessary to determine the best method of physical protection of the circuitry and the painted traces of the custom crack propagation gage.

## References

- Baillet, R. (2004). Crack response of a historic structure to weather effects and construction vibrations. Master's thesis, Northwestern University, Evanston, Illinois.
- Bourns, I. (2006). 4600X Series - Thick Film Conformal SIPs.
- Crossbow Technology, Inc. (2007a). MDA300CA Data Acquisition Board. [http://www.xbow.com/Products/Product\\_pdf\\_files/Wireless\\_pdf/MDA300CA\\_Datasheet.pdf](http://www.xbow.com/Products/Product_pdf_files/Wireless_pdf/MDA300CA_Datasheet.pdf).
- Crossbow Technology, Inc. (2007b). MPR-MIB Users Manual. [http://www.xbow.com/Support/Support\\_pdf\\_files/MPR-MIB\\_Series\\_Users\\_Manual.pdf](http://www.xbow.com/Support/Support_pdf_files/MPR-MIB_Series_Users_Manual.pdf).
- Crossbow Technology, Inc. (2007c). MTS/MDA Sensor Board Users Manual. [http://www.xbow.com/Support/Support\\_pdf\\_files/MTS-MDA\\_Series\\_Users\\_Manual.pdf](http://www.xbow.com/Support/Support_pdf_files/MTS-MDA_Series_Users_Manual.pdf).
- Crossbow Technology, Inc. (2007d). Stargate Gateway. [http://www.xbow.com/Products/Product\\_pdf\\_files/Wireless\\_pdf/Stargate\\_Datasheet.pdf](http://www.xbow.com/Products/Product_pdf_files/Wireless_pdf/Stargate_Datasheet.pdf).
- Crossbow Technology, Inc. (2007e). XMesh Users Manual. [http://www.xbow.com/Support/Support\\_pdf\\_files/XMesh\\_Users\\_Manual.pdf](http://www.xbow.com/Support/Support_pdf_files/XMesh_Users_Manual.pdf).
- Crossbow Technology, Inc. (2009a). ēko pro series data sheet. [http://www.xbow.com/eko/pdf/eKo\\_pro\\_series\\_Datasheet.pdf](http://www.xbow.com/eko/pdf/eKo_pro_series_Datasheet.pdf).
- Crossbow Technology, Inc. (2009b). ēko pro series users manual. [http://www.xbow.com/eko/pdf/eKo\\_Pro\\_Series\\_Users\\_Manual.pdf](http://www.xbow.com/eko/pdf/eKo_Pro_Series_Users_Manual.pdf).
- Crossbow Technology, Inc. (2009c). ESB developer's guide.
- Crossbow Technology, Inc. (2009d). MIB 510 Serial Interface Board. [http://www.xbow.com/Products/Product\\_pdf\\_files/Wireless\\_pdf/MIB510CA\\_Datasheet.pdf](http://www.xbow.com/Products/Product_pdf_files/Wireless_pdf/MIB510CA_Datasheet.pdf).

- Crossbow Technology, Inc. (2009e). MICA2 Wireless Measurement System. [http://www.xbow.com/Products/Product\\_pdf\\_files/Wireless\\_pdf/MICA2\\_Datasheet.pdf](http://www.xbow.com/Products/Product_pdf_files/Wireless_pdf/MICA2_Datasheet.pdf).
- Dowding, C. H. (1996). *Construction Vibrations*. Prentice Hall, Upper Saddle River, New Jersey.
- Dowding, C. H., Kotowsky, M. P., and Ozer, H. (2007). Multi-hop wireless system crack measurement for control of blasting vibrations. In *Proc. 7th Int'l Symposium on Field Measurements in Geomechanics*, Boston, Massachusetts. American Society of Civil Engineers.
- Energizer Holdings, I. (2010a). Product datasheet: Energizer e91. <http://data.energizer.com/PDFs/E91.pdf>.
- Energizer Holdings, I. (2010b). Product datasheet: Energizer 191. <http://data.energizer.com/PDFs/191.pdf>.
- Firstmark Controls (2010). Data sheet - series 150 subminiature position transducer. <http://www.firstmarkcontrols.com/s021f.htm>.
- for Testing, A. S. and Materials (2006). *Standard Test Method for Determination of Resistance to Stable Crack Extension under Low-Constraint Conditions*. ASTM E2472.
- Geo Space Corporation (1980). *GEO GS-14-L3 28 HZ 570 OHM*. Part number 41065.
- Geo Space Corporation (1996). *HS-1-LT 4.5Hz 1250 Ohm Horiz.* Part number 98449.
- Hopwood, T. (2008). Personal communication with University of Kentucky researcher.
- Hopwood, T. and Prine, D. (1987). Acoustic emission monitoring of in-service bridges. Technical Report UKTRP-87-22, Kentucky Transportation Research Program, University of Kentucky, Lexington, Kentucky.
- ITW CHEMTRONICS (2009). CircuitWoprks Conductive Pen TDS Num. CW2200.
- Jevtic, S., Kotowsky, M. P., Dick, R. P., Dinda, P. A., and Dowding, C. H. (2007a). Lucid dreaming: Reliable analog event detection for energy-constrained applications. In *Proc. IPSN-SPOTS 2007*, Cambridge, Massachusetts. Association for Computing Machinery / Institute of Electrical and Electronics Engineers.
- Jevtic, S., Kotowsky, M. P., Dick, R. P., Dinda, P. A., Dowding, C. H., and Mattenson, M. J. (2007b). Lucid dreaming: Reliable analog event detection for energy-constrained applications. Poster presented during live demonstration.

- Kaman Measuring Systems (2009). Sensor data sheet: SMU-9000. <http://www.kamansensors.com/html/products/pdf/wSMU9000-9200.pdf>.
- Kosnik, D. E. (2007). Internet-enabled geotechnical data exchange. In *Proc. 7th Int'l Symposium on Field Measurements in Geomechanics*, Boston, Massachusetts. American Society of Civil Engineers.
- Kotowsky, M. P. (2010). Wireless sensor networks for monitoring cracks in structures: Source code and configuration files. Addendum to MS Thesis.
- Kotowsky, M. P., Dowding, C. H., and Fuller, J. K. (2009). Poster summary: Wireless sensor networks to monitor crack growth on bridges. In *Proceedings, Developing a Research Agenda for Transportation Infrastructure Preservation and Renewal Conference*, Washington, DC. Transportation Research Board.
- Louis, M. (2000). Autonomous Crack Comparometer Phase II. Master's thesis, Northwestern University, Evanston, Illinois.
- Macro Sensors (2009). Macro sensors LVDTs: DC-750 series general purpose DC-LVDT position sensors. [http://www.macrosensors.com/lvdt\\_macro\\_sensors/lvdt\\_products/lvdt\\_position\\_sensors/dc\\_lvdt/free\\_core\\_dc/dc\\_750\\_general\\_purpose.html](http://www.macrosensors.com/lvdt_macro_sensors/lvdt_products/lvdt_position_sensors/dc_lvdt/free_core_dc/dc_750_general_purpose.html).
- Marron, D. R. (2010). Personal communication with Chief Research Engineer at the Infrastructure Technology Institute at Northwestern University.
- Maxim Integrated Products (2003). *SOT23, Dual, Precision, 1.8V, Nanopower Comparators With/Without Reference*. Part number MAX9020EKA-T.
- Maxim Integrated Products, Inc. (2009). 1024-bit, 1-wire eeprom data sheet.
- McKenna, L. M. (2002). Comparison of measured crack response in diverse structures to dynamic events and weather phenomena. Master's thesis, Northwestern University, Evanston, Illinois.
- Moxa, Inc (2010). UC-7410/7420 Series. [http://www.moxa.com/doc/specs/UC-7410\\_7420\\_Series.pdf](http://www.moxa.com/doc/specs/UC-7410_7420_Series.pdf).
- Ozer, H. (2005). Wireless sensor networks for crack displacement measurement. Master's thesis, Northwestern University, Evanston, Illinois.
- Puccio, M. (2010). Personal communication with Application Engineer of Macro Sensors.

- Siebert, D. (2000). Autonomous Crack Comparometer. Master's thesis, Northwestern University, Evanston, Illinois.
- Snider, M. (2003). Crack response to weather effects, blasting, and construction vibrations. Master's thesis, Northwestern University, Evanston, Illinois.
- SOLA HD (2009). SCL Series, 4 and 10 Watt CE Linears. <http://www.solahd.com/products/powersupplies/pdfs/SCL.pdf>.
- SoMat, Inc. (2010). eDAQ Simultaneous High Level Layer. [http://www.somat.com/products/edaq/edaq\\_simultaneous\\_high\\_level\\_layer.html#tabs-1-2](http://www.somat.com/products/edaq/edaq_simultaneous_high_level_layer.html#tabs-1-2).
- Speckman, G. M. (2010). Personal communication with Regional Sales Manager of Kaman Sensors.
- Stolze, F., J.Staszewski, W., Manson, G., and Worden, K. (2009). Fatigue crack detection in a multi-riveted strap joint aluminium panel. In Kundu, T., editor, *Health monitoring of structural and biological systems*, volume 7925. Bellingham, Wash. : SPIE.
- Switchcraft Inc. (2004). EN3™Cord Connector.
- The Sherwin-Williams Company (2019). MACROPOXY 646 FAST CURE EPOXY.
- United States Department of Transportation: Federal Highway Administration (2006). *Bridge Inspector's Reference Manual*, volume 2. National Highway Institute.
- Vishay Intertechnology, Inc. (2008). Special use sensors - crack propagation sensors.
- Waldron, M. (2006). Residential crack response to vibrations from underground mining. Master's thesis, Northwestern University, Evanston, Illinois.

## APPENDIX A

**Experimental Verification of *Shake 'n Wake***

This appendix describes experiments detailing experimental verification of the design criteria of the *Shake 'n Wake* board.

The design criteria of the Shake 'n Wake board are as follows:

- (1) It must not significantly increase the power consumption of a mote.
- (2) Its trigger threshold must be predictable and repeatable.
- (3) It must not contaminate the output signal of its attached sensor.
- (4) It must wake up the mote such that the mote has time to record during the peak of the motion of interest.

Criterion 1 is addressed in Section 3.3.7.3. Verification of the rest of the design criteria are described in the following sections.

### **A.1. Transparency**

Because Shake 'n Wake is intended to be attached in parallel an analog-to-digital conversion unit on the mote, the output of the geophone must not be affected by the presence of the Shake 'n Wake. To determine whether the Shake 'n Wake hardware meets this design criterion, the output of the test geophones attached to Shake 'n Wake boards were compared to control geophones while subjected to identical physical excitation. Figure A.1 shows the experimental setup on which all four geophones – an HS-1 test geophone, an HS-1 control geophone, a GS-14 test geophone, and a GS-14 control geophone, were placed on the end of a cantilevered aluminum springboard at an identical distance from the fulcrum.

By measuring the responses of the geophones connected to Shake 'n Wake boards and comparing them to the responses of the control geophones, it can be determined whether or not the Shake 'n Wake circuitry will contaminate the waveform. Figure A.2 clearly indicates that the positive portion of the output of a test geophone follows the positive portion of the output of its equivalent control geophone. The negative portion of the output of the test geophone is

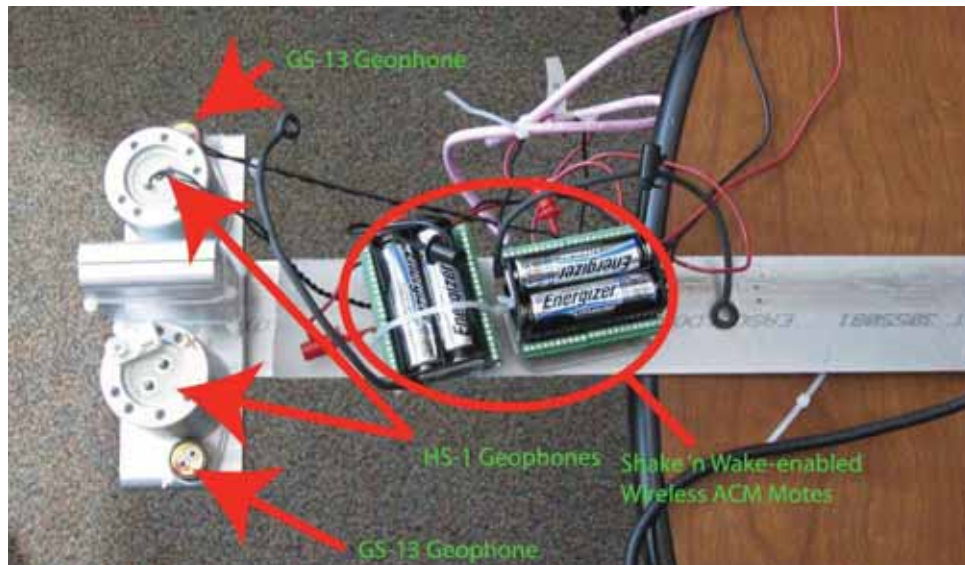


**Figure A.1:** Shake 'n Wake transparency test apparatus

clipped at a value of -200 millivolts. The negative portion of the output of a geophone attached to a Shake 'n Wake is clipped by reverse-current-limiting diodes that prevent voltage of inappropriate polarity from damaging the board's internal electronics. When the same geophone is attached to the opposite connector on the Shake 'n Wake, similar clipping of the positive portion of the waveform can be observed. These results show that the Shake 'n Wake satisfies the requirement of not corrupting the output of the geophone.

## A.2. Verification of Trigger Threshold

Idealized analysis of the Shake 'n Wake's adjustable trigger circuit, pictured in Figure 3.24, indicates that for any trigger setting,  $x$ , the threshold,  $V_{comp}$  at which the Shake 'n Wake will bring the mote out of its low-power sleep state is  $3.558mV * x$ . To verify the validity of this idealized analysis, the output of an HS-1 geophone is recorded on the same time scale as the output of the Shake 'n Wake to which it is attached, and the output of a GS-14 geophone is

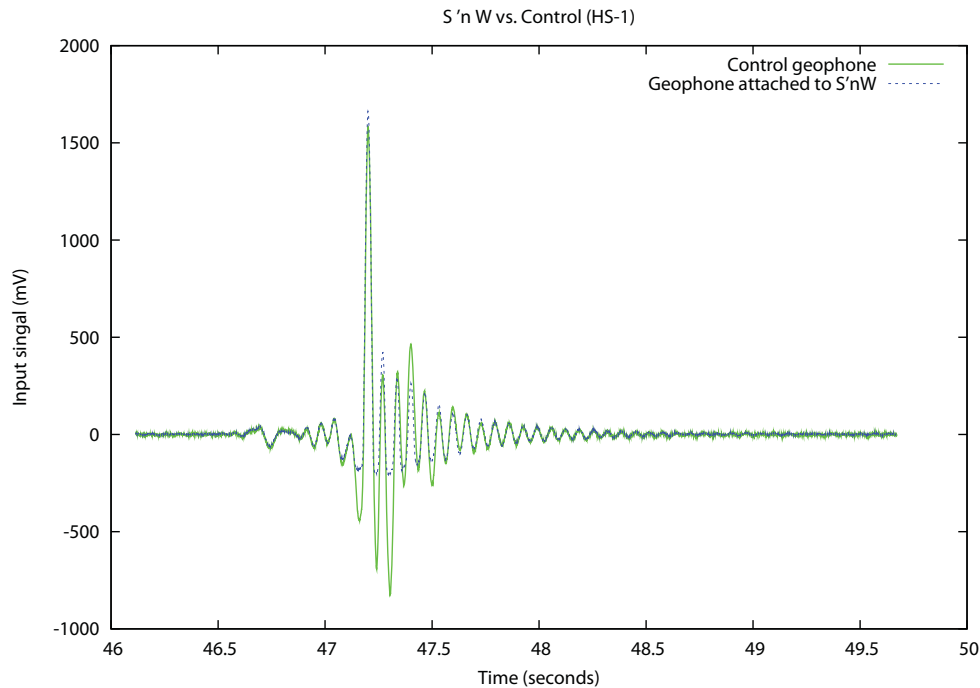


**Figure A.2:** Shake 'n Wake transparency test results for HS-1 geophone

recorded on the same time scale as the output of the Shake 'n Wake to which it is attached. Both geophones were placed on a cantilevered aluminum springboard with identical distances from the fulcrum. Figure A.3 shows this experimental setup.

The length of the springboard was decreased successively to produce response frequencies of 5, 10, 15, and 20 hertz, thereby spanning the frequency range of interest for structural motion in response to a vibration event. The Shake 'n Wake was set to level 2 of 31, the most sensitive level that could be used while avoiding false triggers from ambient vibration of the springboard.

Figures A.4 and A.5 show the voltage level at which each Shake 'n Wake triggers with a threshold setting of level 2 when the geophones are moved at a frequency of 5 hertz.

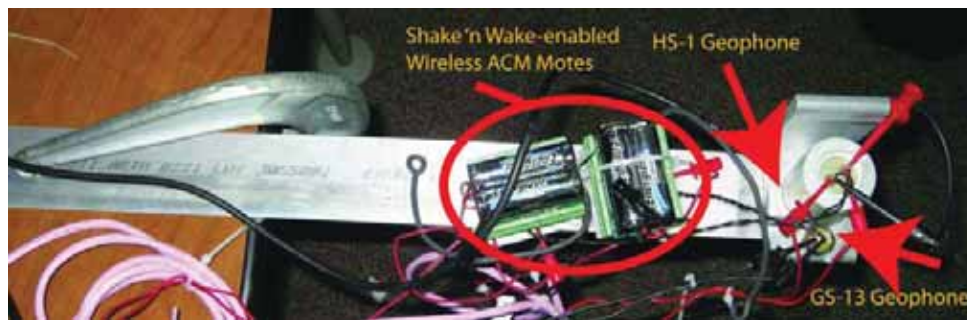


**Figure A.3:** Shake 'n Wake trigger threshold test apparatus

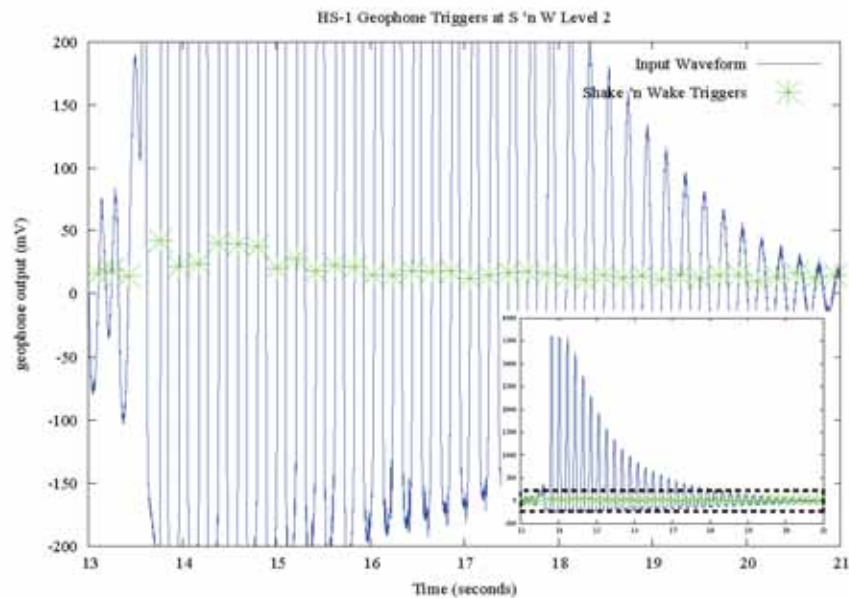


**Figure A.4:** Shake 'n Wake Level 2 trigger threshold test results for HS-1 geophone at 5 hertz

For each of the set of test frequencies, averages of the voltage level at which the Shake 'n Wake triggered were computed. Figure A.6 graphically summarizes these results. Based on the analysis of the idealized trigger threshold reference circuit in Figure 3.24, the theoretical value at which the Shake 'n Wake should trigger – regardless of the sensor to which it is attached – is 7.116 millivolts. Figure A.6 indicates that the Shake 'n Wake is actually triggered at a higher

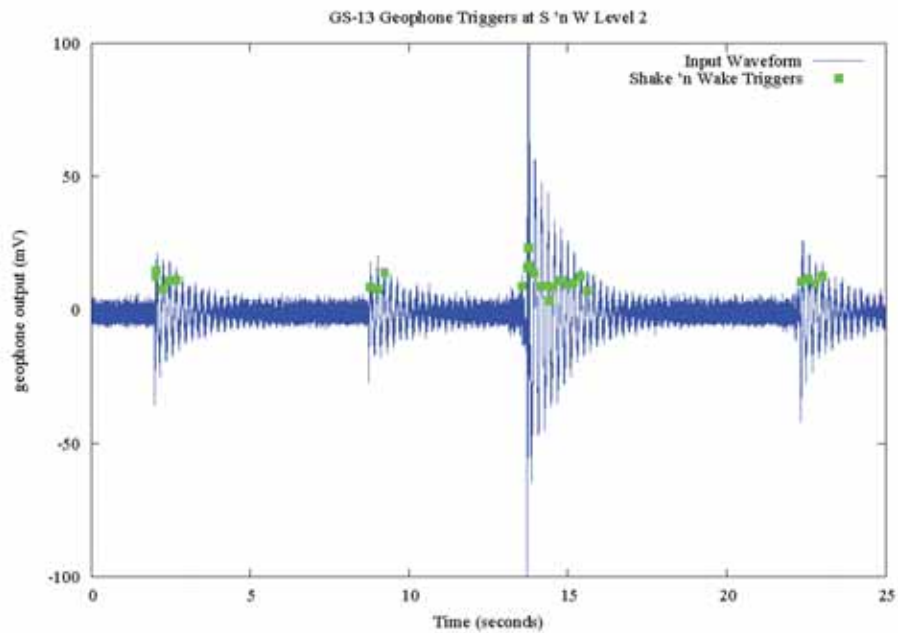


**Figure A.5:** Shake 'n Wake Level 2 trigger threshold test results for GS-14 geophone at 5 hertz voltage threshold than predicted, and the actual trigger threshold varies with frequency of the output of the geophone.

These results indicate that the idealized analysis is not adequate to determine the actual voltage threshold at which the Shake 'n Wake will trigger; frequency also must be taken into account when determining this voltage. The dependence of the Shake 'n Wake's comparators on the frequency of their input voltage can be attributed to the hysteresis of the comparator, described in detail in the comparator's product data sheet in Maxim Integrated Products (2003). In order to accurately determine the threshold voltage, the Shake 'n Wake must be calibrated by the user with the desired sensor over the range of desired input frequencies. Though Figures A.4 and A.5 do indicate that though the trigger threshold varies with frequency, it is predictable; in each period of the input waveform, the trigger occurs at approximately the same input voltage. This

satisfies the requirement that the trigger threshold be both predictable and repeatable, though sensor- and frequency-specific calibration is required for precise predictions.

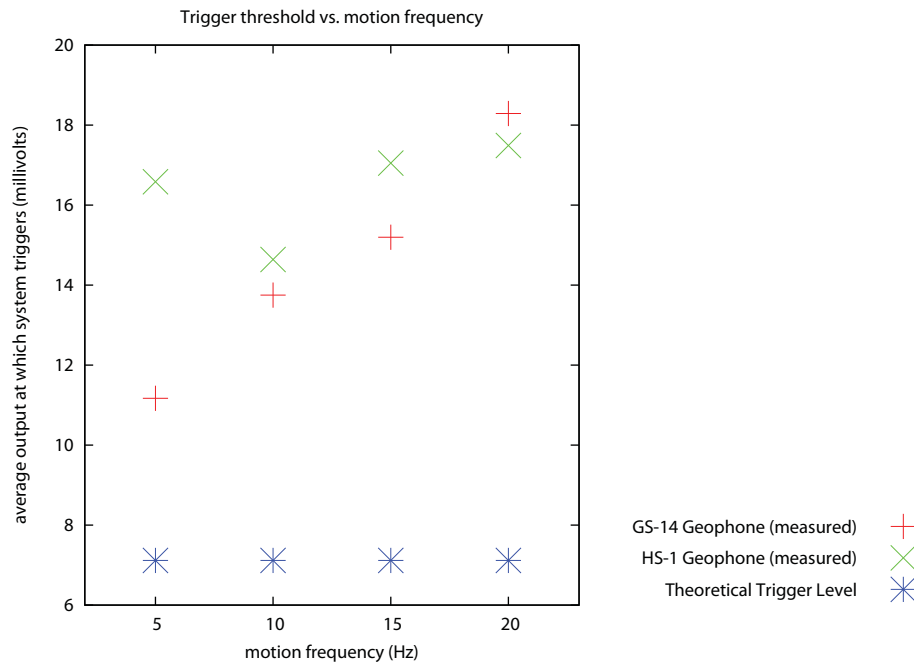


**Figure A.6:** Summary of Shake 'n Wake level 2 trigger threshold voltages

### A.2.1. Physical Meaning of Trigger Threshold

The HS-1 and the GS-14 geophones each have a different characteristic response to vibration phenomena. These responses are shown graphically in Appendices B.8 and B.9, respectively. Figure A.7 shows the trigger levels derived from the springboard experiment translated into terms of particle velocity. Over the frequency range of interest, the response of an undamped HS-1 geophone can be determined using the factory calibration sheet included in Appendix B.9. The GS-14 geophone, however, is not typically used for detection of low-frequency motion, so

the relationship between its voltage and frequency has not been included in the factory calibration curve in Appendix B.8. Its low-frequency response can be extrapolated from the factory-provided curve using a power law formula as follows:

The cantilever vibration displacement  $\delta$  can be held constant during the experiment by applying identical tip displacement. Its velocity is then equal to  $2\pi f\delta$ . Even with a constant  $\delta$ , the velocity increases linearly for the portion of the GS-14's response curve where frequency is less than 20 hertz. Therefore, the portion of the GS-14's response curve can be described with the following power law formula:

$$v = 2\pi\delta k f^n$$

where  $f$  is the frequency of motion,  $k$  is a constant that depends on the damping of the geophone,  $n$  is the slope of the response curve on a logarithmic plot, and  $v$  is the voltage per inch per second of geophone output at frequency  $f$ . For the undamped response curve (A), used in this experiment to provide the largest signal-to-noise ratio to the Shake 'n Wake board, this portion of the response curve can be approximated as:

$$v = 2.455 * 10^{-5} * f^{3.106}$$

### A.3. Speed

The Shake 'n Wake board does not have the ability to digitally record the readings from the sensor to which it is attached. It is therefore crucial to the operation of a system performing Mode 2 recording that the mote to which the Shake 'n Wake is attached begins to operate and execute user code as quickly as possible, as it will be the user code that is responsible for

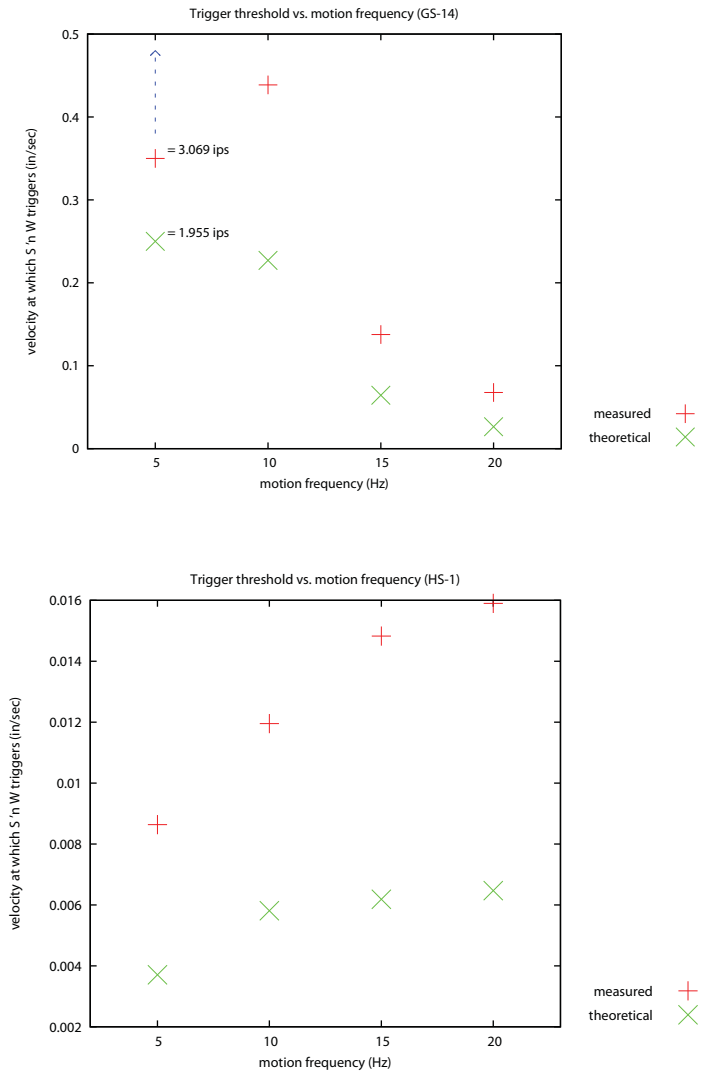


**Figure A.7:** Summary of Shake 'n Wake level 2 trigger threshold velocities

recording the event. If a wireless ACM system were deployed to measure dynamic response of a residential structure, the highest frequency input signal to which the Shake 'n Wake must respond is 20 hertz; this is the highest expected frequency of motion of an instrumented wall.

Figure A.8 shows that a 20 hertz zero-centered sinusoidal input signal will reach its peak absolute amplitude after 12.5 milliseconds.

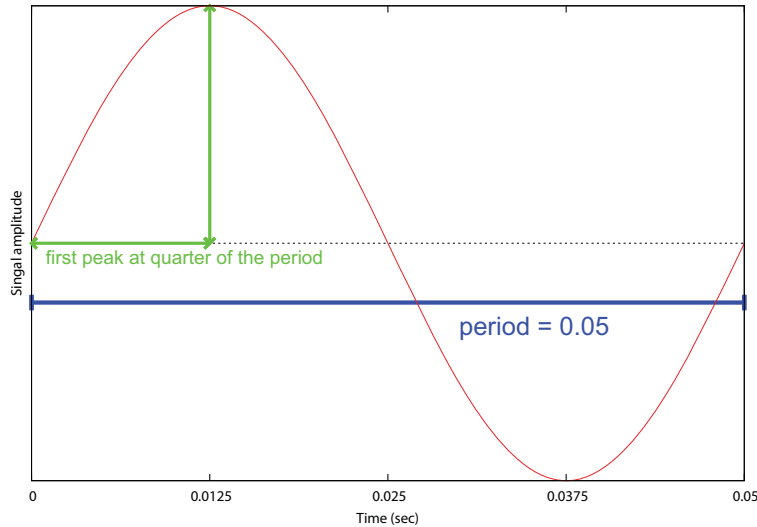


**Figure A.8:** 20 hertz sinusoidal input signal with rise time of 12.5 milliseconds

If it is assumed that the mote must be awake for at least one full sample length before the peak of interest and that it will be sampling at 1000 hertz, then it follows that the time from Shake 'n Wake event detection to the execution of user code by the mote must be less than 11.5 milliseconds.

Output from an oscilloscope connected to various components of a wireless ACM node, shown in Figure A.9, illustrates signal propagation delay from the geophone through the components of the Shake 'n Wake and finally into the mote's processor. At time  $t_1 = 60\mu s$ , the output voltage of the geophone, shown in yellow, crosses the threshold  $V_1$  which corresponds to the software programmable threshold residing in the Shake 'n Wake's memory.  $58\mu s$  later, at time  $t_2$ , the Shake 'n Wake's hardware interrupt request line (IRQ), shown in green, changes to logic low. This change in state of the IRQ is the "wakeup" signal passing from the Shake 'n Wake to

the mote. The mote, which is asleep until  $t_2$ , has already been programmed by the user with an instruction to turn on an LED. The LED active-low hardware line, shown in purple, activates at  $t_3$ ,  $31\mu s$  after the signal from the Shake 'n Wake is sent to the mote. The activation of the LED indicates that the mote has executed its first line of user code. In a real event detection system, this first post-wakeup instruction would be to immediately begin sampling at a high frequency. The power draw of entire system, shown in pink, begins to increase from its sleep level as soon as the Shake 'n Wake sends its “wakeup” signal.

This timing diagram shows that the interval between the moment the input signal reaches the theoretical trigger threshold and the moment the Shake 'n Wake signals a “wakeup” is  $58\mu s$  and the time interval between when the Shake 'n Wake signals a “wakeup” and the time the first line of user code is executed on the mote is  $31\mu s$ . Since this  $89\mu s$  is well within the specified 11.5 millisecond window, it follows that the Shake 'n Wake can perform within the timing requirements.

#### **A.4. Discussion**

These experiments have served to quantify the abilities of the Shake 'n Wake hardware relative to the requirements of a random-event detection scenario. The suitability of the geophones is limited on one end by amplitude: if the vibration frequency is not high enough, the required output amplitude for the Shake 'n Wake to trigger at its most sensitive setting becomes unreachable. On the other end of the frequency range, the limit of functionality is the response speed of the Shake 'n Wake hardware. Table A.1 summarizes the practical limits of the Shake 'n Wake with respect to frequency of geophone output.

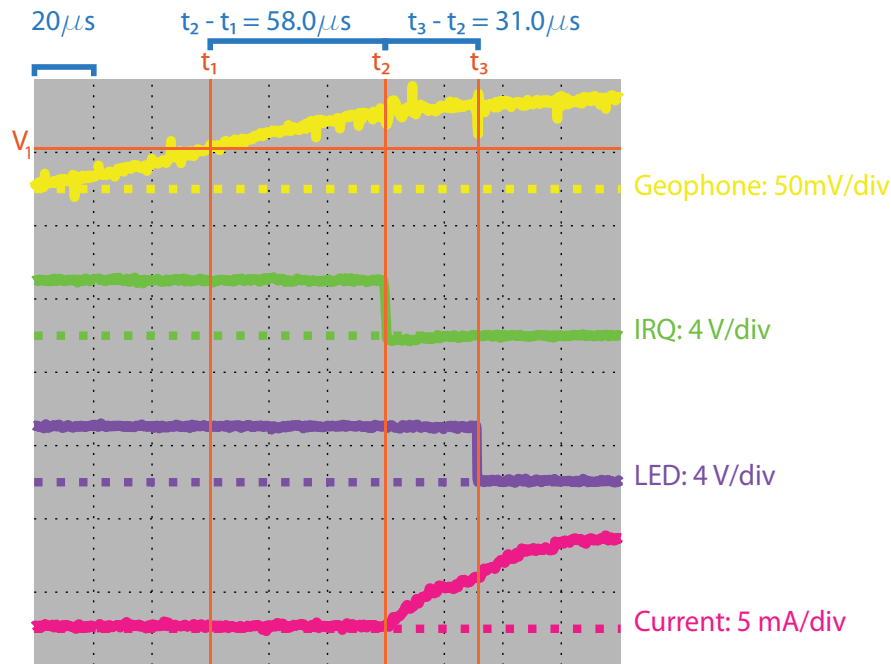


**Figure A.9:** Scope readout indicating the mote can execute user code within 89  $\mu s$  of a signal of interest, after Jevtic et al. (2007b)

#### A.4.1. Upper Frequency Limit: Shake 'n Wake Response Time

A mote attached to a Shake 'n Wake will be executing user code 89  $\mu s$  after a geophone voltage of interest. Using the same assumption that the mote must be awake for at least one full sample period before the peak of interest and that it will be sampling at 1000 hertz once it wakes up, the minimum time between the “wakeup” signal and the arrival of the peak of the event is 1.089 milliseconds. Figure A.8 indicates that the rise time of an idealized sinusoidal input signal is 25% of its period. If the rise time must be at least 1.031 milliseconds, then the period must be at least 4.356 milliseconds and the frequency must be at most 230 hertz. Thus, in order for a node to be executing user code in time to catch the first peak of a dynamic event of interest, the maximum frequency of the event is 230 hertz.

#### A.4.2. Lower Frequency Limit: Geophone Output Amplitude

The GS-14 and HS-1 geophones' output amplitude for a given input velocity varies with frequency, as shown in the response spectra in Appendices B.8 and B.9, respectively. Figure A.7 shows that for the GS-14 geophone, the frequency of motion must be greater than 20 hertz before a 0.05 inch per second velocity can be detected by the Shake 'n Wake at level 2. However, if the amplitude of motion is great enough, the GS-14 can produce sufficient amplitude at low frequencies. For the HS-1 geophone, the frequency of motion can be as low as 2 hertz and still provide a large enough amplitude to trigger the Shake 'n Wake at level 2, no matter what the amplitude of the motion.

input velocity	$> 1ips$	$0.05ips$
GS-14	$2 - 230Hz$	$20 - 230Hz$
HS-1	$2 - 230Hz$	$2 - 230Hz$

**Table A.1:** Summary of functional ranges for Shake 'n Wake event detection at level 2

#### A.5. Appendix Conclusion

The above experiments verify that the Shake 'n Wake:

- does not contaminate the sensor output
- provides a predictable and repeatable threshold voltage
- responds quickly enough to allow the mote to wake up in time to digitally record the signal of interest

- can be used with a GS-14 geophone to detect motions with a frequency 20 hertz and 230 hertz at amplitudes of 0.05 ips, down to 2 hertz if amplitude is sufficiently large
- can be used with an HS-1 geophone to detect motions with a frequency between 2 hertz and 230 hertz regardless of amplitude

## APPENDIX B

### **Data Sheets and Specifications**

The following pages contain specification and data sheets for all relevant commercially manufactured equipment described in this thesis. All documents are reproduced in their entirety as they existed on the Web at the time of publication of this document and without any modification.

## B.1. MICA2 Data Sheet



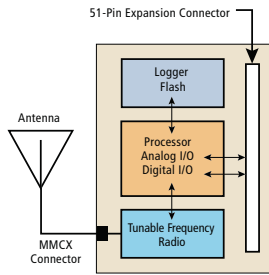
### MICA2

WIRELESS MEASUREMENT SYSTEM

- 3rd Generation, Tiny, Wireless Platform for Smart Sensors
- Designed Specifically for Deeply Embedded Sensor Networks
- > 1 Year Battery Life on AA Batteries (Using Sleep Modes)
- Wireless Communications with Every Node as Router Capability
- 868/916 MHz Multi-Channel Radio Transceiver
- Expansion Connector for Light, Temperature, RH, Barometric Pressure, Acceleration/Seismic, Acoustic, Magnetic and other Crossbow Sensor Boards

#### Applications

- Wireless Sensor Networks
- Security, Surveillance and Force Protection
- Environmental Monitoring
- Large Scale Wireless Networks (1000+ points)
- Distributed Computing Platform



MPR400 Block Diagram



### MICA2

The MICA2 Mote is a third generation mote module used for enabling low-power, wireless, sensor networks. The MICA2 Mote features several new improvements over the original MICA Mote. The following features make the MICA2 better suited to commercial deployment:

- 868/916 MHz multi-channel transceiver with extended range
- Supported by MoteWorks™ wireless sensor network platform for reliable, ad-hoc mesh networking
- Support for wireless remote reprogramming
- Wide range of sensor boards and data acquisition add-on boards

MoteWorks enables the development of custom sensor applications and is specifically optimized for low-power, battery-operated networks. MoteWorks is based on the open-source TinyOS operating system and provides reliable, ad-hoc mesh networking, over-the-air-programming capabilities, cross development tools, server middleware for enterprise network integration and client user interface for analysis and configuration.

#### Processor and Radio Platform (MPR400)

The MPR400 is based on the Atmel ATmega128L. The ATmega128L is a low-power microcontroller which runs MoteWorks from its internal flash memory. A single processor board (MPR400) can be configured to run your sensor application/processing and the network/radio communications stack simultaneously. The MICA2 51-pin expansion connector supports Analog Inputs, Digital I/O, I2C, SPI and UART interfaces. These interfaces make it easy to connect to a wide variety of external peripherals.

#### Sensor Boards

Crossbow offers a variety of sensor and data acquisition boards for the MICA2 Mote. All of these boards connect to the MICA2 via the standard 51-pin expansion connector. Custom sensor and data acquisition boards are also available. Please contact Crossbow for additional information.

Document Part Number: 6020-0042-08 Rev A



Processor/Radio Board	MPR400CB	Remarks
<b>Processor Performance</b>		
Program Flash Memory	128K bytes	
Measurement (Serial) Flash	512K bytes	>100,000 Measurements
Configuration EEPROM	4K bytes	
Serial Communications	UART	0-3V transmission levels
Analog to Digital Converter	10 bit ADC	8 channel, 0-3V input
Other Interfaces		
Current Draw	8 mA	Active mode
	< 15 $\mu$ A	Sleep mode
<b>Multi-Channel Radio</b>		
Center Frequency	868/916 MHz	ISM bands
Number of Channels	4/ 50	Programmable, country specific
Data Rate	38.4 Kbaud	Manchester encoded
RF Power	-20 to +5 dBm	Programmable, typical
Receive Sensitivity	-98 dBm	Typical, analog RSSI at AD Ch. 0
Outdoor Range	500 ft	1/4 Wave dipole, line of sight
Current Draw	27 mA	Transmit with maximum power
	10 mA	Receive
	< 1 $\mu$ A	Sleep
<b>Electromechanical</b>		
Battery	2X AA batteries	Attached pack
External Power	2.7 - 3.3 V	Connector provided
User Interface	3 LEDs	User programmable
Size (in)	2.25 x 1.25 x 0.25	Excluding battery pack
(mm)	58 x 32 x 7	Excluding battery pack
Weight (oz)	0.7	Excluding batteries
(grams)	18	Excluding batteries
Expansion Connector	51-pin	All major I/O signals

Notes: Specifications subject to change without notice

## Base Stations

A base station allows the aggregation of sensor network data onto a PC or other computer platform. Any MICA2 Mote can function as a base station when it is connected to a standard PC interface or gateway board. The MIB510/MIB520 provides a serial/USB interface for both programming and data communications. Crossbow also offers a stand-alone gateway solution, the MIB600 for TCP/IP-based Ethernet networks.



MIB520 Mote Interface Board

## Ordering Information

Model	Description
WSN-START900CA	MICA2 Starter Kit 868/916 MHz
WSN-PRO900CA	MICA2 Professional Kit 868/916 MHz
MPR400CB	868/916 MHz Processor/Radio Board

Document Part Number: 6020-0042-08 Rev A

## B.2. String Potentiometer Data Sheet

Data Sheet - Series 150 Subminiature Position Transducer

http://www.firstmarkcontrols.com/s021f.htm



**Providing the Ultimate Solutions in  
Precision Displacement Sensors**

[Order](#) • [Site Map](#)

Home | All Products | Support | Special Offers | Contact Us

[Home](#)

**Data Sheet - Series 150 Subminiature Position Transducer**

### World's Smallest Cable Position Transducer

**Shaded characteristics are verified during production and test. All others are for REFERENCE and information only.**

#### Key Features

1. 1.5-Inch (38-mm) Maximum Travel
2. Analog Signal Using Precision Conductive Plastic Potentiometer
3. AccuTrak™ Grooved Drum for Enhanced Repeatability
4. Small, Robust Design
5. Choice of Displacement Cable Pull Direction
6. DirectConnect™ Sensor-To-Drum Technology = Zero Backlash, No Torsion Springs or Clutches



#### Potentiometer Specifications

Potentiometer Type	1-turn, precision, conductive plastic
Resistance: Value, Tolerance	5K ohms, ±10%
Travel: Electrical, Mechanical	340°, 340° min
Mechanical Life	5 million shaft revolutions min
Output Signal	analog signal from 0 to supply voltage (voltage divider circuit)
Power Rating	0.75 W at 158° F (70° C)
Supply Current	12 mA max
Supply Voltage	35 VDC max (using voltage divider circuit)
Independent Linearity Error	±1.0% max per VRCl-P-100A
Output Smoothness	0.1% max
Insulation Resistance	1000 Mohms at 500 VDC min
Dielectric Strength	500 VDC min
Resolution	infinite signal
Operating Temperature	-85° to +257° F (-65° to +125° C)
Shock, Vibration	100 g for 6 ms, 10 to 2000 Hz at 15 g per Mil-R-39023
Temperature Coefficient	±400 ppm/°C max

#### Other Specifications

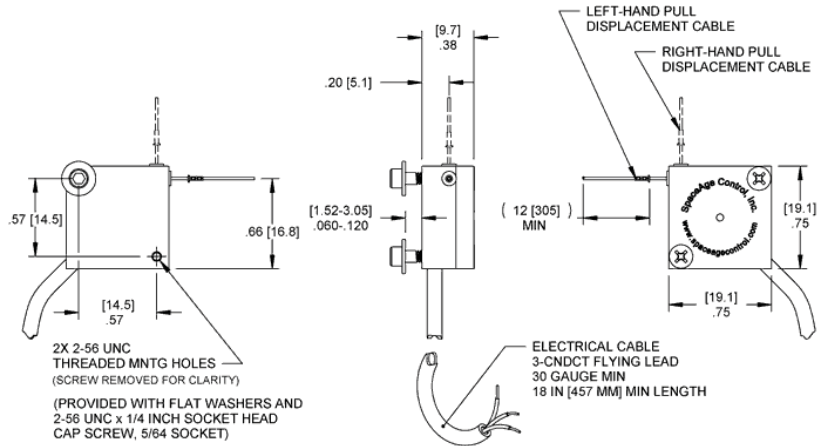
Case Materials	precision-machined anodized 2024 aluminum
Displacement Cable	0.018-inch (0.46-mm) dia., 7-by-7 stranded stainless steel, 40-lb (177-N) min breaking strength
Displacement Cable Hardware	1 each of <a href="#">300196 loop sleeve</a> , <a href="#">300292 copper sleeve</a> , <a href="#">300688 ball-end plug</a> , <a href="#">300495 pull ring</a> , <a href="#">160026 brass swivel</a> , and <a href="#">301003 nickel swivel</a> ; all items provided uncrimped
Nominal Mass	0.5 oz (15.0 g)
Displacement Cable Tension and Cable Acceleration (Nominal): Opt. 1	1 oz 0.3 N min 6 oz 1.7 N max 29 g max
Displacement Cable Tension and Cable Acceleration (Nominal): Opt. 2	3 oz 0.8 N min 14 oz 3.9 N max 49 g max
Environmental Protection	NEMA 3S / IP 54; DO-160D (ED-14D) Env. Cat. E1E1ABXHFDXSAXXXXXXXXXXX

**Model Numbers and Ordering Codes**

150-0121-abc	position transducer (1.50-inch (38-mm) range)
Example: 150-0121-L2N (left-hand displacement cable pull, cable tension: -020, no base)	

Variable	Value	Description
a	L	left-hand displacement cable pull
	R	right-hand displacement cable pull
b	1	cable tension: -010
	2	cable tension: -020
c	N	no base
	B	base: L; pn <a href="#">150015</a>

**Drawing**



Electrical Connection for Increasing Output with Displacement Cable Extraction		
<i>Left-Hand Pull</i>	<i>Right-Hand Pull</i>	<i>Signal</i>
black	red	input, V+
white	white	output, signal, S+
red	black	ground, common, V-, S-

For crimping of hardware to displacement cable, consider the [160001-01 installation kit](#).

Need something not shown? Complete a [Custom Solution Request](#).

All dimensions are REFERENCE and are in inches [mm] • Data Sheet Series 150 Rev. -

Privacy Policy

Firstmark Controls • [info@firstmarkcontrols.com](mailto:info@firstmarkcontrols.com)  
 An ISO9001:2000/AS9100B-Compliant Company  
 1176 Telecom Drive • Creedmoor, NC 27522 USA  
 Phone: 1-919-956-4203 • Fax: 919-682-3786 • Toll Free: 1-866-912-6232

Business hours: Mon-Fri, 8:00am to 5:00pm (Eastern time)  
 All specifications subject to change without notice.  
 © 1996-2010 Firstmark Controls All rights reserved.

### B.3. MDA300CA Data Sheet



## MDA300

DATA ACQUISITION BOARD

- Multi-Function Data Acquisition Board with Temp, Humidity Sensor
- Compatible with MoteView Driver Support
- Up to 11 Channels of 12-bit Analog Input
- Onboard Sensor Excitation and High-Speed Counter
- Convenient Micro-Terminal Screw Connections

### Applications

- Environmental Data Collection
- Agricultural and Habitat Monitoring
- Viticulture and Nursery Management
- HVAC Instrumentation and Control
- General Data Collection and Logging



### MDA300

Developed at UCLA's Center for Embedded Network Sensing (CENS), the MDA300 is an extremely versatile data acquisition board that also includes an onboard temperature/humidity sensor. With its multi-function direct user interface, the MDA300 offers a convenient and flexible solution to those sensor modalities commonly found in areas such as environmental and habitat monitoring as well as many other custom sensing applications.

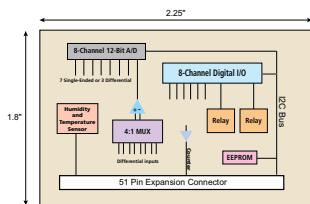
As part of a standard mesh network of Motes, the MDA300's easy access micro-terminals also make it an economical solution for a variety of applications and a key component in the next generation of low-cost wireless weather stations. Data logging and display is supported via Crossbow's MoteView user interface.

Crossbow's MoteView software is designed to be the primary interface between a user and a deployed network of wireless sensors. MoteView provides an intuitive user interface to database management along with sensor data visualization and analysis tools. Sensor data can be logged to a database residing on a host PC, or to a database running autonomously on a Stargate gateway.

### Communication and Control Features Including:

- 7 single-ended or 3 differential ADC channels
- 4 precise differential ADC channels
- 6 digital I/O channels with event detection interrupt
- 2.5, 3.3, 5V sensor excitation and low-power mode
- 64K EEPROM for onboard sensor calibration data
- 2 relay channels, one normally open and one normally closed
- 200 Hz counter channel for wind speed, pulse frequencies
- External I2C interface

Drivers for the MDA300 board are included in Crossbow's MoteWorks™ software platform. MoteWorks enables the development of custom sensor applications and is specifically optimized for low-power, battery-operated networks. MoteWorks is based on the open-source TinyOS operating system and provides reliable, ad-hoc mesh networking, over-the-air-programming capabilities, cross development tools, server middleware for enterprise network integration and client user interface for analysis and configuration.



MDA300C Block Diagram

### Ordering Information

Model	Description
MDA300CA	Mote Data Acquisition Board with Temperature and Humidity

Document Part Number: 6020-0052-03 Rev A

## B.4. MIB510CA Data Sheet



### MIB510

SERIAL INTERFACE BOARD

- Base Station for Wireless Sensor Networks
- Serial Port Programming for IRIS, MICAz and MICA2 Hardware Platforms
- Supports JTAG code debugging

#### Applications

- Programming Interface
- RS-232 Serial Gateway
- IRIS, MICAz, MICA2 Connectivity



### MIB510

The MIB510 allows for the aggregation of sensor network data on a PC as well as other standard computer platforms. Any IRIS/MICAz/MICA2 node can function as a base station when mated to the MIB510 serial interface board. In addition to data transfer, the MIB510 also provides an RS-232 serial programming interface.

The MIB510 has an onboard processor that programs the Mote processor/radio boards. The processor also monitors the MIB510 power voltage and disables programming if the voltage is not within the required limits. Two 51-pin Hirose connectors are available, allowing sensor boards to be attached for monitoring or code development. The MIB510 is also compatible with the Atmel JTAG pod for code development.



MIB510 with Mote and Sensor Board

#### Mote Interface

- Connectors:
  - 51 pin (2)
- Indicators:
  - Mote LEDs: Red, Green, Yellow

#### Programming Interface

- Indicators:
  - LEDs - Power Ok (Green), Programming in Progress (Red)
- Switches:
  - On/Off switch to disable the Mote serial transmission
  - Temporary switch to reset the programming processor and Mote

#### Jtag Interface

- Connector: 10-pin male header (2)

#### Power

- 5V @ 50mA using external power supply (included with unit)
- 3.3-2.7V @ 50mA using Mote batteries

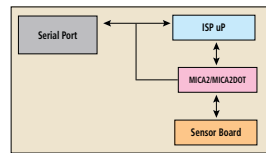
### Specifications

#### RS-232 Interface

- Connector: 9-pin "D"

#### Baud Rates:

- User defined (57.6k typical)
- Programming: 115.2k (uisp controlled)



MIB510 Block Diagram

### Ordering Information

Model	Description
MIB510	Serial PC Interface Board

Document Part Number: 6020-0057-03 Rev A

## B.5. Stargate Data Sheet

### STARGATE

X-SCALE, PROCESSOR PLATFORM

- 400 MHz, Intel PXA255 Processor
- Low Power Consumption <500 mA
- Embedded Linux BSP Package, Source Code Shipped with Kit
- Small, 3.5" x 2.5" Form Factor
- PCMCIA and Compact Flash Connector
- 51-pin Expansion Connector for IRIS/MICAz/MICA2 Motes and other Peripherals
- Ethernet, Serial, JTAG, USB Connectors via 51-pin Daughter Card Interface
- Li-Ion Battery Option

#### Applications

- Sensor Network Gateway
- Robotics Controller Card
- Distributed Computing Platform

### STARGATE

The Stargate is a high-performance processing platform designed for sensor, signal processing, control and wireless sensor networking applications and is based on Intel's Xscale® processor.

The Stargate processor board is the result of the combined design efforts of several different Ubiquitous Computing research groups within Intel. The completed design is licensed to Crossbow Technology for commercial production. The Stargate processor board is preloaded with a Linux distribution and basic drivers. A variety of useful applications and development tools are also provided.

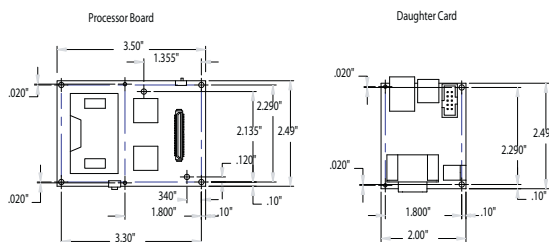
The Stargate processor module is compatible with Crossbow's IRIS/MICAz/MICA2 family of wireless sensor networking products and the public domain software from Intel's Open-Source Robotics initiative. The Stargate processor module is also an ideal solution for standalone Linux-based Single Board Computer (SBC) applications.

With its strong communications capability and Crossbow's ongoing commitment to its open-source architecture, the Stargate platform offers tremendous flexibility. The SPB400CB Processor Board has both Compact Flash and PCMCIA connectors as well as optional installable headers for 2 serial ports and an I2C port. The SDC400CA Daughter Card supports a variety of additional interfaces, including:

- RS-232 Serial
- 10/100 Ethernet
- USB Host
- JTAG

Finally, the standard Mote connector on the SPB400CB Processor Board provides support for synchronous serial port (SSP), UART, and other GPIO connections.

Crossbow



Document Part Number: 6020-0049-05 Rev A

Phone: 408.965.3300 • Fax: 408.324.4840 • E-mail: info@xbow.com • Web: www.xbow.com

Specifications	Remarks
<b>STARGATE Processor Board</b>	
Intel PXA255, Xscale®	400 MHz, RISC Processor
Intel SA1111, StrongARM®	Multiple I/O Companion Chip
<b>Memory</b>	
64 MB SDRAM	
32 MB FLASH	Linux Software < 10 MBytes
<b>Communications</b>	
PCMCIA Slot	Type II
Compact Flash Slot	Type II
51-pin GPIO	UART, SSP via Mote Connector
Optional I2C Port	Installable Header
Optional Serial Port (Z)	Installable Header
<b>General</b>	
Li-Ion Battery Option	
Watch Dog Timer (WDT)	Configurable up to 60 seconds
Battery Gas Gauge	
LED and User Application Switch	
Power Switch	
<b>STARGATE Daughter Card</b>	
<b>Communications</b>	
10 Base-T Ethernet Port	RJ-45 Connector
RS-232 Serial Port	DB-9 Connector
JTAG Debug Port	
USB Host Port	Version 1.1
<b>General</b>	
A/C Power Adaptor	5-6 VDC, 1 Amp
Reset Button	
Real-Time Clock	
<b>Physical</b>	
Processor Board (in)	3.50 x 2.49 x 0.73
(cm)	9.53 x 6.33 x 1.86
Weight (oz)	1.68
(g)	47.47
Daughter Card (in)	2.49 x 2.00 x 0.60
(cm)	6.33 x 5.08 x 1.52
Weight (oz)	1.42
(g)	40.16
<b>Environmental</b>	
Operating Temperature	0 to +70 (°C)

Specifications subject to change without notice

### Ordering Information

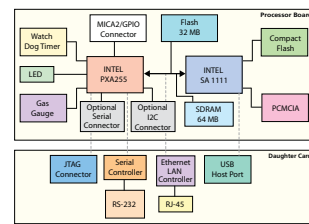
Model	Description
SP-KIT400CA	Stargate Developer's Kit
SPB400CB	Stargate Processor Board
SDC400CA	Stargate Daughter Card - JTAG, 10/100 Ethernet, Serial, USB Host



Processor Board - Top



Daughter Card



Stargate Block Diagram

#### Stargate Kit Contents

- Stargate Processor Board
- Stargate Daughter Card
- Power Supply
- Null Modem Cable
- CD-ROM

#### CD-ROM Contents

- Linux - Kernel & Driver Sources
- GNU Cross Platform Dev. Tools
- Bootloader with Source Code
- Flash Programming Utility
- Shareware & Test Applications
- Developer's Guide - PDF Format

Document Part Number: 6020-0049-05 Rev A

## B.6. Alkaline Battery Data Sheet

**PRODUCT DATASHEET**  1-800-383-7323 USA/CAN  
www.energizer.com

### ENERGIZER E91



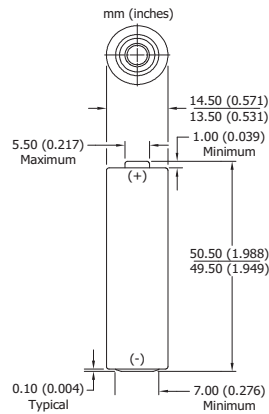
**AA**

#### Specifications

**Classification:** Alkaline  
**Chemical System:** Zinc-Manganese Dioxide (Zn/MnO<sub>2</sub>)  
 No added mercury or cadmium  
**Designation:** ANSI-15A, IEC-LR6  
**Nominal Voltage:** 1.5 volts  
**Nominal IR:** 150 to 300 milliohms (fresh)\*  
**Operating Temp:** -18°C to 55°C (0°F to 130°F)  
**Typical Weight:** 23.0 grams (0.8 oz.)  
**Typical Volume:** 8.1 cubic centimeters (0.5 cubic inch)  
**Jacket:** Plastic Label  
**Shelf Life:** 7 years at 21°C (80% of initial capacity)  
**Terminal:** Flat Contact

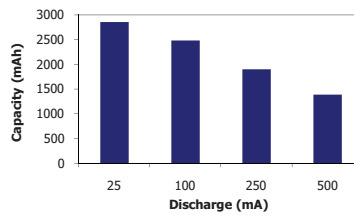
\* For additional information, please reference the IR technical white paper.

#### Industry Standard Dimensions



#### Milliamp-Hours Capacity

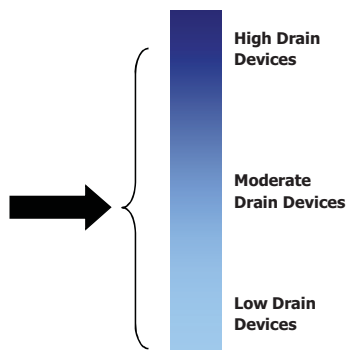
Continuous discharge to 0.8 volts at 21°C



#### Device Selection Guide:

- Digital Camera 
- Photoflash 
- Games, CD's, MD's 
- Tape Player 
- Lighting 
- Toy 
- Remote Control 
- Radio 
- Clock 

#### Battery Selection Indicator



#### Important Notice

This data sheet contains typical information specific to products manufactured at the time of its publication.  
 ©Energizer Holdings, Inc. - Contents herein do not constitute a warranty.

PRODUCT DATASHEET



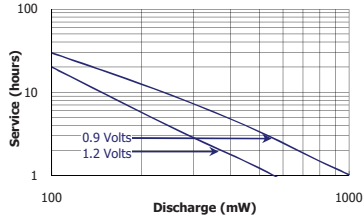
1-800-383-7323 USA/CAN  
www.energizer.com

ENERGIZER E91

AA

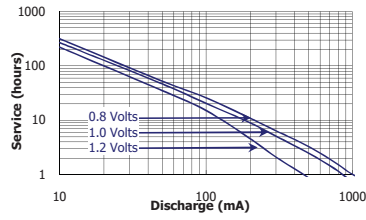
**Constant Power Performance**

Typical Characteristics (21°C)



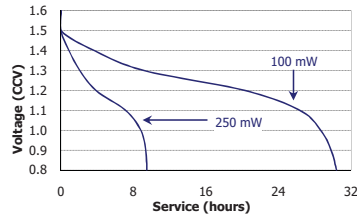
**Constant Current Performance**

Typical Characteristics (21°C)



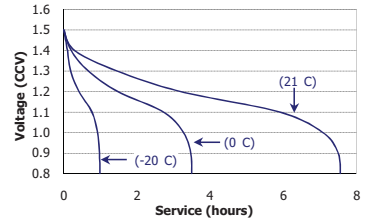
**Constant Power Performance**

Discharge Characteristics (21°C)

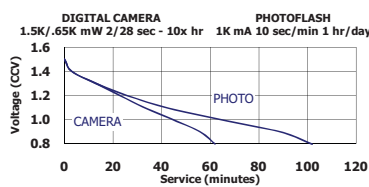
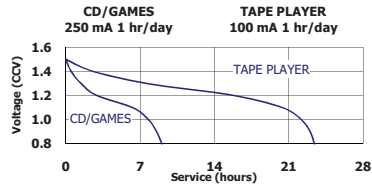
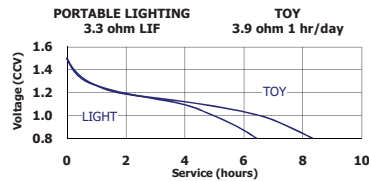
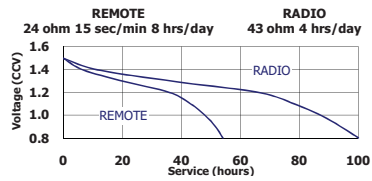


**Constant Current Performance**

250 mA Discharge (-20°C / 0°C / 21°C)



**Industry Standard Tests (21°C)**



**Important Notice**

This data sheet contains typical information specific to products manufactured at the time of its publication.  
©Energizer Holdings, Inc. - Contents herein do not constitute a warranty.

## B.7. Lithium Battery Data Sheet

PRODUCT DATASHEET



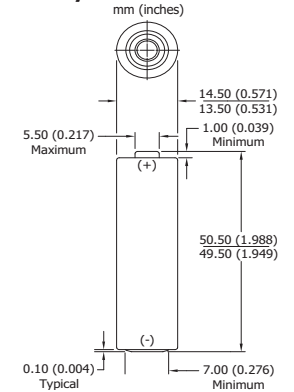
1-800-383-7323 US/CAN  
www.energizer.com

### ENERGIZER L91

Ultimate Lithium



#### Industry Standard Dimensions



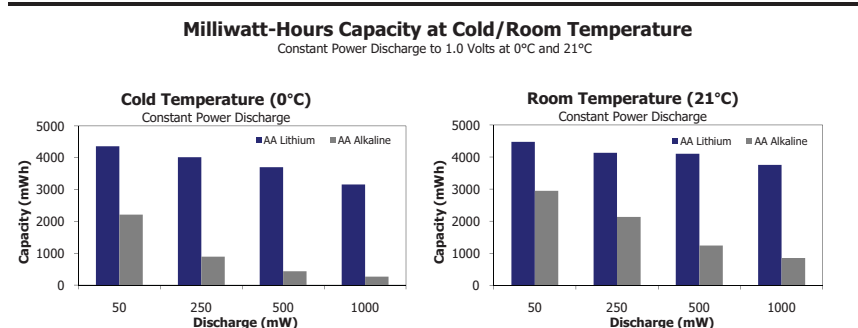
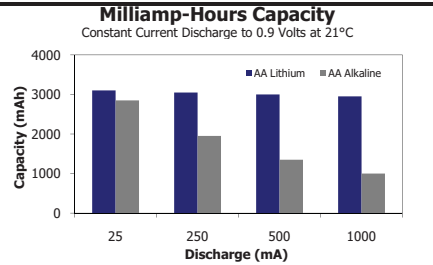
This battery has Underwriters Laboratories component recognition (M429988)

#### Specifications

AA

<b>Classification:</b>	"Cylindrical Lithium"
<b>Chemical System:</b>	Lithium/Iron Disulfide (Li/FeS <sub>2</sub> )
<b>Designation:</b>	ANSI 15-LF, IEC-FR6
<b>Nominal Voltage:</b>	1.5 Volts
<b>Storage Temp:</b>	-40°C to 60°C (-40°F to 140°F)
<b>Operating Temp:</b>	-40°C to 60°C (-40°F to 140°F)
<b>Typical Weight:</b>	14.5 grams (0.5 oz.)
<b>Typical Volume:</b>	8.0 cubic centimeters (0.5 cubic inch)
<b>Max Discharge:</b>	2.0 Amps Continuous
(single battery only)	3.0 Amps Pulse (2 sec on / 8 sec off)
<b>Max Rev Current:</b>	2 uA
<b>Typical Li Content:</b>	0.98 grams (0.03 oz.)
<b>Typical IR:</b>	90 to 150 milliohms*
<b>Shelf Life:</b>	15 years at 21°C (90% of rated capacity)
<b>Transportation:</b>	For complete details, please reference: Global (except US): Special Provision A45 of the International Air Transport Association Dangerous Goods Regulations United States: 49 CFR 173.185

\* For additional information, please reference the IR technical white paper



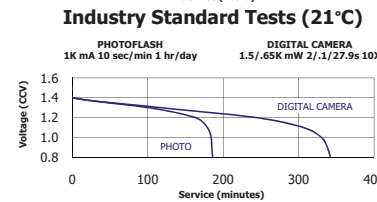
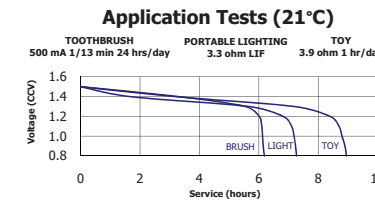
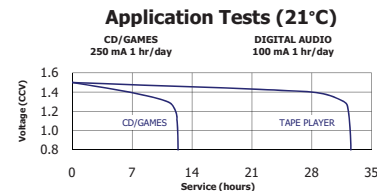
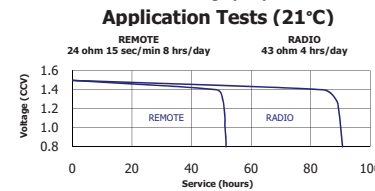
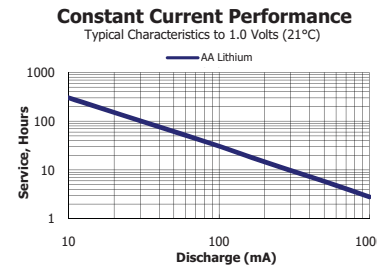
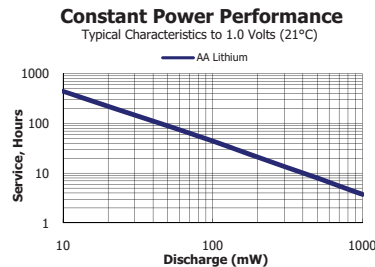
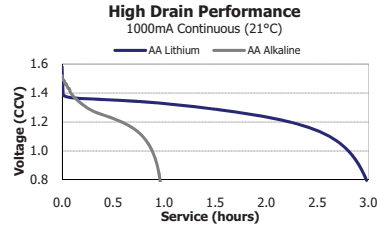
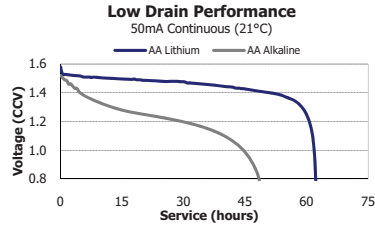
**Important Notice**  
This datasheet contains typical information specific to products manufactured at the time of its publication.  
©Energizer Holdings, Inc. - Contents herein do not constitute a warranty.

ENERGIZER L91

AA

**Typical Discharge Curve Characteristics**

Constant Current Discharge at 21°C (low and high drains)



**Important Notice**

This datasheet contains typical information specific to products manufactured at the time of its publication.  
©Energizer Holdings, Inc. - Contents herein do not constitute a warranty.

**B.8. GS-14 Geophone Data Sheet**

A	SEE E.C.O.	418-533	E.T.	21
B	.09 COIL EXCURSION WAS.120	001065	Z/m	R/

SENSING SYSTEMS ENGINEERING  
 PRODUCT/CUSTOMER  
 SPECIFICATIONS

FOR

GS-14-L3 28 HZ 570 OHMS 0 - 180°

P/N

41065

		<b>GEOSPACE</b>	
		<b>PROPRIETARY INFORMATION</b> <small>"This document contains Geo Space Corporation proprietary and confidential information. It is transmitted to the recipient for limited purposes only, and remains the property of Geo Space Corporation. It may not be reproduced, in whole or in part, without the written consent of Geo Space Corporation, and need not be disclosed to persons not having need of such disclosure consistent with the purpose of the transmittal."</small>	<b>DATE DWN.</b> 7-24-80
			<b>TITLE</b> GEO GS-14-L3 28 HZ 570 OHM 0 - 180°
		<b>CHK. BY</b> <i>[Signature]</i>	<b>SCALE</b>
		<b>APP. BY</b> <i>[Signature]</i>	<b>SHEET 1 OF 4</b>
<b>NEXT ASSY.</b> DWS. NO.	<b>TOP ASSY.</b> MODEL NO.	<b>REL BY</b> <i>[Signature]</i>	<b>CLASS</b> S 41065
<b>APPLICATION</b>			

## GEOPHONE SPECIFICATIONS

GEOPHONE MODEL GS-14-L3 28 Hz 570 OhmsORIENTATION OPERATES IN ANY POS. PART NUMBER 41065

DESCRIPTION	SPECIFICATION	TOLERANCE
NATURAL FREQUENCY (Fn)	<u>28</u> Hz	$\pm 5$ Hz
TILT ANGLE, MEASURED FROM	<u>          </u> Degrees	
FREQUENCY TOLERANCE WITH TILT	<u>          </u> Hz	$\pm 5$
COIL RESISTANCE @ 25°C (Rc)	<u>570</u> Ohms	$\pm 15$ %
INTRINSIC VOLTAGE SENSITIVITY (G)	<u>.29</u> V/in/sec	$\pm 15$ %
	<u>.11</u> V/cm/sec	$\pm 15$ %
NORMALIZED TRANSDUCTION CONSTANT (V/IN/SEC)	<u>.012</u> $\sqrt{Rc}$	$\pm 30$ %
OPEN CIRCUIT DAMPING (Bo)	<u>.18</u>	
DAMPING CONSTANT (B <sub>c</sub> R <sub>c</sub> )	<u>172</u>	
MOVING MASS	<u>2.15</u> g	
COIL EXCURSION P-P	TYPICAL <u>.09</u> in	
	<u>.23</u> cm	
OPERATING TEMPERATURE	<u>-40 +158</u> °F	(-40 +70 °C)
STORAGE TEMPERATURE	<u>-60 +185</u> °F	(-51 +85 °C)
DIMENSIONS:		
CASE HEIGHT:	<u>.68</u> in	(1.73 cm)
HEIGHT ( WITH TERMINALS)	<u>.80</u> in	(2.0 cm)
DIAMETER:	<u>.66</u> in	
	<u>1.68</u> cm	
WEIGHT:	<u>.67</u> oz	
	<u>19</u> g	

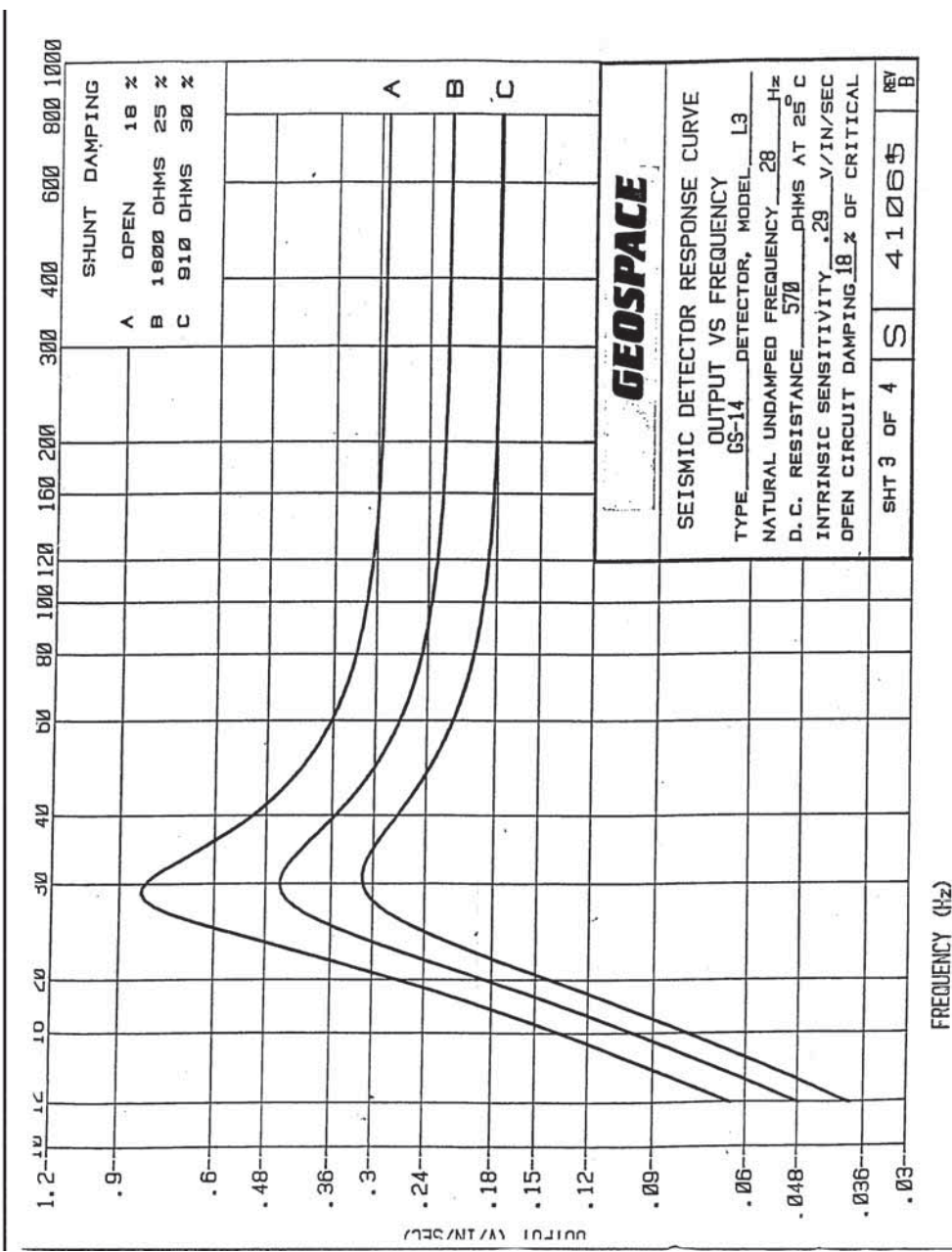
**GEOSPACE**

SHT 2 OF 4

S

41065

B



FREQUENCY (Hz)

**B.9. HS-1 Geophone Data Sheet**

REV	DESCRIPTION OF CHANGE	ECO NO	CHG BY	DATE
A	REDRAWN		<i>H. G.</i>	<i>11/96</i>

**SENSING SYSTEMS ENGINEERING**  
**PRODUCT / CUSTOMER**  
**SPECIFICATION**  
**FOR**  
**HS-1-LT 4.5Hz 1250Ω Horizontal**

**P / N**  
**98449**

<p style="text-align: center;">                     ©Geo Space Corporation 1991                      PROPRIETARY NOTICE                 </p> <p>                     This document, whether patentable or non-patentable subject matter, embodies proprietary and confidential information and is the exclusive property of Geo Space Corporation. It may not be reproduced, used or disclosed to others for any purpose except that for which it is loaned, and it shall be returned on demand.                 </p>	<b>GEO SPACE CORPORATION</b> Houston, Texas U.S.A.	
	DATE DWN.	<u>TITLE</u> <b>HS-1-LT 4.5Hz 1250Ω Horiz.</b>
	11/14/96	
	CHECK BY	SHEET 1 OF 3
APP. BY <i>JMM</i> <i>11-20-96</i>	SPECIFICATION # <b>S-98449</b>	REV. <b>A</b>

**PRODUCT/CUSTOMER  
SPECIFICATION**

GEPHONE MODEL: HS-1-LT

PART NUMBER: 98449

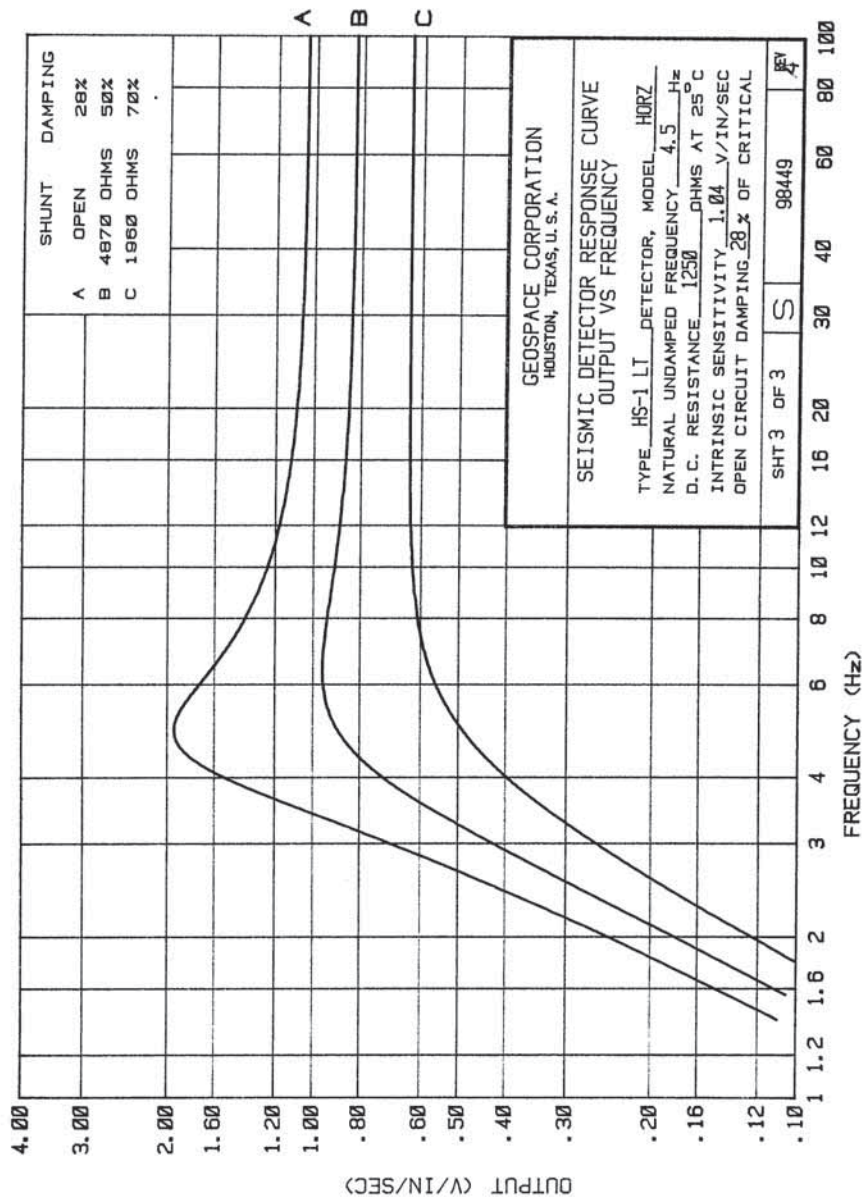
<u>DESCRIPTION</u>	<u>SPECIFICATION @ 25°C</u>	<u>TOL±</u>
*ORIENTATION	<u>HORIZONTAL</u>	
NATURAL FREQUENCY (F <sub>n</sub> )	<u>4.5 Hz</u>	<u>.75 Hz</u>
TILT ANGLE, MEASURED FROM <u>Horizontal</u>	<u>±2.5 °</u>	
FREQUENCY SHIFT AT TILT ANGLE	<u>.5 Hz</u>	
FREQUENCY TOLERANCE WITH TILT	<u>3.25 - 5.75 Hz</u>	<u>1.25 Hz</u>
CLEAN BAND PASS (SPURIOUS RESPONSE)	<u>&gt;140 Hz (TYPICAL)</u>	
DC RESISTANCE @ 25°C (R <sub>c</sub> )	<u>1250 Ω</u>	<u>5 %</u>
INTRINSIC VOLTAGE SENSITIVITY (G)	<u>1.04 V/in/sec</u>	<u>10 %</u>
NORMALIZED TRANSDUCTION CONSTANT Coil Resistance (R <sub>c</sub> ) <u>1240 Ω</u>	<u>.0295 √R<sub>c</sub> V/in/sec</u>	
OPEN CIRCUIT DAMPING (B <sub>a</sub> )	<u>.28</u>	<u>20 %</u>
MOVING MASS (M)	<u>22 g</u>	<u>5 %</u>
COIL EXCURSION P-P	<u>≥.100 in</u> <u>≥.254 cm</u>	
HARMONIC DISTORTION @ <u>----</u> Hz WITH DRIVING VELOCITY OF .7 in/sec (1.8 cm/sec) P-P @ TILT <u>-----°</u>	<u>N.S.</u> <u>N.S.</u>	
DAMPING CONSTANT (B <sub>r</sub> )	<u>1348</u>	
OPERATING AND STORAGE TEMPERATURE	<u>-45 to +100 °C</u>	
MAXIMUM OPERATING TEMPERATURE	<u>+100 °C</u> continuous duty	
DIMENSIONS		
WEIGHT	<u>8.75 oz, 248 g</u>	
DIAMETER	<u>1.625 in, 4.128 cm</u>	
HEIGHT (Less Stud)	<u>2.00 in, 5.08 cm</u>	
STUD LENGTH	<u>.310 in, .787 cm</u>	

**GEO SPACE CORPORATION**

SHEET 2 OF 3

S-98449

A



## B.10. UC-7420 Data Sheet

►►► Embedded Computers

### UC-7410/7420 Series

**RISC ready-to-run computers with 8 serial ports, dual LANs, USB, PCMCIA, CompactFlash, web server**



- > 128 MB RAM onboard, 32 MB flash
- > 8 RS-232/422/485 serial ports
- > Dual 10/100 Mbps LANs for network redundancy
- > USB 2.0 host
- > CompactFlash socket for storage expansion
- > PCMCIA supporting WLAN, GPRS, UMTS, HSDPA
- > LCM display and keypad for HMI
- > Built-in firewall and VPN function
- > Apache web server supporting PHP and XML
- > Ready-to-run Linux or WinCE 5.0 platform
- > DIN-rail or wallmount installation
- > Robust, fanless design

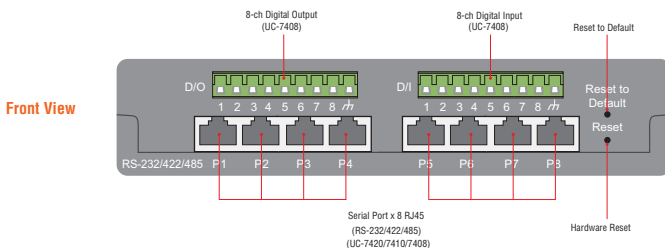


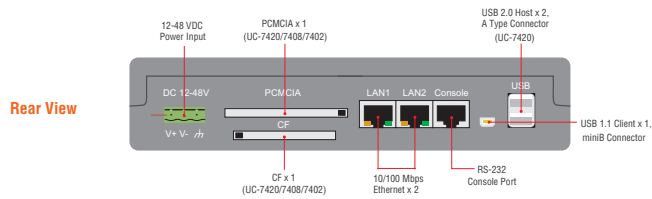
#### Overview

The UC-7410/7420 Series RISC-based ready-to-run Linux and WinCE computers are designed for embedded applications. The computers feature 8 RS-232/422/485 serial ports, a PCMCIA interface for wireless LAN communication, CompactFlash, and USB ports for adding external memory. The built-in firewall, VPN, and web server make these computers ideal for applications that require a web server and front-end controller in the industrial embedded system.

The pre-installed open-standard Linux or WinCE OS operating system provide a convenient platform for software development. In fact, software written for a desktop PC can be ported as is to the UC-7410/7420 platform using readily available development tools, and the code can be stored in the UC-7410/7420's Flash memory. System integrators will find it easy to use the UC-7410/7420 computers as part of distributed control systems based on embedded technology.

#### Appearance





## Hardware Specifications

### Computer

**CPU:**  
 UC-7410/7420: Intel XScale IXP422 266 MHz  
 UC-7410/7420 Plus: Intel XScale IXP425 533 MHz  
**OS (pre-installed):** Embedded Linux or Windows CE 5.0  
**DRAM:** 128 MB onboard  
**Flash:** 32 MB onboard  
**PCMCIA:** Cardbus card and 16-bit PCMCIA 2.1 ro JEIDA 4.2 card (UC-7420 only)

### USB:

- USB 2.0 compliant hosts x 2, A-type connector
- USB 1.1 client x 1, mini B connector

### Storage

**Storage Expansion:** CompactFlash socket (UC-7420, UC-7420 Plus)

### Ethernet Interface

**LAN:** 2 auto-sensing 10/100 Mbps ports (RJ45)

**Magnetic Isolation Protection:** 1.5 KV built-in

### Serial Interface

**Serial Standards:** RS-232/422/485 software-selectable (8-pin RJ45), 8 ports

**ESD Protection:** 15 KV for all signals

**Console Port:** RS-232 (all signals), RJ45 connector, supports PPP

### Serial Communication Parameters

**Data Bits:** 5, 6, 7, 8

**Stop Bits:** 1, 1.5, 2

**Parity:** None, Even, Odd, Space, Mark

**Flow Control:** RTS/CTS, XON/XOFF, ADDC® (automatic data direction control) for RS-485

**Baudrate:** 50 bps to 921.6 Kbps (supports non-standard baudrates; see user's manual for details)

### Serial Signals

**RS-232:** TxD, RxD, DTR, DSR, RTS, CTS, DCD, GND

**RS-422:** TxD+, TxD-, RxD+, RxD-, GND

**RS-485-4w:** TxD+, TxD-, RxD+, RxD-, GND

**RS-485-2w:** Data+, Data-, GND

### LEDs

**System:** OS Ready, Console (TxD/RxD)

**LAN:** 10M/100M x 2

**Serial:** TxD x 8, RxD x 8 (UC-7408/7410/7420, UC-7408/7410/7420 Plus only)

### Physical Characteristics

**Housing:** SECC sheet metal (1 mm)

### Weight:

UC-7410: 810 g

UC-7420: 875 g

**Dimensions:** 197 x 44 x 125 mm (7.76 x 1.73 x 4.92 in)

**Mounting:** DIN-Rail, wall

### Environmental Limits

**Operating Temperature:** -10 to 60°C (14 to 140°F)

**Operating Humidity:** 5 to 95% RH

**Storage Temperature:** -20 to 80°C (-4 to 176°F)

**Anti-vibration:** 1 g @ IEC-68-2-6, sine wave (resonance search), 5-500 Hz, 1 Oct/min, 1 cycle, 13 min 17 sec per axis

**Anti-Shock:** 5 g @ IEC-68-2-27, half sine wave, 30 ms

### Power Requirements

**Input Voltage:** 12 to 48 VDC

### Power Consumption:

UC-7410: 10 W

• 415mA @ 24 VDC

• 830 mA @ 12 VDC

UC-7420: 11 W

• 450 mA @ 24 VDC

• 890 mA @ 12 VDC

### Regulatory Approvals

**EMC:** CE (EN55022 Class A, EN61000-3-2 Class A, EN61000-3-3, EN55024), FCC (Part 15 Subpart B, CISPR 22 Class A)

**Safety:** UL/cUL (UL60950-1, CSA C22.2 No. 60950-1-03), TÜV (EN60950-1)

### Reliability

**Alert Tools:** Built-in buzzer and RTC (real-time clock)

**Automatic Reboot Trigger:** Built-in WDT (watchdog timer)

### Warranty

**Warranty Period:** 5 years

**Details:** See [www.moxa.com/warranty](http://www.moxa.com/warranty)

## Software Specifications

### Linux

**Kernel Version:** 2.6.10

**Protocol Stack:** TCP, UDP, IPv4, SNMP V1, ICMP, IGMP, ARP, HTTP, CHAP, PAP, SSH 1.0/2.0, SSL, DHCP, NTP, NFS, SMTP, Telnet, FTP, PPP, PPPoE

**File System:** JFFS2 (on-board flash)

**System Utilities:** bash, busybox, tinylogin, telnet, ftp, scp

**telnetd:** Telnet Server daemon

**ftpd:** FTP server daemon

**sshd:** Secure shell server

**Apache:** Web server daemon, supporting PHP and XML

**openvpn:** Virtual private network service manager

**iptables:** Firewall service manager

**pppd:** dial in/out over serial port daemon & PPPoE

**snmpd:** snmp agent daemon

**inetd:** TCP server manager program

**Application Development Software:**

- Moxa Linux API Library for device control

- Linux Tool Chain: Gcc, Glibc, GDB

### Windows Embedded CE 5.0

**System Utilities:** Windows command shell, telnet, ftp, web-based administration manager

**File System:** FAT (on-board flash)

**Protocol Stack:** TCP, UDP, IPv4, IPv6 Tunneling, SNMP V2, ICMP, IGMP, ARP, HTTP, CHAP, PAP, SSL, DHCP, SNTP, SMTP, Telnet, FTP, PPP

**Telnet Server:** Allows remote administration through a standard telnet client.

**FTP Server:** Used for transferring files to and from remote computer systems over a network.

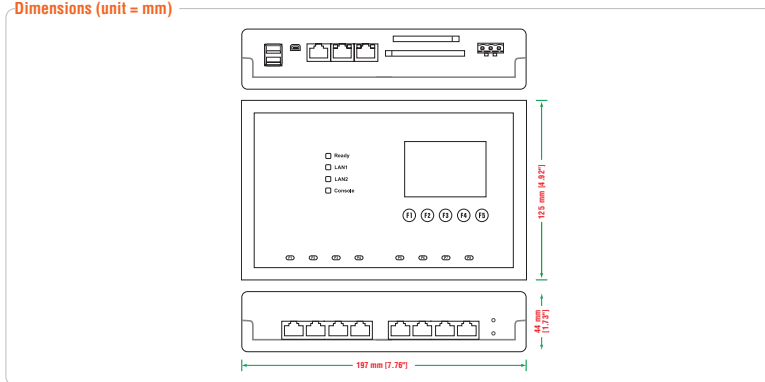
**Web Server (httpd):** WinCE IIS, including ASP, ISAPI Secure Socket Layer support, SSL 2, SSL 3, and Transport Layer Security (TLS/SSL 3.1) public key-based protocols, and Web Administration ISAPI Extensions.

**Dial-up Networking Service:** RAS client API and PPP, supporting Extensible Authentication Protocol (EAP) and RAS scripting.

**Application Development Software:**

- Moxa WinCE 5.0 SDK
- C Libraries and Run-times
- Component Services (COM and DCOM)
- Microsoft Foundation Classes (MFC)
- Microsoft® .NET Compact Framework 2.0 SP2
- XML, including DOM, XPath, XSLT, SAX2
- SOAP Toolkit
- Winsock 2.2

### Dimensions (unit = mm)



## Ordering Information

### Available Models

**UC-7410-LX Plus:** RISC-based IXP425 embedded computer with 8 serial ports, dual LANs, Linux 2.6

**UC-7410-CE:** RISC-based IXP422 embedded computer with 8 serial ports, dual LANs, WinCE 5.0

**UC-7420-LX Plus:** RISC-based IXP425 embedded computer with 8 serial ports, dual LANs, USB, PCMCIA, CompactFlash, Linux 2.6

**UC-7420-CE:** RISC-based IXP422 embedded computer with 8 serial ports, dual LANs, USB, PCMCIA, CompactFlash, WinCE 5.0

### Package Checklist

- 1 UC-7410 or UC-7420 computer
- Wall mounting kit
- DIN-Rail mounting kit
- Ethernet cable: RJ45 to RJ45 cross-over cable, 100 cm
- CBL-RJ45F9-150: 8-pin RJ45 to DB9 female console port cable, 150 cm
- CBL-RJ45M9-150: 8-pin RJ45 to DB9 male serial port cable, 150 cm
- Universal power adaptor
- Document and Software CD
- Quick Installation Guide (printed)
- Product Warranty Statement (printed)

## B.11. Bus Resistor Data Sheet



### Features

- RoHS compliant\*
- Low profile is compatible with DIPs
- Wide assortment of pin packages enhances design flexibility
- Ammo-pak packaging available
- Recommended for rosin flux and solvent clean or no clean flux processes
- Marking on contrasting background for permanent identification

### 4600X Series - Thick Film Conformal SIPs

#### Product Characteristics

Resistance Range ..... 10 ohms to 10 megohms  
 Maximum Operating Voltage ..... 100 V  
 Temperature Coefficient of Resistance  
 50 Ω to 2.2 MΩ ..... ±100 ppm/°C  
 below 50 Ω ..... ±250 ppm/°C  
 above 2.2 MΩ ..... ±250 ppm/°C  
 TCR Tracking ..... 50 ppm/°C maximum; equal values  
 Resistor Tolerance ..... See circuits  
 Insulation Resistance ..... 10,000 megohms minimum  
 Dielectric Withstanding Voltage ..... 200 VRMS  
 Operating Temperature ..... -55 °C to +125 °C

#### Environmental Characteristics

TESTS PER MIL-STD-202.....ΔR MAX.  
 Short Time Overload.....±0.25 %  
 Load Life.....±1.00 %  
 Moisture Resistance.....±0.50 %  
 Resistance to Soldering Heat.....±0.25 %  
 Terminal Strength.....±0.25 %  
 Thermal Shock.....±0.25 %

#### Physical Characteristics

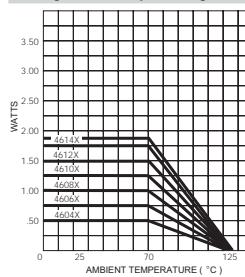
Flammability .....Conforms to UL94V-0  
 Body Material.....Epoxy resin  
 Standard Packaging .....Bulk, Ammo-pak available

#### How To Order

**46 06 X - 101 - 222 LF**

Model (46 = Conformal SIP)  
 Number of Pins  
 Physical Configuration (X = Thick Film Low Profile)  
 Electrical Configuration  
 • 101 = Bussed  
 • 102 = Isolated  
 • 104 = Dual Terminator  
 • AP1 = Bussed Ammo\*\*  
 • AP2 = Isolated Ammo\*\*  
 • AP4 = Dual Ammo\*\*  
 Resistance Code  
 • First 2 digits are significant  
 • Third digit represents the number of zeros to follow.  
 Resistance Tolerance  
 • Blank = ±2 % (see "Resistance Tolerance" on next page for resistance range)  
 • F = ±1 % (100 ohms - 5 megohms)  
 Terminations  
 • All electrical configurations EXCEPT 104 & AP4:  
 LF = Sn/Ag/Cu-plated (RoHS compliant)  
 • ONLY electrical configurations 104 & AP4:  
 L = Sn/Ag/Cu-plated (RoHS compliant)  
 Consult factory for other available options.  
 \*\*Available for packages with 10 pins or less.

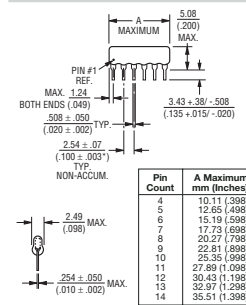
#### Package Power Temp. Derating Curve



#### Package Power Ratings (Watts)

Pkg.	Ambient Temperature	
	70 °C	70 °C
4604X	0.50	1.25
4605X	0.63	1.38
4606X	0.75	1.50
4607X	0.88	1.63
4608X	1.00	1.75
4609X	1.13	

#### Product Dimensions



Maximum package length is equal to 2.54mm (.100") times the number of pins, less .005mm (.002").

Governing dimensions are in metric. Dimensions in parentheses are inches and are approximate.

\*Terminal centerline to centerline measurements made at point of emergence of the lead from the body.

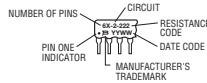
For Standard Values Used in Capacitors, Inductors, and Resistors, [click here](#).

#### Typical Part Marking

Represents total content. Layout may vary.

Part Number	Part Number
4606X-101-RC	6X-1-RC
4608X-102-RC	8X-2-RC
4610X-104-RC/RC	10X-4-RC/RC

RC = ohmic value, 3-digit resistance code.

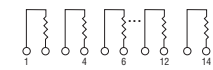


\*RoHS Directive 2002/95/EC Jan 27 2003 including Annex  
 Specifications are subject to change without notice.  
 Customers should verify actual device performance in their specific applications.

For information on specific applications, download Bourns' application notes:  
[DRAM Applications](#)  
[Dual Terminator Resistor Networks](#)  
[R/ZR Ladder Networks](#)  
[SCSI Applications](#)

**4600X Series - Thick Film Conformal SIPs** **BOURNS®**

**Isolated Resistors (102 Circuit)**  
**Model 4600X-102-RC**  
 4, 6, 8, 10, 12, 14 Pin

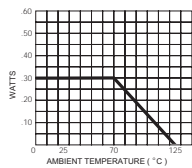


These models incorporate 2 to 7 isolated thick-film resistors of equal value, each connected between two pins.

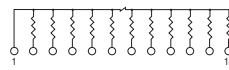
**Resistance Tolerance**  
 10 ohms to 49 ohms .....±1 ohm  
 50 ohms to 5 megohms.....±2 %\*  
 Above 5 megohms.....±5 %

**Power Rating per Resistor**  
 At 70 °C .....0.30 watt

**Power Temperature Derating Curve**



**Bussed Resistors (101 Circuit)**  
**Model 4600X-101-RC**  
 4 through 14 Pin

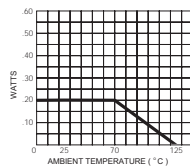


These models incorporate 3 to 13 thick-film resistors of equal value, each connected between a common bus (pin 1) and a separate pin.

**Resistance Tolerance**  
 10 ohms to 49 ohms .....±1 ohm  
 50 ohms to 5 megohms.....±2 %\*  
 Above 5 megohms.....±5 %

**Power Rating per Resistor**  
 At 70 °C .....0.20 watt

**Power Temperature Derating Curve**



**Popular Resistance Values (101, 102 Circuits)\*\***

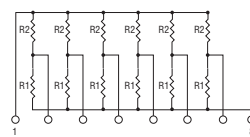
Ohms	Code	Ohms	Code	Ohms	Code	Ohms	Code	Ohms	Code
10	100	180	181	1,800	182	15,000	153	120,000	124
22	220	220	221	2,000	202	18,000	183	150,000	154
27	270	270	271	2,200	222	20,000	203	180,000	184
33	330	330	331	2,700	272	22,000	223	220,000	224
39	390	390	391	3,300	332	27,000	273	270,000	274
47	470	470	471	3,900	392	33,000	333	330,000	334
56	560	560	561	4,700	472	39,000	393	390,000	394
68	680	680	681	5,600	562	47,000	473	470,000	474
82	820	820	821	6,800	682	56,000	563	560,000	564
100	101	1,000	102	8,200	822	68,000	683	680,000	684
120	121	1,200	122	10,000	103	82,000	823	820,000	824
150	151	1,500	152	12,000	123	100,000	104	1,000,000	105

\* ±1% TOLERANCE IS AVAILABLE BY ADDING SUFFIX CODE "F" AFTER THE RESISTANCE CODE.  
 \*\*NON-STANDARD VALUES AVAILABLE, WITHIN RESISTANCE RANGE.

REV. 12/06

Specifications are subject to change without notice.  
 Customers should verify actual device performance in their specific applications.

**Dual Terminator (104 Circuit)**  
**Model 4600X-104-R1/R2**  
 4 through 14 Pin

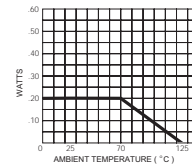


The 4608X-104 (shown above) is an 8-pin configuration and terminates 6 lines. Pins 1 and 8 are common for ground and power, respectively. Twelve thick-film resistors are paired in series between the common lines (pins 1 and 8).

**Resistance Tolerance**  
 Below 100 ohms.....±2 ohms  
 100 ohms to 5 megohms.....±2 %\*  
 Above 5 megohms.....±5 %

**Power Rating per Resistor**  
 At 70 °C .....0.20 watt

**Power Temperature Derating Curve**



**Popular Resistance Values (104 Circuit)\*\***

Resistance			
(Ohms)		Code	
R <sub>1</sub>	R <sub>2</sub>	R <sub>1</sub>	R <sub>2</sub>
160	240	161	241
180	390	181	391
220	270	221	271
220	330	221	331
330	390	331	391
330	470	331	471
3,000	6,200	302	622

## B.12. Conductive Pen Data Sheet

<b>CHEMTRONICS®</b> <b>Technical Data Sheet</b>	<b>TDS # CW2200</b>
<b>CircuitWorks® Conductive Pen</b>	

### PRODUCT DESCRIPTION

CircuitWorks® Conductive Pen makes instant highly conductive silver traces on circuit boards. CW2200 is used in prototype, rework, and repair of circuit boards by linking components, repairing defective traces, and making smooth jumpers. The silver traces dry in minutes and have excellent adhesion to most electronic materials. Engineers, repair technicians, and manufacturers will find that the CircuitWorks® Conductive Pen speeds project completion and cuts rework time.

- Single component system
- High electrical conductivity
- Fast drying
- Highly adherent to circuit boards
- Operating temperature to 400°F (205°C)

### TYPICAL APPLICATIONS

CircuitWorks® Conductive Pen may be used for electronics applications including:

- Circuit Trace Repair
- Solderless Linking of Components
- EMI Shielding
- Solderable Terminations
- Quick Prototype Modifications

### TYPICAL PRODUCT DATA AND PHYSICAL PROPERTIES

<b>Composition</b>	
Material	Silver Filled Polymer
Silver Particle Size	10-15 microns
Color	Silver Gray
Setting Rate	<2mm/hr.
<b>Properties</b>	
Conductivity	0.02-0.05 ohms/sq/mil 0.00005-0.000125 ohm cm
Max. Temperature	400°F (205°C)
Tack-Free Time @ 25°C	3 to 5 Minutes
Cure Time @ 25°C	20 to 30 Minutes
Solder Wetting	2 to 3 Seconds
Electrical Conductivity	Excellent
Adhesion	Excellent
Flexibility	Good
Chemical Resistance	Good
Tip Diameters	
MTP	0.8 mm (0.03 inches)
STP	1.2 mm (0.05 inches)
<b>Shelflife</b>	12 months

### COMPATIBILITY

CircuitWorks® Conductive Pen material has excellent compatibility with materials used in printed circuit board fabrication. As with any chemical system, compatibility with the substrate must be determined on a non-critical area prior to use.

**USAGE INSTRUCTIONS**

**Read MSDS carefully prior to use.**

**Cleaning:** For best adhesion, clean board with one of Chemtronics Electro-Wash<sup>®</sup> or Pow-R-Wash<sup>®</sup> solvents in order to remove any surface contamination which may prevent adequate material contact.

**Mixing:** Although this system has been formulated to resist hard-packing, it should be shaken vigorously for 30 seconds to insure the proper dispersion of the silver flakes. If pen has been allowed to sit idle for a long period of time, the mixing ball may seize in the barrel. To free the ball use force to tap the barrel end of the pen until the ball begins to move inside the pen.

**Application:** The conductive ink is dispensed through the CircuitWorks<sup>®</sup> Conductive Pen. Squeezing the pen body while pressing down on the surface will allow the material to flow, enabling the trace to be drawn. Practice with the pen before attempting detail work. The bulk form of this material may be applied by brushing, banding, or automatic dispensing equipment.

**Thinning:** The conductive ink has been optimized for the CircuitWorks<sup>®</sup> Conductive Pen and thinning is not normally necessary. However, Butyl Acetate may be added with thorough mixing to make slight adjustments for ease of application in the bulk form.

**Clean-up/Removal:** The conductive ink may be cleaned or removed using a strong organic solvent such as Chemtronics<sup>®</sup> Electro-Wash<sup>®</sup> PX.

**Curing:** Tack-free in 3 to 5 minutes at room temperature. Achieves electrical conductivity within 30 minutes. Heat cure for 5 minutes at 250 to 300°F (120 to 150°C) for maximum conductivity, durability and chemical resistance.

**Soldering:** Low temperature soldering is possible to the *heat-cured* silver conductive traces if done at 350°F (177°C) for <5 seconds.

**AVAILABILITY**

CW2200STP 8.5 g (0.3 oz.), Standard 1.2 mm tip  
CW2200MTP 8.5g (0.3 oz.), MicroTip 0.8 mm tip

**TECHNICAL & APPLICATION****ASSISTANCE**

Chemtronics<sup>®</sup> provides a technical hotline to answer your technical and application related questions. The toll free number is: **1-800-TECH-401**.

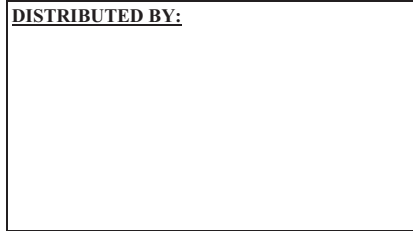
**NOTE:**

This information is believed to be accurate. It is intended for professional end users having the skills to evaluate and use the data properly. ITW CHEMTRONICS<sup>®</sup> does not guarantee the accuracy of the data and assumes no liability in connection with damages incurred while using it.

**MANUFACTURED BY:**

ITW CHEMTRONICS<sup>®</sup>  
8125 COBB CENTER DRIVE  
KENNESAW, GA 30152  
1-770-424-4888

REV. F (06/09)

**DISTRIBUTED BY:**

B.13. "Bridge Paint" Data Sheet



**Protective  
&  
Marine  
Coatings**

**MACROPOXY® 646  
FAST CURE EPOXY**

**PART A B58-600 SERIES**  
**PART B B58V600 HARDENER**

Revised 2/10

**PRODUCT INFORMATION**

4.53

PRODUCT DESCRIPTION		PRODUCT CHARACTERISTICS (Cont'd)																																																																
<p><b>MACROPOXY 646 FAST CURE EPOXY</b> is a high solids, high build, fast drying, polyamide epoxy designed to protect steel and concrete in industrial exposures. Ideal for maintenance painting and fabrication shop applications. The high solids content ensures adequate protection of sharp edges, corners, and welds. This product can be applied directly to marginally prepared steel surfaces.</p> <ul style="list-style-type: none"> <li>• Low VOC</li> <li>• Low odor</li> <li>• Outstanding application properties</li> <li>• Chemical resistant</li> <li>• Abrasion resistant</li> </ul>		<p><b>Shelf Life:</b> 36 months, unopened Store indoors at 40°F (4.5°C) to 100°F (38°C).</p> <p><b>Flash Point:</b> 91°F (33°C), TCC, mixed</p> <p><b>Reducer/Clean Up:</b> Reducer, R7K15</p> <p><b>In California:</b> Reducer R7K111 or Oxsol 100</p>																																																																
PRODUCT CHARACTERISTICS		RECOMMENDED USES																																																																
<p><b>Finish:</b> Semi-Gloss</p> <p><b>Color:</b> Mill White, Black and a wide range of colors available through tinting</p> <p><b>Volume Solids:</b> 72% ± 2%, mixed, Mill White</p> <p><b>Weight Solids:</b> 85% ± 2%, mixed, Mill White</p> <p><b>VOC (EPA Method 24):</b> Unreduced: &lt;250 g/L; 2.08 lb/gal mixed Reduced 10%: &lt;300 g/L; 2.50 lb/gal</p> <p><b>Mix Ratio:</b> 1:1 by volume</p>		<p><b>RECOMMENDED USES</b></p> <ul style="list-style-type: none"> <li>• Marine applications</li> <li>• Fabrication shops</li> <li>• Pulp and paper mills</li> <li>• Power plants</li> <li>• Offshore platforms</li> <li>• Refineries</li> <li>• Chemical plants</li> <li>• Tank exteriors</li> <li>• Water treatment plants</li> </ul> <p>• Mill White and Black are acceptable for immersion use for salt water and fresh water, not acceptable for potable water</p> <ul style="list-style-type: none"> <li>• Suitable for use in USDA inspected facilities</li> <li>• Conforms to AWWA D102-03 OCS #5</li> <li>• Conforms to MPI # 108</li> </ul>																																																																
Recommended Spreading Rate per coat:		PERFORMANCE CHARACTERISTICS																																																																
<table border="1"> <thead> <tr> <th></th> <th>Minimum</th> <th>Maximum</th> </tr> </thead> <tbody> <tr> <td><b>Wet mils (microns)</b></td> <td>7.0 175</td> <td>13.5 338</td> </tr> <tr> <td><b>Dry mils (microns)</b></td> <td>5.0* 125</td> <td>10.0* 250</td> </tr> <tr> <td><b>-Coverage sq ft/gal (m<sup>2</sup>/L)</b></td> <td>116 2.8</td> <td>232 5.7</td> </tr> <tr> <td><b>Theoretical coverage sq ft/gal (m<sup>2</sup>/L) @ 1 mil / 25 microns dft</b></td> <td>1152 28.2</td> <td></td> </tr> </tbody> </table> <p>*May be applied at 3.0-10.0 mils dft as an intermediate coat. Refer to Recommended Systems (page 2).</p> <p><i>NOTE: Brush or roll application may require multiple coats to achieve maximum film thickness and uniformity of appearance.</i></p>			Minimum	Maximum	<b>Wet mils (microns)</b>	7.0 175	13.5 338	<b>Dry mils (microns)</b>	5.0* 125	10.0* 250	<b>-Coverage sq ft/gal (m<sup>2</sup>/L)</b>	116 2.8	232 5.7	<b>Theoretical coverage sq ft/gal (m<sup>2</sup>/L) @ 1 mil / 25 microns dft</b>	1152 28.2		<p><b>Substrate*:</b> Steel</p> <p><b>Surface Preparation*:</b> SSPC-SP10/NACE 2</p> <p><b>System Tested*:</b> 1 ct. Macropoxy 646 Fast Cure @ 6.0 mils (150 microns) dft *unless otherwise noted below</p> <table border="1"> <thead> <tr> <th>Test Name</th> <th>Test Method</th> <th>Results</th> </tr> </thead> <tbody> <tr> <td><b>Abrasion Resistance</b></td> <td>ASTM D4060, CS17 wheel, 1000 cycles, 1 kg load</td> <td>84 mg loss</td> </tr> <tr> <td><b>Accelerated Weathering-QUV<sup>1</sup></b></td> <td>ASTM D4587, QUV-A, 12,000 hours</td> <td>Passes</td> </tr> <tr> <td><b>Adhesion</b></td> <td>ASTM D4541</td> <td>1,037 psi</td> </tr> <tr> <td><b>Corrosion Weathering<sup>1</sup></b></td> <td>ASTM D5894, 36 cycles, 12,000 hours</td> <td>Rating 10 per ASTM D714 for blistering; Rating 9 per ASTM D610 per rusting</td> </tr> <tr> <td><b>Direct Impact Resistance</b></td> <td>ASTM D2794</td> <td>30 in. lb.</td> </tr> <tr> <td><b>Dry Heat Resistance</b></td> <td>ASTM D2485</td> <td>250°F (121°C)</td> </tr> <tr> <td><b>Exterior Durability</b></td> <td>1 year at 45° South</td> <td>Excellent, chalks</td> </tr> <tr> <td><b>Flexibility</b></td> <td>ASTM D522, 180° bend, 3/4" mandrel</td> <td>Passes</td> </tr> <tr> <td><b>Humidity Resistance</b></td> <td>ASTM D4585, 6000 hours</td> <td>No blistering, cracking, or rusting</td> </tr> <tr> <td><b>Immersion</b></td> <td>1 year fresh and salt water</td> <td>Passes, no rusting, blistering, or loss of adhesion</td> </tr> <tr> <td><b>Irradiation-Effects on Coatings used in Nuclear Power Plants</b></td> <td>ANSI 5.12 / ASTM D4082-89</td> <td>Passes</td> </tr> <tr> <td><b>Pencil Hardness</b></td> <td>ASTM D3363</td> <td>3H</td> </tr> <tr> <td><b>Salt Fog Resistance<sup>1</sup></b></td> <td>ASTM B117, 6,500 hours</td> <td>Rating 10 per ASTM D610 for rusting; Rating 9 per ASTM D1654 for corrosion</td> </tr> <tr> <td><b>Slip Coefficient, Mill White</b></td> <td>ASCE Specification for Structural Joints Using ASTM A325 or ASTM A490 Bolts</td> <td>Class A, 0.36</td> </tr> <tr> <td><b>Water Vapor Permeance</b></td> <td>ASTM D1653, Method B</td> <td>1.16 US perms</td> </tr> </tbody> </table> <p>Epoxy coatings may darken or discolor following application and curing.</p> <p><b>Footnotes:</b> <sup>1</sup>Zinc Clad II Plus Primer</p>		Test Name	Test Method	Results	<b>Abrasion Resistance</b>	ASTM D4060, CS17 wheel, 1000 cycles, 1 kg load	84 mg loss	<b>Accelerated Weathering-QUV<sup>1</sup></b>	ASTM D4587, QUV-A, 12,000 hours	Passes	<b>Adhesion</b>	ASTM D4541	1,037 psi	<b>Corrosion Weathering<sup>1</sup></b>	ASTM D5894, 36 cycles, 12,000 hours	Rating 10 per ASTM D714 for blistering; Rating 9 per ASTM D610 per rusting	<b>Direct Impact Resistance</b>	ASTM D2794	30 in. lb.	<b>Dry Heat Resistance</b>	ASTM D2485	250°F (121°C)	<b>Exterior Durability</b>	1 year at 45° South	Excellent, chalks	<b>Flexibility</b>	ASTM D522, 180° bend, 3/4" mandrel	Passes	<b>Humidity Resistance</b>	ASTM D4585, 6000 hours	No blistering, cracking, or rusting	<b>Immersion</b>	1 year fresh and salt water	Passes, no rusting, blistering, or loss of adhesion	<b>Irradiation-Effects on Coatings used in Nuclear Power Plants</b>	ANSI 5.12 / ASTM D4082-89	Passes	<b>Pencil Hardness</b>	ASTM D3363	3H	<b>Salt Fog Resistance<sup>1</sup></b>	ASTM B117, 6,500 hours	Rating 10 per ASTM D610 for rusting; Rating 9 per ASTM D1654 for corrosion	<b>Slip Coefficient, Mill White</b>	ASCE Specification for Structural Joints Using ASTM A325 or ASTM A490 Bolts	Class A, 0.36	<b>Water Vapor Permeance</b>	ASTM D1653, Method B	1.16 US perms
	Minimum	Maximum																																																																
<b>Wet mils (microns)</b>	7.0 175	13.5 338																																																																
<b>Dry mils (microns)</b>	5.0* 125	10.0* 250																																																																
<b>-Coverage sq ft/gal (m<sup>2</sup>/L)</b>	116 2.8	232 5.7																																																																
<b>Theoretical coverage sq ft/gal (m<sup>2</sup>/L) @ 1 mil / 25 microns dft</b>	1152 28.2																																																																	
Test Name	Test Method	Results																																																																
<b>Abrasion Resistance</b>	ASTM D4060, CS17 wheel, 1000 cycles, 1 kg load	84 mg loss																																																																
<b>Accelerated Weathering-QUV<sup>1</sup></b>	ASTM D4587, QUV-A, 12,000 hours	Passes																																																																
<b>Adhesion</b>	ASTM D4541	1,037 psi																																																																
<b>Corrosion Weathering<sup>1</sup></b>	ASTM D5894, 36 cycles, 12,000 hours	Rating 10 per ASTM D714 for blistering; Rating 9 per ASTM D610 per rusting																																																																
<b>Direct Impact Resistance</b>	ASTM D2794	30 in. lb.																																																																
<b>Dry Heat Resistance</b>	ASTM D2485	250°F (121°C)																																																																
<b>Exterior Durability</b>	1 year at 45° South	Excellent, chalks																																																																
<b>Flexibility</b>	ASTM D522, 180° bend, 3/4" mandrel	Passes																																																																
<b>Humidity Resistance</b>	ASTM D4585, 6000 hours	No blistering, cracking, or rusting																																																																
<b>Immersion</b>	1 year fresh and salt water	Passes, no rusting, blistering, or loss of adhesion																																																																
<b>Irradiation-Effects on Coatings used in Nuclear Power Plants</b>	ANSI 5.12 / ASTM D4082-89	Passes																																																																
<b>Pencil Hardness</b>	ASTM D3363	3H																																																																
<b>Salt Fog Resistance<sup>1</sup></b>	ASTM B117, 6,500 hours	Rating 10 per ASTM D610 for rusting; Rating 9 per ASTM D1654 for corrosion																																																																
<b>Slip Coefficient, Mill White</b>	ASCE Specification for Structural Joints Using ASTM A325 or ASTM A490 Bolts	Class A, 0.36																																																																
<b>Water Vapor Permeance</b>	ASTM D1653, Method B	1.16 US perms																																																																
<p><b>Drying Schedule @ 7.0 mils wet (175 microns):</b></p> <table border="1"> <thead> <tr> <th></th> <th>@ 35°F/1.7°C</th> <th>@ 77°F/25°C</th> <th>@ 100°F/38°C</th> </tr> </thead> <tbody> <tr> <td><b>To touch:</b></td> <td>4-5 hours</td> <td>2 hours</td> <td>1.5 hours</td> </tr> <tr> <td><b>To handle:</b></td> <td>48 hours</td> <td>8 hours</td> <td>4.5 hours</td> </tr> <tr> <td><b>To recoat:</b></td> <td></td> <td></td> <td></td> </tr> <tr> <td>  <b>minimum:</b></td> <td>48 hours</td> <td>8 hours</td> <td>4.5 hours</td> </tr> <tr> <td>  <b>maximum:</b></td> <td>1 year</td> <td>1 year</td> <td>1 year</td> </tr> <tr> <td><b>To cure:</b></td> <td></td> <td></td> <td></td> </tr> <tr> <td>  <b>Service:</b></td> <td>10 days</td> <td>7 days</td> <td>4 days</td> </tr> <tr> <td>  <b>Immersion:</b></td> <td>14 days</td> <td>7 days</td> <td>4 days</td> </tr> </tbody> </table> <p><i>If maximum recoat time is exceeded, abrade surface before recoating. Drying time is temperature, humidity, and film thickness dependent. Paint temperature must be at least 40°F (4.5°C) minimum.</i></p> <p><b>Pot Life:</b> 10 hours 4 hours 2 hours</p> <p><b>Sweat-in-time:</b> 30 minutes 30 minutes 15 minutes</p>			@ 35°F/1.7°C	@ 77°F/25°C	@ 100°F/38°C	<b>To touch:</b>	4-5 hours	2 hours	1.5 hours	<b>To handle:</b>	48 hours	8 hours	4.5 hours	<b>To recoat:</b>				<b>minimum:</b>	48 hours	8 hours	4.5 hours	<b>maximum:</b>	1 year	1 year	1 year	<b>To cure:</b>				<b>Service:</b>	10 days	7 days	4 days	<b>Immersion:</b>	14 days	7 days	4 days																													
	@ 35°F/1.7°C	@ 77°F/25°C	@ 100°F/38°C																																																															
<b>To touch:</b>	4-5 hours	2 hours	1.5 hours																																																															
<b>To handle:</b>	48 hours	8 hours	4.5 hours																																																															
<b>To recoat:</b>																																																																		
<b>minimum:</b>	48 hours	8 hours	4.5 hours																																																															
<b>maximum:</b>	1 year	1 year	1 year																																																															
<b>To cure:</b>																																																																		
<b>Service:</b>	10 days	7 days	4 days																																																															
<b>Immersion:</b>	14 days	7 days	4 days																																																															
<p><b>When used as an intermediate coat as part of a multi-coat system:</b></p> <p><b>Drying Schedule @ 5.0 mils wet (125 microns):</b></p> <table border="1"> <thead> <tr> <th></th> <th>@ 35°F/1.7°C</th> <th>@ 77°F/25°C</th> <th>@ 100°F/38°C</th> </tr> </thead> <tbody> <tr> <td><b>To touch:</b></td> <td>3 hours</td> <td>1 hour</td> <td>1 hour</td> </tr> <tr> <td><b>To handle:</b></td> <td>48 hours</td> <td>4 hours</td> <td>2 hours</td> </tr> <tr> <td><b>To recoat:</b></td> <td></td> <td></td> <td></td> </tr> <tr> <td>  <b>minimum:</b></td> <td>16 hours</td> <td>4 hours</td> <td>2 hours</td> </tr> <tr> <td>  <b>maximum:</b></td> <td>1 year</td> <td>1 year</td> <td>1 year</td> </tr> </tbody> </table>			@ 35°F/1.7°C	@ 77°F/25°C	@ 100°F/38°C	<b>To touch:</b>	3 hours	1 hour	1 hour	<b>To handle:</b>	48 hours	4 hours	2 hours	<b>To recoat:</b>				<b>minimum:</b>	16 hours	4 hours	2 hours	<b>maximum:</b>	1 year	1 year	1 year																																									
	@ 35°F/1.7°C	@ 77°F/25°C	@ 100°F/38°C																																																															
<b>To touch:</b>	3 hours	1 hour	1 hour																																																															
<b>To handle:</b>	48 hours	4 hours	2 hours																																																															
<b>To recoat:</b>																																																																		
<b>minimum:</b>	16 hours	4 hours	2 hours																																																															
<b>maximum:</b>	1 year	1 year	1 year																																																															



**Protective  
&  
Marine  
Coatings**

**MACROPOXY® 646  
FAST CURE EPOXY**

**PART A B58-600**      **SERIES**  
**PART B B58V600**      **HARDENER**

**PRODUCT INFORMATION**

4.53

<b>RECOMMENDED SYSTEMS</b>			
		<b>Dry Film Thickness / ct.</b>	
		<b>Mils</b>	<b>(Microns)</b>
<b>Immersion and atmospheric:</b>			
<b>Steel:</b>			
2 cts.	Macropoxy 646	5.0-10.0	(125-250)
<b>Concrete/Masonry, smooth:</b>			
2 cts.	Macropoxy 646	5.0-10.0	(125-250)
<b>Concrete Block:</b>			
1 ct.	Kem Cati-Coat HS Epoxy Filler/Sealer <i>as needed to fill voids and provide a continuous substrate.</i>	10.0-20.0	(250-500)
2 cts.	Macropoxy 646	5.0-10.0	(125-250)
<b>Atmospheric:</b>			
<b>Steel:</b>			
(Shop applied system, new construction, AWWA D102-03, can also be used at 3 mils minimum dft when used as an intermediate coat as part of a multi-coat system)			
1 ct.	Macropoxy 646 Fast Cure Epoxy	3.0-6.0	(75-150)
1-2 cts.	of recommended topcoat		
<b>Steel:</b>			
1 ct.	Recoat Epoxy Primer	4.0-6.0	(100-150)
2 cts.	Macropoxy 646	5.0-10.0	(125-250)
<b>Steel:</b>			
1 ct.	Macropoxy 646	4.0-6.0	(100-150)
1-2 cts.	Acrolon 218 Polyurethane or Hi-Solids Polyurethane or SherThane 2K Urethane or Hydrogloss	3.0-6.0 3.0-5.0 2.0-4.0 2.0-4.0	(75-150) (75-125) (50-100) (50-100)
<b>Steel:</b>			
2 cts.	Macropoxy 646	5.0-10.0	(125-250)
1-2 cts.	Tile-Clad HS Epoxy	2.5-4.0	(63-100)
<b>Steel:</b>			
1 ct.	Zinc Clad II Plus	3.0-6.0	(75-150)
1 ct.	Macropoxy 646	3.0-10.0	(75-250)
1-2 cts.	Acrolon 218 Polyurethane	3.0-6.0	(75-150)
<b>Steel:</b>			
1 ct.	Zinc Clad III HS or Zinc Clad IV	3.0-5.0 3.0-5.0	(75-125) (75-125)
1 ct.	Macropoxy 646	3.0-10.0	(75-250)
1-2 cts.	Acrolon 218 Polyurethane	3.0-6.0	(75-150)
<b>Aluminum:</b>			
2 cts.	Macropoxy 646	5.0-10.0	(125-250)
<b>Galvanizing:</b>			
2 cts.	Macropoxy 646	5.0-10.0	(125-250)
The systems listed above are representative of the product's use, other systems may be appropriate.			
<b>DISCLAIMER</b>			
The information and recommendations set forth in this Product Data Sheet are based upon tests conducted by or on behalf of The Sherwin-Williams Company. Such information and recommendations set forth herein are subject to change and pertain to the product offered at the time of publication. Consult your Sherwin-Williams representative to obtain the most recent Product Data Information and Application Bulletin.			

<b>SURFACE PREPARATION</b>					
Surface must be clean, dry, and in sound condition. Remove all oil, dust, grease, dirt, loose rust, and other foreign material to ensure adequate adhesion.					
Refer to product Application Bulletin for detailed surface preparation information.					
Minimum recommended surface preparation:					
<b>Iron &amp; Steel</b>					
Atmospheric:	SSPC-SP2/3				
Immersion:	SSPC-SP10/NACE 2, 2-3 mil (50-75 micron) profile				
Aluminum:	SSPC-SP1				
Galvanizing:	SSPC-SP1				
<b>Concrete &amp; Masonry</b>					
Atmospheric:	SSPC-SP13/NACE 6, or ICR1 03732, CSP 1-3				
Immersion:	SSPC-SP13/NACE 6-4.3.1 or 4.3.2, or ICR1 03732, CSP 1-3				
<b>Surface Preparation Standards</b>					
Condition of Surface	ISO 8501-1	Swedish Std.	SSPC	NACE	
White Metal	BS7079:A1	Sa 3	SP 5		
Near White Metal	Sa 2.5	Sa 2.5	SP 10	2	
Commercial Blast	Sa 2	Sa 2	SP 7	4	
Brush-Off Blast	CSa 1	CSa 1	SP 3		
Hand Tool Cleaning	Rusted	CSa 2	SP 2		
	Pitted & Rusted	D St 2	SP 3		
Power Tool Cleaning	Rusted	CSa 3	SP 3		
	Pitted & Rusted	D St 3	SP 3		
<b>TINTING</b>					
Tint Part A with Maxitoner at 150% strength. Five minutes minimum mixing on a mechanical shaker is required for complete mixing of color.					
Tinting is not recommended for immersion service.					
<b>APPLICATION CONDITIONS</b>					
Temperature:	35°F (1.7°C) minimum, 120°F (49°C) maximum (air and surface) 40°F (4.5°C) minimum, 120°F (49°C) maximum (material) At least 5°F (2.8°C) above dew point				
Relative humidity:	85% maximum				
Refer to product Application Bulletin for detailed application information.					
<b>ORDERING INFORMATION</b>					
Packaging:	Part A: 1 gallon (3.78L) and 5 gallon (18.9L) containers Part B: 1 gallon (3.78L) and 5 gallon (18.9L) containers				
Weight:	12.9 ± 0.2 lb/gal ; 1.55 Kg/L mixed, may vary by color				
<b>SAFETY PRECAUTIONS</b>					
Refer to the MSDS sheet before use.					
Published technical data and instructions are subject to change without notice. Contact your Sherwin-Williams representative for additional technical data and instructions.					
<b>WARRANTY</b>					
The Sherwin-Williams Company warrants our products to be free of manufacturing defects in accord with applicable Sherwin-Williams quality control procedures. Liability for products proven defective, if any, is limited to replacement of the defective product or the refund of the purchase price paid for the defective product as determined by Sherwin-Williams. NO OTHER WARRANTY OR GUARANTEE OF ANY KIND IS MADE BY SHERWIN-WILLIAMS, EXPRESSED OR IMPLIED, STATUTORY, BY OPERATION OF LAW OR OTHERWISE, INCLUDING MERCHANTABILITY AND FITNESS FOR A PARTICULAR PURPOSE.					



**Protective  
&  
Marine  
Coatings**

**MACROPOXY® 646  
FAST CURE EPOXY**

**PART A** B58-600 **SERIES**  
**PART B** B58V600 **HARDENER**

Revised 2/10

**APPLICATION BULLETIN**

4.53

**SURFACE PREPARATIONS**

Surface must be clean, dry, and in sound condition. Remove all oil, dust, grease, dirt, loose rust, and other foreign material to ensure adequate adhesion.

**Iron & Steel, Atmospheric Service:**

Minimum surface preparation is Hand Tool Clean per SSPC-SP2. Remove all oil and grease from surface by Solvent Cleaning per SSPC-SP1. For better performance, use Commercial Blast Cleaning per SSPC-SP6/NACE 3, blast clean all surfaces using a sharp, angular abrasive for optimum surface profile (2 mils / 50 microns). Prime any bare steel within 8 hours or before flash rusting occurs.

**Iron & Steel, Immersion Service:**

Remove all oil and grease from surface by Solvent Cleaning per SSPC-SP1. Minimum surface preparation is Near White Metal Blast Cleaning per SSPC-SP10/NACE 2. Blast clean all surfaces using a sharp, angular abrasive for optimum surface profile (2-3 mils / 50-75 microns). Remove all weld spatter and round all sharp edges by grinding. Prime any bare steel the same day as it is cleaned.

**Aluminum**

Remove all oil, grease, dirt, oxide and other foreign material by Solvent Cleaning per SSPC-SP1.

**Galvanized Steel**

Allow to weather a minimum of six months prior to coating. Solvent Clean per SSPC-SP1 (recommended solvent is VM&P Naphtha). When weathering is not possible, or the surface has been treated with chromates or silicates, first Solvent Clean per SSPC-SP1 and apply a test patch. Allow paint to dry at least one week before testing adhesion. If adhesion is poor, brush blasting per SSPC-SP7 is necessary to remove these treatments. Rusty galvanizing requires a minimum of Hand Tool Cleaning per SSPC-SP2, prime the area the same day as cleaned.

**Concrete and Masonry**

For surface preparation, refer to SSPC-SP13/NACE 6, or ICR 03732, CSP 1-3. Surfaces should be thoroughly clean and dry. Concrete and mortar must be cured at least 28 days @ 75°F (24°C). Remove all loose mortar and foreign material. Surface must be free of laitance, concrete dust, dirt, form release agents, moisture curing membranes, loose cement and hardeners. Fill bug holes, air pockets and other voids with Steel-Seam FT910.

**Concrete, Immersion Service:**

For surface preparation, refer to SSPC-SP13/NACE 6, Section 4.3.1 or 1.3.2 or ICR 03732, CSP 1-3.

**Always follow the standard methods listed below:**

ASTM D4258 Standard Practice for Cleaning Concrete.  
ASTM D4259 Standard Practice for Abrading Concrete.  
ASTM D4260 Standard Practice for Etching Concrete.  
ASTM F1869 Standard Test Method for Measuring Moisture Vapor Emission Rate of Concrete.  
SSPC-SP 13/Nace 6 Surface Preparation of Concrete.  
ICRI 03732 Concrete Surface Preparation.

**Previously Painted Surfaces**

If in sound condition, clean the surface of all foreign material. Smooth, hard or glossy coatings and surfaces should be dulled by abrading the surface. Apply a test area, allowing paint to dry one week before testing adhesion. If adhesion is poor, or if this product attacks the previous finish, removal of the previous coating may be necessary. If paint is peeling or badly weathered, clean surface to sound substrate and treat as a new surface as above.

Condition of Surface	Surface Preparation Standards			
	ISO 8501-1 BS7079:A1	Swedish Std. SIS055900	SSPC	NACE
White Metal	Sa 3	Sa 3	SP 5	1
Near White Metal	Sa 2.5	Sa 2.5	SP 10	2
Commercial Blast	Sa 2	Sa 2	SP 8	3
Brush-Off Blast	Sa 1	Sa 1	SP 7	4
Hand Tool Cleaning	OC St 2	OC St 2	-	-
Rusted	OC St 3	OC St 3	-	-
Pitted & Rusted	OC St 3	OC St 3	-	-
Power Tool Cleaning	D St 3	D St 3	SP 3	-

**APPLICATION CONDITIONS**

Temperature: 35°F (1.7°C) minimum, 120°F (49°C) maximum (air and surface)  
40°F (4.5°C) minimum, 120°F (49°C) maximum (material)  
At least 5°F (2.8°C) above dew point

Relative humidity: 85% maximum

**APPLICATION EQUIPMENT**

The following is a guide. Changes in pressures and tip sizes may be needed for proper spray characteristics. Always purge spray equipment before use with listed reducer. Any reduction must be compliant with existing VOC regulations and compatible with the existing environmental and application conditions.

**Reducer/Clean Up** ..... Reducer R7K15  
In California.....Reducer R7K111

**Airless Spray**

Pump.....30:1  
Pressure.....2800 - 3000 psi  
Hose.....1/4" ID  
Tip......017" - .023"  
Filter.....60 mesh  
Reduction.....As needed up to 10% by volume

**Conventional Spray**

Gun.....DeVilbiss MBC-510  
Fluid Tip.....E  
Air Nozzle.....704  
Atomization Pressure.....60-65 psi  
Fluid Pressure.....10-20 psi  
Reduction.....As needed up to 10% by volume  
Requires oil and moisture separators

**Brush**

Brush.....Nylon/Polyester or Natural Bristle  
Reduction.....Not recommended

**Roller**

Cover.....3/8" woven with solvent resistant core  
Reduction.....Not recommended

If specific application equipment is not listed above, equivalent equipment may be substituted.



## Protective & Marine Coatings

# MACROPOXY® 646 FAST CURE EPOXY

PART A B58-600 SERIES  
PART B B58V600 HARDENER

### APPLICATION BULLETIN

4.53

#### APPLICATION PROCEDURES

Surface preparation must be completed as indicated.

Mix contents of each component thoroughly with low speed power agitation. Make certain no pigment remains on the bottom of the can. Then combine one part by volume of Part A with one part by volume of Part B. Thoroughly agitate the mixture with power agitation. Allow the material to sweat-in as indicated prior to application. Re-stir before using.

If reducer solvent is used, add only after both components have been thoroughly mixed, after sweat-in.

Apply paint at the recommended film thickness and spreading rate as indicated below:

#### Recommended Spreading Rate per coat:

	Minimum	Maximum
Wet mils (microns)	7.0 175	13.5 338
Dry mils (microns)	5.0* 125	10.0* 250
~Coverage sq ft/gal (m <sup>2</sup> /L)	116 2.8	232 5.7
Theoretical coverage sq ft/gal (m <sup>2</sup> /L) @ 1 mil / 25 microns dft	1152 28.2	

\*May be applied at 3.0-10.0 mils dft as an intermediate coat. Refer to Recommended Systems (page 2).

NOTE: Brush or roll application may require multiple coats to achieve maximum film thickness and uniformity of appearance.

#### Drying Schedule @ 7.0 mils wet (175 microns):

	@ 35°F/1.7°C	@ 77°F/25°C	@ 100°F/38°C
		50% RH	
To touch:	4-5 hours	2 hours	1.5 hours
To handle:	48 hours	8 hours	4.5 hours
To recoat:			
minimum:	48 hours	8 hours	4.5 hours
maximum:	1 year	1 year	1 year
To cure:			
Service:	10 days	7 days	4 days
Immersion:	14 days	7 days	4 days
If maximum recoat time is exceeded, abrade surface before recoating. Drying time is temperature, humidity, and film thickness dependent. Paint temperature must be at least 40°F (4.5°C) minimum.			
Pot Life:	10 hours	4 hours	2 hours
Sweat-in-time:	30 minutes	30 minutes	15 minutes

#### When used as an intermediate coat as part of a multi-coat system:

	@ 35°F/1.7°C	@ 77°F/25°C	@ 100°F/38°C
		50% RH	
To touch:	3 hours	1 hour	1 hour
To handle:	48 hours	4 hours	2 hours
To recoat:			
minimum:	16 hours	4 hours	2 hours
maximum:	1 year	1 year	1 year

Application of coating above maximum or below minimum recommended spreading rate may adversely affect coating performance.

#### CLEAN UP INSTRUCTIONS

Clean spills and spatters immediately with Reducer R7K15. Clean tools immediately after use with Reducer R7K15. In California use Reducer R7K111. Follow manufacturer's safety recommendations when using any solvent.

#### PERFORMANCE TIPS

Stripe coat all crevices, welds, and sharp angles to prevent early failure in these areas.

When using spray application, use a 50% overlap with each pass of the gun to avoid holidays, bare areas, and pinholes. If necessary, cross spray at a right angle.

Spreading rates are calculated on volume solids and do not include an application loss factor due to surface profile, roughness or porosity of the surface, skill and technique of the applicator, method of application, various surface irregularities, material lost during mixing, spillage, overthinning, climatic conditions, and excessive film build.

Excessive reduction of material can affect film build, appearance, and adhesion.

Do not mix previously catalyzed material with new.

Do not apply the material beyond recommended pot life.

In order to avoid blockage of spray equipment, clean equipment before use or before periods of extended downtime with Reducer R7K15. In California use Reducer R7K111.

Tinting is not recommended for immersion service.

Use only Mil White and Black for immersion service.

Insufficient ventilation, incomplete mixing, miscatalyzation, and external heaters may cause premature yellowing.

Excessive film build, poor ventilation, and cool temperatures may cause solvent entrapment and premature coating failure.

Quik-Kick Epoxy Accelerator is acceptable for use. See data page 4.99 for details.

Refer to Product Information sheet for additional performance characteristics and properties.

#### SAFETY PRECAUTIONS

Refer to the MSDS sheet before use.

Published technical data and instructions are subject to change without notice. Contact your Sherwin-Williams representative for additional technical data and instructions.

#### DISCLAIMER

The information and recommendations set forth in this Product Data Sheet are based upon tests conducted by or on behalf of The Sherwin-Williams Company. Such information and recommendations set forth herein are subject to change and pertain to the product offered at the time of publication. Consult your Sherwin-Williams representative to obtain the most recent Product Data Information and Application Bulletin.

#### WARRANTY

The Sherwin-Williams Company warrants our products to be free of manufacturing defects in accord with applicable Sherwin-Williams quality control procedures. Liability for products proven defective, if any, is limited to replacement of the defective product or the refund of the purchase price paid for the defective product as determined by Sherwin-Williams. NO OTHER WARRANTY OR GUARANTEE OF ANY KIND IS MADE BY SHERWIN-WILLIAMS, EXPRESSED OR IMPLIED, STATUTORY, BY OPERATION OF LAW OR OTHERWISE, INCLUDING MERCHANTABILITY AND FITNESS FOR A PARTICULAR PURPOSE.